Zrf1's Role in mESC Differentiation and Breast Cancer Progression

Dissertation zur Erlangung des Grades

"Doktor der Naturwissenschaften"

im Promotionsfach Pharmazie

am Fachbereich Chemie, Pharmazie und Geowissenschaften

der Johannes Gutenberg-Universität in Mainz

vorgelegt von Aysegul Kaymak

geb. am 18.07.1987 in Izmir, Türkei

Mainz, 2017

SUMMARY

Zuotin-related factor 1 (Zrf1) has recently been identified as an epigenetic regulator of gene transcription. Upon a differentiation stimulus, Zrf1 facilitates the expression of its target genes via specifically binding to mono-ubiquitinated histone H2A and simultaneous displacement of PRC1 from chromatin. So far, Zrf1 was shown to primarily operate during differentiation into the neuronal lineage. As a multifunctional protein, Zrf1 plays a crucial role in carcinogenesis. Zrf1 is overexpressed in many cancers and was suggested to have an oncogenic role in cancer progression. Zrf1 provides leukemogenic potential in acute myeloid leukemia and it contributes to Ras-oncogene induced senescence through the *INK4-ARF* locus.

In the present study, I elucidated a broader role for Zrf1 during during *in vitro* differentiation. Zrf1 depleted mESCs have defects in the generation of all three germ layers. I observed a particularly pronounced effect during mesoderm development and I was able to rescue the observed phenotype by re-expression of Zrf1 in Zrf1 knockdown cells. I found that Zrf1 plays a prominent role in cardiomyocyte differentiation and Zrf1 knockdown results in impaired beating function of cardiomyocytes *in vitro*. At the molecular level, Zrf1 plays an essential regulatory role for the expression of the first and second heart field related genes, thereby promoting faithful cardiomyocyte differentiation. Taken together, the function of Zrf1 needs to be considered when addressing molecular mechanisms of cardiovascular diseases.

In addition to studying the function of Zrf1 during differentiation, I have studied the function of Zrf1 in breast invasive ductal carcinoma. Upon Zrf1 depletion, breast cancer cells increase their cell motility, decrease their cellular adhesion and are able to form organoid like structures in cell suspension. Hence, Zrf1 depleted cells can mimic the events during cancer metastasis *in vitro.* Zrf1 knockdown also contributes to hormone independent growth of cells which represents a phenotype that is observed in more aggressive forms of breast cancer. Zrf1 depletion disrupts the balance between anti-apoptotic and pro-apoptotic genes, thereby favoring cell survival and contributing to drug resistance. My data suggest that Zrf1 is a potential novel target to be explored for new treatment

strategies in breast cancer, moreover it plays a critical regulatory role in the progression of breast invasive ductal carcinoma.

ZUSAMMENFASSUNG

Zuotin-related factor 1 (Zrf1) wurde vor kurzem als ein epigenetischer Regulator der Transkription beschrieben. Während der Zelldifferenzierung unterstützt Zrf1 die Gen-Expression durch ein spezifisches Binden an mono-ubiquitiniertes Histone H2A und gleichzeitiger Verdrängung der PRC1 Komplexe vom Chromatin. Bislang wurde gezeigt, dass Zrf1 hauptsächlich während der Zelldifferenzierung in die neuronale Linie beteiligt ist. Als ein multi-funktionales Protein spielt Zrf1 auch eine wichtige Rolle während der Krebsentstehung. Zrf1 ist in vielen Krebsarten überexpremiert und es wird vermutet, dass es eine Funktion in der Metastasierung hat. In akuter Leukämie spielt Zrf1 eine signifikante Rolle, und es trägt zur Ras-induzierten Seneszenz durch den *INK4A-ARF* locus bei.

In der hier vorliegenden Arbeit wurde eine globale Analyse der Zrf1 Funktion während der *In-vitro*-Differenzierung vorgenommen. Zrf1-depletierte embryonale Maus-Stammzellen zeigen Defekte in der Formation aller drei Keimblätter. Es konnte gezeigt werden, dass insbesondere die Entwicklung des Mesoderms in Zrf1-*Knockdown* Zellen gestört ist. Die Ausbildung dieses Phänotyps konnte nach ektopischer Expression von Zrf1 in den *Knockdown* Zelllinien verhindert werden. Es konnte weiterhin gezeigt werden, dass Zrf1 eine essentielle Funktion während der Differenzierung von Kardiomyozyten einnimmt. Unter anderem zeigen Zrf1 *Knockdown* Zellen eine verminderte Schlagrate *in vitro*. Auf molekularer Ebene spielt Zrf1 eine wichtige regulative Rolle bei der Expression der Gene des ersten und zweiten Herzfelds. Zusammengenommen sollte in Zukunft die Funktion von Zrf1 berücksichtigt werden, wenn molekulare Mechanismen von kardiovaskulären Krankheiten untersucht werden.

Weiterhin widmet sich die vorliegende Arbeit der Rolle von Zrf1 in invasivem Brustkrebs. Ein Zrf1 *Knockdown* in Brustkrebszellen bewirkt eine höhere Zellmobilität, eine verringerte Adhäsion und eine Ausbildung von Organoid-Strukturen. Ein Zrf1 *Knockdown* führt daher zu einer erhöhten Metastasierung *in vitro* und trägt ebenfalls zu einem Hormon-unabhängigen Wachstum der Zellen bei, einem Phänotyp den man gewöhnlich in aggresiven Formen des Brustkrebs findet. Eine Depletion von Zrf1 hebt die Balance der Expression von pro-apoptotischen und anti-apoptotischen Genen auf, wodurch es zu

einem Überleben der Zellen und Resistenz gegenüber Medikamenten kommen kann. Daher stellt Zrf1 eine neues *drug target* dar, welches neue Behandlungsstrategien eröffnen könnte.

Zrf1 controls mesoderm lineage genes and cardiomyocyte differentiation

INDEX OF CONTENT

1 INTRODUCTION 10

1.1 STEM CELLS 10

1.2 TRANSCRIPTIONAL REGULATION IN PLURIPOTENCY AND DIFFERENTIATION 12

1.2.1 CORE EMBRYONIC STEM CELL REGULATORY CIRCUITRY 12

1.2.2 CHROMATIN REGULATORS 13

1.2.3 BIVALENT CHROMATIN STATE 14

1.2.4 POLYCOMB GROUP PROTEINS 15

1.2.5 RECRUITMENT OF POLYCOMB GROUP PROTEINS 18

1.3 DIFFERENTIATION 19

1.3.1 EMBRYOGENESIS AND GASTRULATION 20

1.3.2 ECTODERM DEVELOPMENT 20

1.3.3 ENDODERM DEVELOPMENT 20

1.3.4 MESODERM DEVELOPMENT 21

1.3.5 HEART DEVELOPMENT (CARDIOGENESIS) 22

1.3.6 ANATOMY OF THE HEART 22

1.3.7 CELL PRECURSORS OF THE HEART 23

1.3.8 EARLY CARDIOGENESIS AND IDENTIFICATION OF HEART FIELDS 24

1.3.9 IMPORTANT SIGNALING PATHWAYS AND TRANSCRIPTION FACTORS IN CARDIOGENESIS 25

1.3.10 *IN VITRO* DIFFERENTIATION OF EMBRYONIC STEM (ES) OR EMBRYONIC CARCINOMA (EC) CELLS 34

1.4 ZRF1 AND ITS ROLE IN DIFFERENTIATION 36

2 AIM OF THE STUDY 38

3 MATERIAL AND METHODS 39
3.1 CELL CULTURE 39
3.1.1 E14TG2A ES CELLS 39
3.1.2 P19 TERATOCARCINOMA CELLS 39
3.1.3 HEK293T CELLS 39
3.1.4 GENERATION OF STABLE ES KNOCKDOWN AND RESCUE CELL LINES 39
3.1.5 GENERATION OF STABLE ZRF1 KNOCKDOWN P19 CELL LINES 40
3.2 *IN VITRO* DIFFERENTIATION 41
3.2.1 EMRBYOID BODIES 41
3.2.2 P19 CARDIOMYOCYTE DIFFERENTIATION 41
3.3 BEATING ASSAYS AND ANALYSIS 41
3.4 HISTOLOGICAL STAINING 42
3.4.1 FIXATION AND SECTIONING OF EBS 42
3.4.2 HEMATOXYLIN AND EOSIN STAINING 42
3.4.3 ALCIAN BLUE AND HEMATOXYLIN STAINING 43
3.4.4 OIL RED O STAINING 44
3.5 IMMUNOFLUORESCENCE STAINING AND ANALYSIS 44
3.6 RNA EXTRACTION, CDNA SYNTHESIS AND RT-QPCR 45
3.7 WESTERN BLOT 48
3.8 CHROMATIN IMMUNOPRECIPITATION 48
3.9 FLOW CYTOMETRY 51
4 RESULTS 53
4.1 KNOCKDOWN OF ZRF1 IN MESC PROVOKES DEFORMATION OF THE MESODERM 53

4.2 RE-ESTABLISHING ZRF1 EXPRESSION IN ZRF1 KNOCKDOWN CELLS RESCUES THE MESODERM PHENOTYPE 57
4.3 ZRF1 DEPLETION LEADS TO ABERRANT GENE EXPRESSION IN CARDIOMYOGENESIS RELATED GENES AND IMPAIRS THE EXPRESSION OF GENES SPECIFIC FOR CARDIAC SUBTYPES 61
4.4 ZRF1 CONTROLS THE TEMPORAL EXPRESSION OF CARDIOMYOGENESIS SPECIFIC GENES 64
4.5 ZRF1 IS ESSENTIAL FOR CARDIOMYOCYTE DIFFERENTIATION IN P19 CELLS 67
5 DISCUSSION 73
6 REFERENCES 76

INDEX OF FIGURES

INTRODUCTION

Figure 1. Stem Cell Hierarchy. 11
Figure 2. Chromatin during ES-cell differentiation. 13
Figure 3. Bivalent chromatin state of ES cells. 15
Figure 4. Classical PRC2 and PRC1 complexes. 16
Figure 5. Hierarchical models for recruitment of PcGs to chromatin. 19
Figure 6. Mesoderm derived tissues during gastrulation. 21
Figure 7. Cardiac Cell Types in Adult Human Heart. 22
Figure 8. Heart Progenitor Cells. 23
Figure 9. Four major stages of cardiogenesis in mouse. 24
Figure 10. Cellular hierarchy of cardiac progenitor cells and their lineage specification. 26
Figure 11. Roles of Wnt/β-catenin signaling during vertebrate heart development. 29
Figure 12. Summary of in vitro differentiation of ES cells and EC cells 35

RESULTS

Figure 1. Zrf1 knockdown cells have abnormal gene expression for the germ layer related genes. 54
Figure 2. Zrf1 knockdown derived EBs can't properly differentiate into structures important for germ layers. 55
Figure 3. Mesoderm is particularly effected at early differentiation of Zrf1 depleted cells. 56
Figure 4. Zrf1 re-expression partially restores the differentiation properties of knockdown cells. 58
Figure 5. Restoration of Zrf1 expression in Zrf1 knockdown ES cells rescues the mesoderm phenotype 59
Figure 6. Zrf1 knockdown cells can't properly differentiate into cardiomyoyctes during in vitro development. 60
Figure 7. Schematic illustration of cardiomyogenesis 61

Figure 8. Zrf1 controls the temporal expression of the genes related to cardiomyogenesis. 62
Figure 9. Zrf1 depletion affects the genes essential for the generation of atrium, ventricle and the nodal conduction system. 64
Figure 10. Zrf1 plays a direct role in the transcriptional activation of some cardiomyogenesis specific genes. 65
Figure 11. Zrf1 is specifically recruited the TSSs of its target genes at day 4 of differentiation. 66
Figure 12. P19 cells are capable of generating functional cardiomyoyctes. 68
Figure 13. Zrf1 functions early during P19 differentiation. 69
Figure 14: Zrf1 is essential for the cardiomyocyte differentiation in P19 cells. 71
Figure 15. Zrf1 is essential for cardiomyocyte differentiation in P19 cells. 72

INDEX OF TABLES

Table 1. Comparison of PRC1 and PRC2 complexes in *Drosophila melanogaster* and *Homo sapiens* with known functions. 17
Table 2. shRNA plasmids used for the cell line generations. 41
Table 3. Receipts for the solutions used in Hematoxylen and Eosin staining. 43
Table 4. Receipts for the solutions used in Alcian Blue and Hematoxylen staining. 44
Table 5. Receipts for the solutions used in Oil O Red staining. 44
Table 6. Antibodies used in immunofluorescence staining. 45
Table 7. Primers used for RT-qPCR experiments. 47
Table 8. Antibodies used in western blot experiments. 48
Table 9. Receipts for the buffers used in ChIP experiments. 51
Table 10. Primers used in ChiP-qPCR experiments 51

INDEX OF ABBREVIATIONS

ICM: Inner cell mass

mESC: Mouse embryonic stem cells

LIF: Leukemia inhibitory factor

MEFs: Mouse embryonic fibroblasts

gp130: Glycoprotein 130

JAK/STAT: Janus kinase/ Signal transduction and activation of transcription

PI3K: Phosphoinositide 3-kinase

SHP2: SH2 (Src homology 2) domain-containing tyrosine phosphatase

MAPK: Mitogen-activated protein kinase

PcG: Polycomb

TrX: Trithorax

EZH: Enhancer of zeste (E(z))

Esc: Extra sex combs

Suz12: Suppressor of Zeste 12

PCL: Polycomblike

Psc: Posterior sex combs

CBX: Chromobox protein homologue

Scm: Sex comb on midleg

H3K27me: Methylation of H3 at lysine 27

H3K4me: Methylation of H3 at lysine 4

H2AK119ub1: Histone H2A monoubiquitination at lysine 119

PRE: Polycomb responsive elements

CMC: Cardiogenic mesoderm cells

CNCC: Cardiac neural crest cells

PE: Proepicardium

FHF: First heart field

SHF: Second heart field

Flk-1: Fetal liver kinase-1

BMP: Bone morphogenic protein

TGF-β: Transforming growth factor-β

APC: Adenomatosis polyposis coli

Fzd: Frizzled

Lpr: Lipoprotein receptor related

Dkk1: Dickkopf1

FGF: Fibroblast growth factor

Eomes: Eomesodermin

Mesp1: Mesoderm posterior-1

Isl-1: Islet-1

MyocD: Myocardin

ECC: Embronic carcinoma cells

EB: Embryoid body

Zrf1: Zoutin Related Factor-1

NPC: Neural progenitor cells

H&E: Hematoxylen and Eosin

α-MHC: Alpha myosin heavy chain

β-MHC: Beta myosin heavy chain

MLC2a: Myosin light chain 2a

MLC2v: Myosin light chain 2v

Cx: Connexin

ANP: Atrial natriuretic peptide

CVD: Cardiovascular Disease

TSS: Transcription start site

1 INTRODUCTION

1.1 STEM CELLS

In 1961, Till JA and McCulloch A. injected bone marrow cells intravenously to previously irradiated mice and observed the formation of colonies of proliferating cells in the spleen of those animals. This was the first hint regarding the existence of some kind of special cell groups, today known as stem cells (Romito A. and Cobellis G. 2015; Till J.E. and McCulloch E.A., 1961). The isolation of murine embryonic stem cells (mESC) from the inner cell mass (ICM) of mouse blastocyst was accomplished in 1981 (Evans M.J. and Kauffman M.H., 1981; Martin G.R., 1981). Since then, the field of stem cell research expanded because of their capacity of wide range of application.

Stem cells are unspecialized cells which can generate special tissues or organs with unique features in response to particular physiological or experimental conditions. Their definition is based on three important properties: pluripotency, self-renewal and limitless proliferation. With their self-renewal and limitless proliferation capacities, stem cells can divide for long periods maintaining their progenitor cell properties without differentiation. At the same time, they are capable of existing from self-renewal and can program themselves into all kinds of specialized cell types deriving from the three germ layers (ectoderm, mesoderm and endoderm) (Keller G.M., 1995; Morrison S.J. et al., 1997; Smith, A.G. 2001; Till J.E. and McCulloch E.A., 1980; Weissman I.L., 2000; He S. et al., 2009)

After the fusion of sperm and egg gametes during fertilization, a diploid zygote which has the ability to generate an entire organism is formed. This so called totipotency capacity is maintained until the eight cell stage of the morula. Subsequently, cell differentiation leads to formation of the blastocyst stage that is characterized by the presence of a blastocyst cavity, outer cell mass (outer trophoblast cells) and inner cell mass (ICM). Whereas the cells in the ICM are no longer totipotent, they retain the ability to develop into all cell types of the embryo (pluripotent). Embryonic stem (ES) cells are derived from the inner cell mass of the blastocyst (Figure 1) (Wobus A.M. and Boheler K.R., 2005; O'Connor T.P. and Crystal R.G., 2006). ES cells can generate all cell types

of the body *in vivo* and *in vitro* cell culture except extraembryonic trophoblast lineage (Jaenisch R. and Young R. 2008).

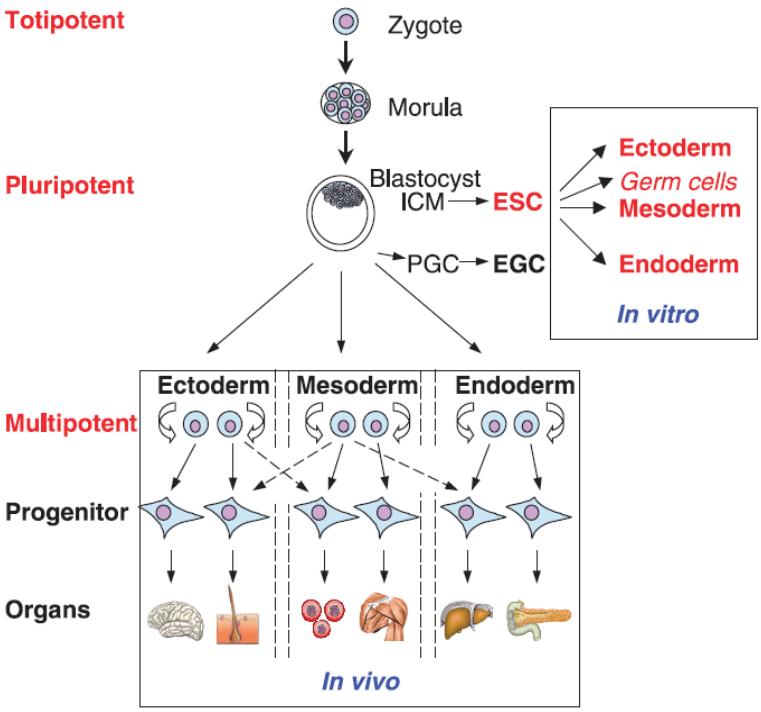

Figure 1. Stem Cell Hierarchy. From zygote to early cell division stages of the morula are defined as totipotent. At the blastocyst stage, only the cells in the inner cell mass (ICM) retain the capacity to generate all three primary germ layers (ectoderm, mesoderm, endoderm) and the primordial germ cells (PGC), the founder cells of male and female gametes. Multipotent cells can give rise all cell types only in one lineage (Wobus A.M. and Boheler K.R., 2005).

Initially generation of murine embryonic stem cells (mESC) required a monolayer of inactivated mouse embryonic fibroblasts (MEFs) in the presence of the serum (Robertson E.J., 1987). Therefore it was reasoned that somehow fibroblasts are able to provide critical factors to maintain pluripotency state. Leukemia inhibitory factor (LIF) was identified as a responsible protein for the maintenance of self-renewal of mESCs and the inhibition of differentiation (Smith A.G. and Hooper M.L. 1987; Smith A.G. et al., 1988; Williams R.L. et al., 1988).

LIF is a soluble glycoprotein which belongs to the interleukin (IL)-6 family of cytokines. This family contains eight cytokines and all of them use glycoprotein 130 (gp130) as a signal transducer. The LIF/gp130 receptor interaction on the cell surface activates three signaling pathways: 1. the JAK (Janus kinase)/ STAT3 (signal transduction and

activation of transcription 3) 2. the PI3K (phosphoinositide 3-kinase)/ AKT 3. the SHP2 [SH2 (Src homology 2) domain-containing tyrosine phosphatase 2]/ MAPK (mitogen-activated protein kinase) (Niwa H. et al., 1998; Hirai H. et al., 2011). Interestingly in serum free conditions, LIF is not sufficient to block neural differentiation and maintain pluripotency. It was much later revealed that the serum component BMP4, is essential to sustain self-renewal in the presence of LIF, by inducing the expression of Id proteins via the Smad pathway (Ying Q.L. et al., 2003).

1.2 TRANSCRIPTIONAL REGULATION IN PLURIPOTENCY AND DIFFERENTIATION

1.2.1 CORE EMBRYONIC STEM CELL REGULATORY CIRCUITRY

Due to their unique features, stem cells hold great promise from basic research to regenerative medicine. Hence it is fundamental to understand the underlying mechanism of self-renewal and pluripotency to achieve the clinical usage of stem cells.

The gene expression program of pluripotency, also known as molecular circuitry of pluripotency is controlled by specific transcription factors, chromatin modifying enzymes, regulatory RNA molecules, and signal transduction pathways (Jaenisch R. and Young R., 2008). Among many other transcription factors (TFs), Oct4, Nanog and Sox2 come into prominence and the pluripotent state is mainly regulated by three of them (Loh K.M. and Lim B., 2011; Thomson M. et al., 2011). Oct4 and Nanog are two homeodomain TFs identified as essentials for early development and identity of pluripotent cell population in mammalian embryo (Chambers I. et al., 2003; Hay D.C. et al., 2004; Matin M.M. et al., 2004; Mitsui K. et al., 2003; Nichols J. et al., 1998; Zaehres H. et al., 2005). However Oct4 is considered to be the most upstream gene of the molecular circuitry of pluripotency (Jaenisch R. and Young R., 2008). Because Oct4 deficient embryos can’t develop a proper pluripotent inner cell mass and these cells can’t differentiate into extraembryonic endoderm (Nichols J. et al., 1998). Nanog, on the other hand, is described as a stabilizer of pluripotent state rather than being essential for the maintenance of pluripotency (Chambers I. et al., 2007). Deletion of Nanog causes early embryonic lethality and Nanog deficient ICM fails to generate epiblast and only differentiate into parietal endoderm-like cells (Mitsui K. et al., 2003). The

contribution of Sox2 in pluripotency is partially attributed to its function to regulate Oct4 levels (Masui S. et al., 2007). Because Oct4 can activate its own expression through a positive auto-regulatory loop with Sox2 (Okumura-Nakanishi S. et al., 2005). Genome wide analysis of Oct4, Nanog and Sox2 showed that these three TFs bind together at their own promoters and often co-occupy their target genes by forming an interconnected auto-regulatory loop (Boyer L.A. et al., 2005; Loh Y.H. et al., 2006). They can occupy both actively expressed genes and repressed genes which are poised for differentiation (Boyer L. A. et al., 2005).

1.2.2 CHROMATIN REGULATORS

Emerging data suggest the importance of the epigenetic regulation for the maintenance of self-renewal and pluripotency of ES cells. These epigenetic regulations include various mechanisms from nuclear architecture, chromatin structure, and chromatin dynamics to histone modifications (Loden M. and van Steensel B., 2005). The spatial organization of chromatin into higher-order structure promotes the genome regulation. Chromatin structure can influence gene function in two ways: 1. changing the accessibility of regulatory proteins to their target sites, 2. modifying the affinity of transcriptional regulators with their targets. ES cells seem to exhibit a higher-order global chromatin structure (Figure 2) (Meshorer E. and Misteli T., 2006).

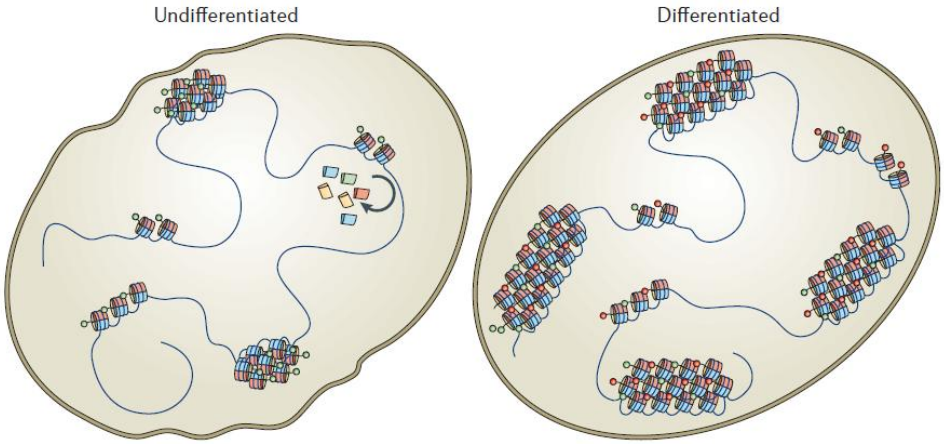

Figure 2. Chromatin during ES-cell differentiation. In pluripotent embryonic stem (ES) cells (left), chromatin is globally decondensed, enriched in active histone marks (green circular tags), and contains loosely bound architectural chromatin proteins. When cells differentiate (right), tightly packed chromatin regions (heterochromatin) form, silencing histone marks (red circular tags) accumulate, architectural proteins become more stable (Meshorer E.and Misteli T., 2006).

1.2.3 BIVALENT CHROMATIN STATE

The chromatin organization is largely maintained by the structural chromatin proteins, which are prominently referred as the core and linker histones. According to 'beads on a string' model, 147 bp of DNA occupy one nucleosome octomer unit which consists of two pairs of each of H2A-H2B and H3-H4 core histone dimers. Core histones provide structural backbone and are largely regulated by post-translational covalent histone modifications such as methylation, acetylation, phosphorylation, ubiquitylation and sumoylation. The protruding N-terminal tails of the core histones are subjects to those kind of posttranslational modifications (Alberts B. et al., 2002). Histone modifications can serve as docking sites for proteins and can recruit other factors to relevant genomic loci. Charged modifications, such as lysine acetylation, can promote transcriptional activation by loosening the chromatin structure (Kouzarides T., 2007). Among histone modifications, histone H3 lysine 4 (H3K4) and lysine 27 (H3K27) methylations are of particular interest. They can contribute to maintenance of an epigenetic memory for lineage-specific expression or repression of important genes over cell divisions (Ringrose L. and Paro R., 2004). Lysine 4 methylation encourages transcriptionally active chromatin by recruiting nucleosome remodeling enzymes and histone acetylation (Santos-Rosa H. et al., 2003; Pray-Grant M.G. et al., 2005; Wysocka J. et al., 2005). Lysine 27 methylation, on the other hand, promotes a transcriptionally inactive chromatin by causing a compact chromatin structure (Francis N.J. et al., 2004; Ringrose L. et al., 2004). In ES cells, the promoters of important developmental genes exhibit a bivalent chromatin. These promoters contain both activating (H3K4 methylation) and repressive marks (H3K27 methylation) at the same time. Hence, chromatin structure can be kept in a poised state until a differentiation signal occurs. Upon differentiation signal, the genes that are important for development lose their repressive marks, retain in an active state and are transcribed. On the other hand, genes, which are responsible for pluripotency, lose their activating marks, retain in a repressed state and are not transcribed (Figure 3) (Bernstein B.E. et al., 2006; Schuettengruber B. and Cavalli G., 2009).

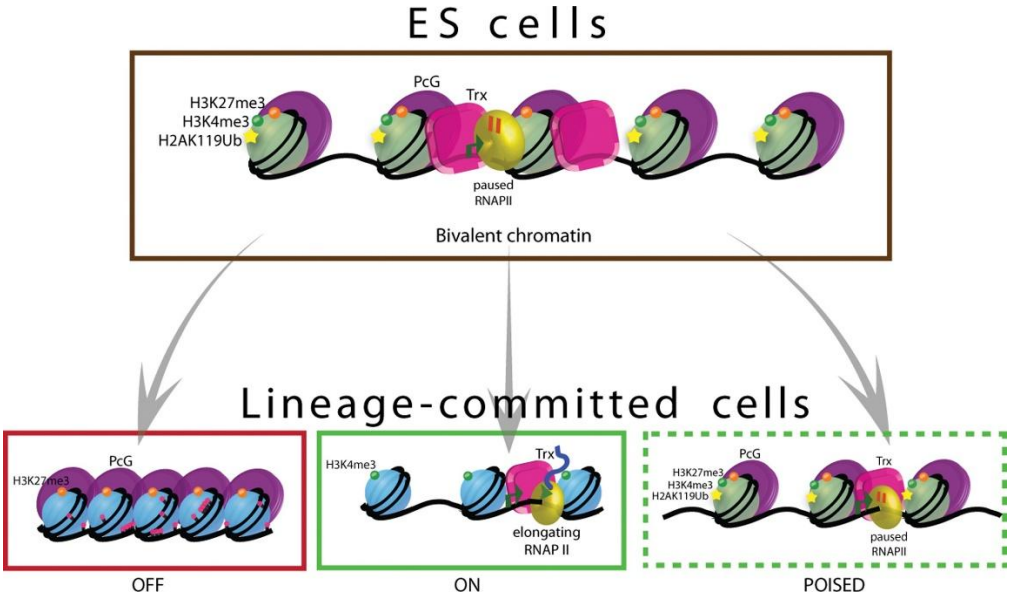

Figure 3. Bivalent chromatin state of ES cells. Bivalent chromatin domains mark the promoters of developmentally important genes in pluripotent ES cells. Polycomb (PcG) and Tritorax (TrxG) group proteins play critical role in the regulation of bivalent chromatin state. While PRC2 (Polycomb repressive complex 2) catalyze the tri-methylation of histone H3 on lysine 27 (H3K27me3), TrxG catalyzed the tri-methylation of Histone H3 on lysine 4 (H3K4me3). In addition, PRC1 (Polycomb repressive complex 1) is recruited to many of these genes and can mono-ubiquitinylate histone H2A on lysine 119, a modification that is also thought to be important for gene silencing. Hence, bivalent genes are kept in silenced but poised state. Upon differentiation, the bivalent histone marks can be resolved to monovalent modifications in which the gene is "ON" or "OFF". Bivalent domains can also be maintained or newly established in lineage-committed cells (Sha K. and Boyer L.A., 2009).

1.2.4 POLYCOMB GROUP PROTEINS

Polycomb (PcG) group proteins are a special group of proteins which assist the maintenance of bivalent chromatin state of ES cells by repressing the expression of the differentiation genes, thus govern the pluripotency (Bracken A.P. and Helin K., 2009; Sauvageau M. and Sauvageau G., 2010; Schwartz Y.B. and Pirrotta V., 2007; Simon J.A. and Kingston R.E., 2009). Polycomb proteins were first discovered *in Drosophila melanogaster* as regulators of *Hox* genes which encode transcription factors for the proper development of the anterior-posterior axis of the body plan (Duncan D.M. et al. 1982; Lewis E.B., 1978). PcG mutants were found to exhibit defects in axis specification and body patterning (Jürgens G., 1985; Schwartz Y.B. and Pirrotta V., 2007) indicating the importance of PcG-mediated repression of gene expression. Recent findings revealed that PcG proteins can regulate numerous developmental factors and signaling pathways besides *Hox* genes (Simon J.A. and Kingston R.E, 2013).

PcG proteins are found in large multi-protein complexes; the two best characterized are Polycomb repressive complex 1 (PRC1) (Saurin A.J. et al., 2001; Shao Z. et al., 1999) and Polycomb repressive complex 2 (PRC2) (Cao R. et al., 2002; Czermin B. et al., 2002; Kuzmichev A. et al., 2002; Müller J. et al., 2002) (Figure 4). Each complex is composed of several proteins with different biochemical functions, many of which are not well understood. In mammals, PRC2 complex consists of four core components: EZH1/2, SUZ12, EED and RbAp46/48 (also known as RBBP7/4). Mammalian PRC1 contains several homologs of each of the *Drosophila* components: five CBX homologs (CBX2/4/6/7/8), two ubiquitin ligases (RING1A/B), six PCGF family members (PCFG1-6) and three PHC family members (Table 1) (Di Croce L. and Helin K., 2013; Laugesen A. and Helin K., 2014).

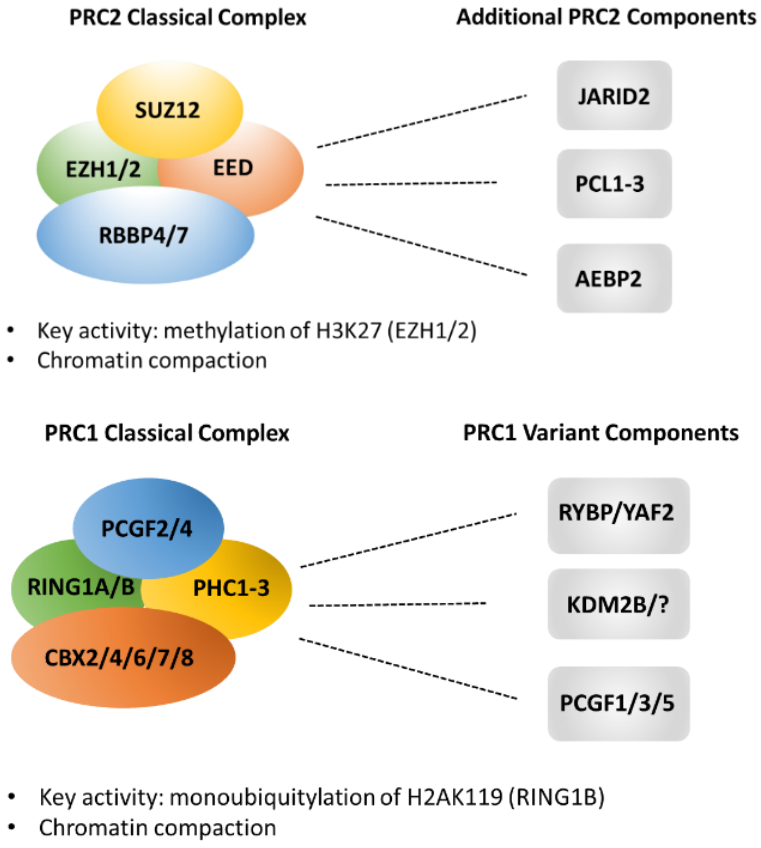

Figure 4. Classical PRC2 and PRC1 complexes. The core component of PRC2 consists of EZH1/2, SUZ12, EED and RBP4/7. EZH1/2 subunit is responsible for the methylation H3K27. With addition of other components, PRC2 facilitates chromatin compaction. The core component of PRC1 consists of RIGB1A/B, PCGF2/4, PHC1-3 and CBX/2/4/6/7/8. RING1A/B subunit is responsible for monoubiquitylation of H2AK119. Like PRC2, PRC1 also contributes to chromatin compaction.

***Drosophila melanogaster* subunits**	**Homologous subunits in *Homo sapiens***	**Function**
PRC2	**PRC2**	**PRC2**
Enhancer of zeste (E(z))	Enhancer of zeste homologue 2 (**EZH2**=KMT6) and **EZH1**	Methylation of H3 at lysine 27 (H3K27)
Extra sex combs (Esc) and Extra sex combs-like (Escl)	Embryonic ectoderm development (**EED**)	Stimulation of Lysine 27 methylation
Suppressor of Zeste 12 (Su(z)12)	**SUZ12**	Unknown, required for ES cell differentiation
Chromatin assembly factor 1 subunit Caf1	Histone-binding protein **RBBP4** (=RBAP48) and **RBBP7** (=RBAP46)	Histone chaperone
Jing	Zinc-finger protein **AEBP2**	
Polycomblike	**PCL1** (PHF1), **PCL2** (MTF2) and **PCL3** (PHF19)	
	Jarid 2	
PRC1	**PRC1**	**PRC1**
E3-ubiquitin-protein ligase RING1 (=Sce)	RING2 (=**RING1B** and RNF2) and RING1 (=**RING1A** and RNF1)	Monoubiquitination of H2A at lysine 119
Posterior sex combs (Psc) and Suppressor of Zeste 12 (Su(z)12)	BMI1 (=**PCGF4**) and MEL18 (=**PCGF2**)	Unknown, required for self-renewal
Polyhomeotic-proximal (Ph-p) and Polyhomeotic-distal (Ph-d)	Polyhomeotic-like protein 1 (**PHC1**=EDR1), **PHC2** (=EDR2) and **PH3** (=EDR3)	Unknown
Polycomb (Pc)	Chromobox protein homologue 2 (**CBX2**), **CBX4**, **CBX6**, **CBX7** and **CBX8**	Chromodomain proteins, bind H3K27me3
Sex comb on midleg (Scm)	Sex comb on midleg homologue 1 (SCMH1) and Sex comb on midleg-like protein 2 (SCMH2)	

Table 1. Comparison of PRC1 and PRC2 complexes in *Drosophila melanogaster* and *Homo sapiens* with known functions (Modified from Beisel C. and Paro R., 2011).

Drosophila Sce and mammalian RING1B are ubiquitin E3 ligases that are responsible for the monoubiquitylation of histone H2A at lysine 119 (H2AK119ub1). This histone mark promotes chromatin compaction that is often observed within nuclear foci called PcG bodies (Bantignies F. et al., 2011; Sexton T. et al., 2012).The compact state of

chromatin mediates transcriptional repression (Cao R. et al., 2005; Wang H. et al., 2004) by reducing the accessibility of TFs and ATP-dependent chromatin-remodeling machineries (Bantignies F. et al. 2011; Di Croce L. and Helin K., 2013).

1.2.5 RECRUITMENT OF POLYCOMB GROUP PROTEINS

Although the exact mechanism of Polycomb recruitment hasn't been fully understood, there are several different mechanisms that have been suggested. In *Drosophila*, PcG group proteins are recruited to chromatin via specific cis-regulatory DNA elements, called Polycomb response elements (PREs). PREs are shown to function as general silencer elements of PcG mediated transcriptional repression (Sengupta A.K. et al., 2004; (Schuettengruber B. and Cavalli G., 2009). The genome wide analysis of DNA binding elements for PREs indicates that the combination of these factors are responsible for the recruitment of PcG proteins (Margueron R. and Reinberg D., 2011). However in mammals, such PREs don't exist as seen in *Drosophila*. For PRC2 recruitment, some GC enriched sequences (CpG islands) are identified, but these sequences alone don't point a common response element (Ku M. et al., 2008; Mendenhall E.M. et al., 2010). Yin Yang 1 (YY1) protein may be regarded as a possible PcG recruiter for mammals which mimics the PREs in *Drosophila*. Yet limited overlap between YY1 and PRC2 target genes (Squazzo S.L. et al., 2006) suggests a role for YY1 as one of the upstream regulators of PRC2 rather than a general recruiter function (Ku M. et al., 2008; Margueron R. and Reinberg D., 2011). Growing evidence pinpoints a key role for non-coding RNAs (ncRNA) as important participants in PRC2 function (Simon J.A. and Kingston R.E., 2009).

According to classical or canonical hierarchical model, after recruitment of PRC2 complex to its target genes, the catalytic subunit of PRC2, EZH1/2 marks the H3K27 trimethylation (Kuzmichev A. et al., 2002). This mark which is believed to be a prerequisite for PRC1 binding, leads to recruitment of PRC1 complexes via protein interactions. Then E3 ligase subunit of PRC1, RING1B catalyzes the monoubiquitination of histone H2A (H2AK119ub1) (Figure 5) (Cao R.et al., 2005; Wang H. et al., 2004) that results in chromatin compaction. Thereby two Polycomb group proteins acting together

mediates transcriptional silencing and ensures epigenetic maintenance through H3K4me3 (Comet I. and Helin K., 2014).

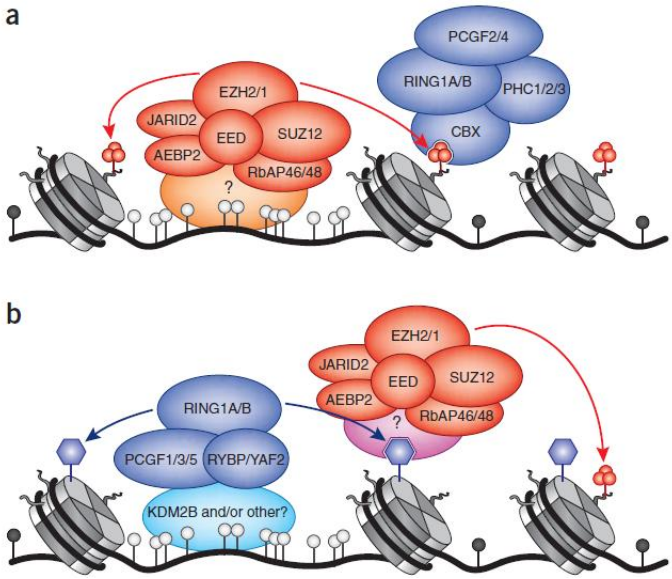

Figure 5. Hierarchical models for recruitment of PcGs to chromatin. a) Classical model for PcG recruitment. PRC1 is recruited to chromatin through recognition of H3K27me3 via its CBX subunit. b) New hierarchical model for PcG recruitment. PRC1 variants are recruited to unmethylated CpG islands, leading to H2AK199ub1 deposition and recruitment of PRC2 via a yet unresolved mechanism (Comet I. and Helin K., 2014).

However recent findings suggest a more complicated hierarchical model for PcG group protein recruitment. Interestingly, tethering of variant PRC1 complexes (PCGF1, 3, 5) to chromatin leads to recruitment of PRC2 complex and concomitant H3K27 trimethylation whereas canonical PRC1 complexes (PCGF2 or 4) don't lead to such recruitment. Experiments done in RING1B-PCGF4 fusion proteins revealed that H2AK119ub1 is sufficient to trigger PRC2 recruitment (Blackledge N.P. et al., 2014). Moreover Cooper et al. showed that this recruitment via H2AK119ub1 is affected by DNA methylation (Cooper S. et al., 2014). In this case PRC1 exists in a variant form containing PCGF1, RYBP or YAF2 and KDM2B (Figure 5) (Comet I. and Helin K., 2014).

1.3 DIFFERENTIATION

Early mammalian development has always been an exciting topic for scientists as the findings in this field can open new windows for regenerative medicine. In this concept, establishment of embryonic stem cells lines from mouse (Evans M.J. and Kauffman

M.H., 1981; Martin G.R., 1981) and human (Thomson J.A. et al., 1998) embryos is regarded as one of the major breakthroughs for developmental biology. The ease use of unlimited, pluripotent, renewable ES cells enables the investigation of early events taking place during early development. With identification of specific genes and pathways that are involved in embryonic development, it will be possible to differentiate ES cells into all kinds of cell type in culture conditions and later use them for cell replacement therapy.

1.3.1 EMBRYOGENESIS AND GASTRULATION

Embryogenesis is the process of cell division and cellular differentiation of the embryo that occurs during the early stages of development. It starts with the fertilization of the egg and sperm cells which forms one-celled zygote and continues with the division and the cleavage of zygote. Subsequently these cleavages result in the formation of morula which consists of blastomeres inside and blastocyst with a cavity inside zona pellucida. Blastocyst contains an embryoblast (or inner cell mass) and a trophoblast which will eventually give rise to germ layers of the embryo and the extra-embryonic tissues, respectively (Figure 1) (Boklage C.E., 2010). Embryogenesis continues with gastrulation when single-layered blastocyst is reorganized into a three-layered structure known as the gastrula. These germ layers are known as ectoderm, mesoderm and endoderm. Each germ layer develops into internal organs of the organism with a process called organogenesis (Pansky B. and Gilbert S.F., 2000).

1.3.2 ECTODERM DEVELOPMENT

The ectoderm which from the outer layer of very early embryo gives rise to the central nervous system (the brain and spinal cord); the peripheral nervous system; the epidermis and its appendages; the sensory epithelia of the eye, ear and nose; the mammary glands; the hypophysis; the subcutaneous glands; and the enamel of the teeth (Pansky B. and Gilbert S.F., 2000).

1.3.3 ENDODERM DEVELOPMENT

The endoderm which emerges from the innermost layer of the embryo gives rise to the epithelial lining of the gastrointestinal and respiratory tracts; the parenchyma of the

tonsils, the liver, the thymus, the thyroid, the parathyroids, and the pancreas; the epithelial lining of the urinary bladder and urethra; and the epithelial lining of the tympanic cavity, tympanic antrum, and auditory tube (Pansky B. and Gilbert S.F., 2000).

1.3.4 MESODERM DEVELOPMENT

The mesoderm layer appears in the third week of embryonic development and lies between the outer germ layer ectoderm and the inner germ layer endoderm. During gastrulation mesoderm develops into three different compartments: the paraxial mesoderm, the intermediate mesoderm and the lateral plate mesoderm (Figure 6).

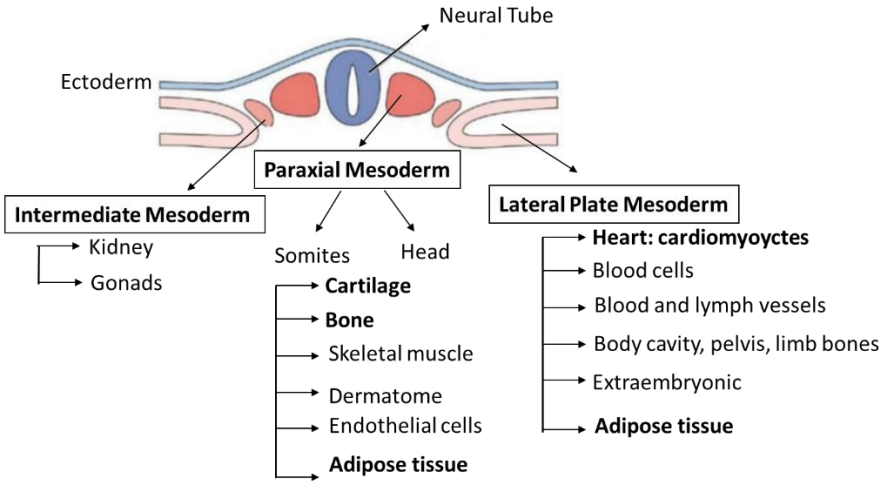

Figure 6. Mesoderm derived tissues during gastrulation. Mesoderm develops into three different compartments during gastrulation: the paraxial mesoderm, the intermediate mesoderm and the lateral plate mesoderm. Generally, the paraxial mesoderm gives rise to the head and somites; the lateral plate mesoderm gives rise to the cardiovascular system; the intermediate mesoderm gives rise to the urogenital structures.

The paraxial mesoderm gives rise to the head and somites including cartilage, bone, skeletal muscle, endothelial cells and dermatome. The intermediate mesoderm which connects the paraxial and lateral plate mesoderm gives rise to the urogenital structures consisting of the kidney and gonads. The lateral plate mesoderm gives rise to all circulatory system including the heart muscles (cardiomyoyctes), blood cells, blood and lymph vessels, extraembryonic, body cavity, pelvis and limb bones (Rupert E.E. et al., 2004; Gilbert S. 2010) (Figure 6). It is generally suggested that adipocyte tissue develops from the paraxial mesoderm with contributions from the somites and lateral plate mesoderm (Atit R. et al., 2006; Gesta S. et al., 2007). Although it has been

suggested that adipose tissue can be differentiated from neural crest cells (Billon N. et al., 2007), there are some studies suggesting that is not valid for all the adipose tissue derivatives (Wrage P.C. et al., 2008).

1.3.5 HEART DEVELOPMENT (CARDIOGENESIS)

1.3.6 ANATOMY OF THE HEART

The heart is a muscular organ that pumps the blood to your body through the circulatory system by rhythmic contraction and dilation. It is located between the right and left lungs, in the middle of the chest and slightly towards the left of the breastbone. The heart lies in a double walled fibroserous sac called the pericardial sac. The heart wall is composed of three layers: epicardium (the outer lining of the cardiac chambers), myocardium (the intermediate layer of the heart) and endocardium (the innermost layer of the heart). A functional heart contains four distinct chambers (left and right atrium, left and right ventricule); four valves (aortic, mitral, tricuspid, and pulmonary); cardiac conduction system (purkinje fiber, sinoatrial node and atrioventricular node); coronary arteries, cardiac veins, smooth muscle and endothelial cells of the coronary arteries (Figure 7) (Shah S. et al., 2009).

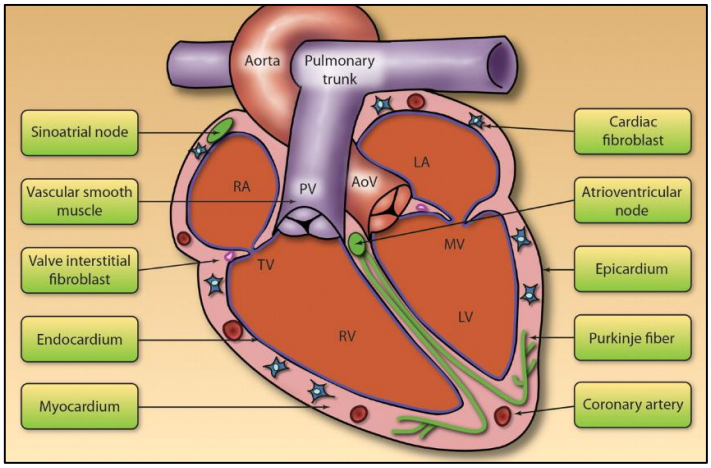

Figure 7. Cardiac Cell Types in Adult Human Heart. The heart is composed of endocardium, myocardium, and epicardium. Both ventricular and atrial region are filled with myocardium and cardiac fibroblasts along with the coronary vasculature. The 4 cardiac valves are surrounded by valve endothelium. The valve annulus and vascular wall of the aorta and pulmonary trunk are predominantly made up of smooth muscle cells. The cardiac conduction system mainly consists of purkinje fiber, atrioventricular and sinoatrial nodes. RA: right atrium; TV: tricuspid valve; RV: right ventricle; LV: left ventricle; MV: mitral valve; LA: left atrium; AoV: aortic valve; PV: pulmonary valve.

1.3.7 CELL PRECURSORS OF THE HEART

The heart comprises both muscular and non-muscular cells. One of the major questions regarding the heart development is to fully understand where the progenitor cells originate from and how they terminally differentiate into specific cell types of the heart.

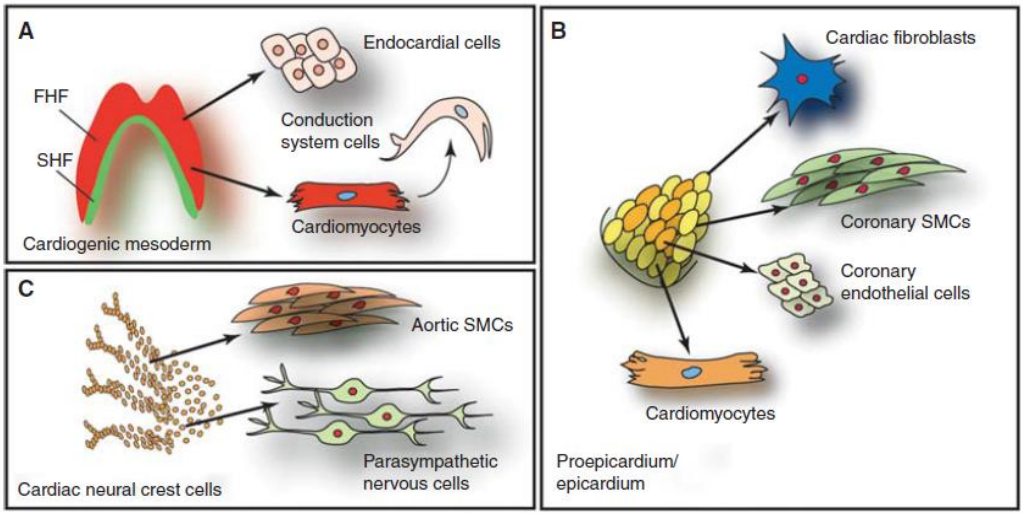

Figure 8. Heart Progenitor Cells. The precursor cells of the heart contribute to different cardiac compartments during heart morphogenesis in mouse development. A) Cardiogenic mesoderm, B) Proepicardium/epicardium, C) Cardiac neural crest cells. FHF: first heart field; SHF: second heart field; SMC: smooth muscle cells (Brade T. et al., 2013).

In the developing embryo, three major sources of heart cell precursors have been identified: the cardiogenic mesoderm cells (CMC), the cardiac neural crest cells (CNCC) and the proepicardium (PE). Each of these precursors represents a spatially and temporally distinct pool of cells which give rise to all cell types of the heart tissue e.g. atrial and ventricular myocytes from cardiogenic mesoderm; aorta smooth muscle cells from cardiac neural crest (Laugwitz K.L. et al., 2008; Brade T. et al., 2013). The cardiogenic mesoderm which harbors so-called first and second heart fields (FHF, SHF respectively), is mostly responsible for the generation of the cardiomyocytes. At the same time, it contributes to the endocardium, conduction system and the aortic and pulmonary cushions. Cardiac neural crest cells give rise to the smooth muscle cells of the outflow tract as well as the autonomous nervous system of the heart. Proper CNC development is also essential for the cardiac valve development and the heart septation. Finally the proepicardium cells differentiate into cardiac fibroblasts in the

myocardium, vascular smooth muscle cells of the coronary vessels, endothelial cells of coronary vessels and some cardiomyocytes (Figure 8) (Brade T. et al., 2013).

1.3.8 EARLY CARDIOGENESIS AND IDENTIFICATION OF HEART FIELDS

The mesoderm derived heart is the first organ to develop in order to supply increasing oxygen and nutrient demands of the growing embryo. Cardiogenesis begins with mesoderm formation via gastrulation (Roche P. et al., 2013).

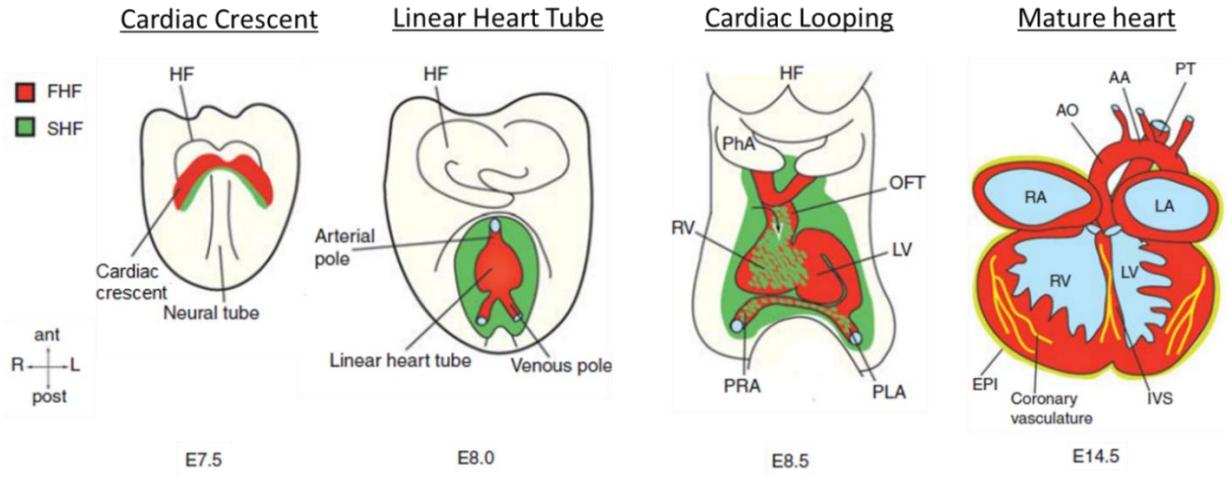

Figure 9. Four major stages of cardiogenesis in mouse. At E7.5, cardiac progenitor cells form the cardiac crescent comprising the FHF and SHF at the midline of the embryo. At 8.0 the cardiac crescent fuses and give rise to the beating, linear heart tube. After the addition of SHF derived cells, the linear heart tube undergoes rightward looping at E8.5. Finally cardiac neural crest and proepicardial cells complete their contribution to the heart and at E14.5 fully septated four chambered heart is finally generated. AA: Aortic arch; ant: anterior; AO: dorsal aorta; EPI: epicardium; FHF: first heart field; HF: headfolds; IVS: interventricular septum; L: left; LA: left atrium; LV: left ventricle; OFT: outflow tract; PE: proepicardium; PhA: pharyngeal arch; PLA: primitive left atrium; post: posterior; PRA: primitive right atrium; PT: pulmonary trunk; R: right; RA: right atrium; RV: right ventricle; SHF: second heart field; SMCs: smooth muscle cells; ven: ventral (Modified from Brade T. et al., 2013).

The naïve cardiogenic mesoderm cells arising from the anterior lateral mesoderm (Lawson K.A. et al., 1991; Tam P.P. et al., 1997; Abu-Issa R. et al., 2007) migrate away from the primitive streak (PS) and merge in an anterior-lateral direction to generate so-called splanchnic mesoderm. These progenitor cells on both sides of the embryo form the cardiac crescent which comprise the first heart field (FHF) and the second heart field (SHF) (E7.5) (Buckingham M. et al., 2005). At E8.0, the cardiac crescent fuses at the midline and give rise to the FHF-derived linear heart tube. Subsequently, this tube starts beating and undergoes rightward looping followed by a series of septation and fusion event (E8.5-9.5) (Zaffran S. et al., 2004). After addition of SHF derived cells

which originate from the pharyngeal mesoderm, CCNCs, epicardial and endocardial cells to the arterial and venous poles of the linear heart, the generation of the four-chambered mature heart is completed (Figure 9) (Buckingham M. et al., 2005; Kelly R.G. et al., 2012; Brade T. et al., 2013; Mjaatvedt C.H. et al., 2001; Moorman A. et al., 2013; Waldo K.L. et al., 2001; Brade T. et al., 2013).

1.3.9 IMPORTANT SIGNALING PATHWAYS AND TRANSCRIPTION FACTORS IN CARDIOGENESIS

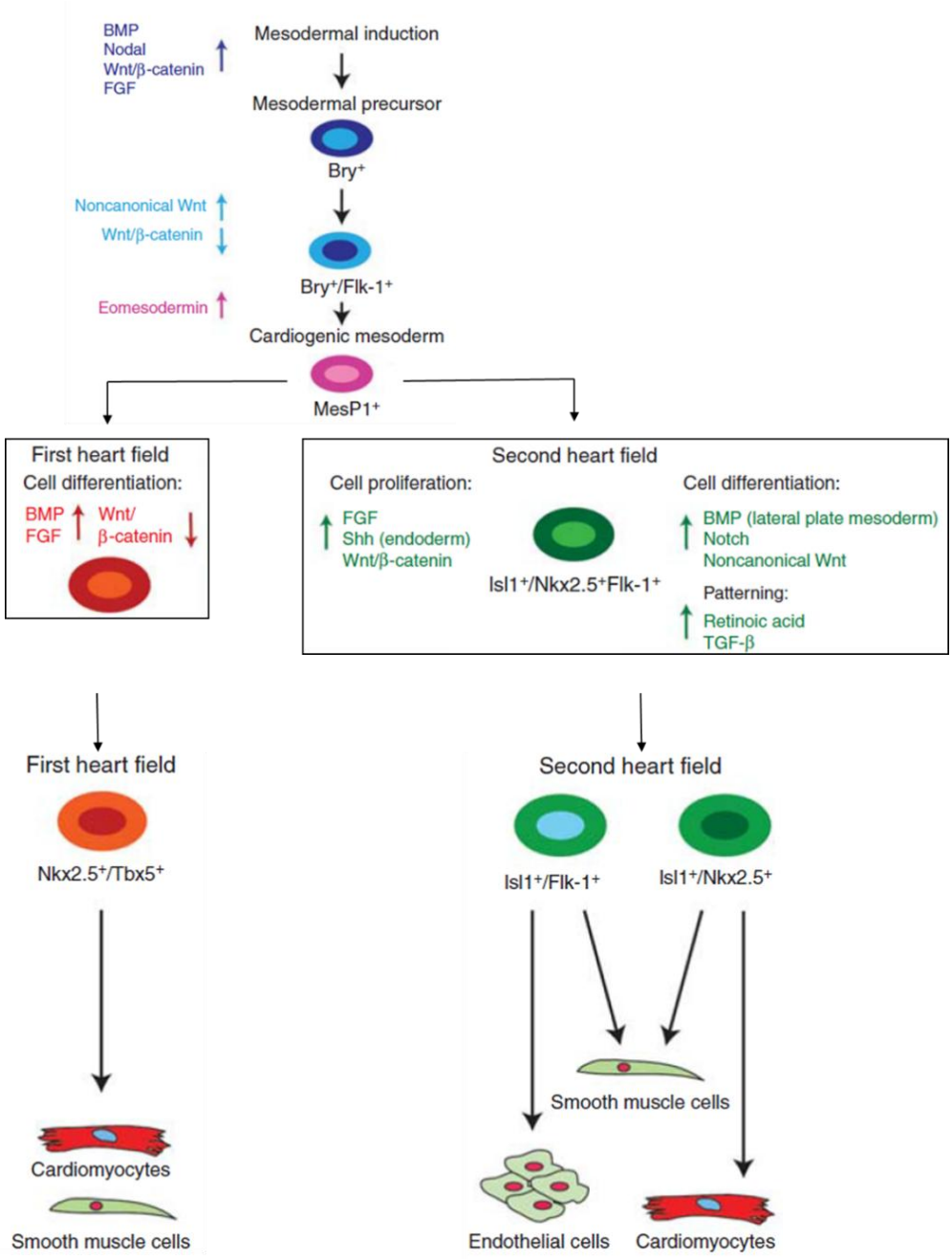

Figure 10. Cellular hierarchy of cardiac progenitor cells and their lineage specification. Induction of mesoderm by several signaling pathways (BMP, Nodal, Wnt/β-catenin, FGF) leads to formation of mesodermal precursors. After downregulation of Wnt/β-catenin signaling and induction of non-canonical Wnt signaling, Brachyury and Flk-1 (fetal liver kinase-1) positive progenitors appear. Eomesodermin signaling promotes cardiogenic mesoderm specification from these mesodermal precursors. Cardiogenic mesoderm is marked by the expression of mesoderm posterior 1 (Mesp1). Early mesoderm-derived cardiac precursors differentiate into first heart field (FHF) and second heart field precursors. FHF progenitors start to differentiate upon BMP and FGF action toward cardiomyocytes and smooth muscle cells. SHF progenitors which are marked by Isl-1^{+}/Nkx2.5^{+}/Flk-1^{+}, divide into two subpopulations. One population marked by the expression of Isl-1 and Flk-1 differentiates into endothelial cells and smooth muscle cells, whereas a second popultion of Isl-1 and Nkx2.5 positive precursors provide smooth muscle cells and cardiomyocytes as well as contributing to the proepicardial lineages which later form cardiac fibroblasts (CF), smooth muscle cells (SMCs), endothelial cells (EC), and cardiomyocytes (CM) (Modified from Brade T. et al., 2013).

The proper development of heart tissue relies on specific orchestrated roles of signaling pathways and cardiogenic transcription factors, most of which are evolutionarily conserved. After induction of mesoderm by several signaling pathways, Brachyury and Flk-1 (fetal liver kinase-1) positive progenitors appear. These progenitors give rise to cardiogenic mesoderm which is marked by the expression of mesoderm posterior 1 (Mesp1). Subsequently, early mesoderm-derived cardiac precursors differentiate into first heart field (FHF) and second heart field (SHF) precursors. FHF and SHF progenitors later differentiate into all cell types within the mature heart (Figure 10) (Brade T. et al., 2013).

1.3.9.1 SIGNALING PATHWAYS

1.3.9.1.1 Nodal Signaling

The Nodal signaling pathway is essential for early embryonic patterning in vertebrates. Nodal is a signaling molecule that belongs to the transforming growth factor-β (TGF-β) family and functions through core TGF-β receptors to activate a Smad transcription factor signaling cascade. (Shen M.M. et al., 2007). Unlike TGF-β signaling pathway, the Nodal signaling requires additional co-receptors, Cripto and Cryptic, to activate intracellular signaling (Shen M.M. et al., 2002). In addition, Nodal-dependent activation of TGF-β receptors is negatively regulated by the proteins of Lefty family, specifically by Lefty1 and Lefty2 (Chen C. and Shen M.M., 2004).

The Nodal signaling plays a critical role in germ layer formation, anterior-posterior axis patterning during gastrulation and left-right axis determination in the developing embryo (Brennan J. et al., 2002; Conlon F.L. et al., 1994). Improper Nodal signaling leads to

aberrant organogenesis and left-right patterning problems that result in a wide range of congenital defects in organs including the heart (Ralston M. B. and Black B.L., 2016). Mutant mice for *Tdgf1* gene which encodes Cripto, lack a primitive streak, fail to form embryonic mesoderm and exhibit anterior-posterior axis defect (Gritsman K. et al., 1999). Conditional deletion of Nodal in the lateral plate mesoderm in mice results in transposition of the great arteries of the heart (Kumar A. et al., 2008).

1.3.9.1.2 BMP Signaling

Bone morphogenetic proteins (BMPs) are growth factors that represent the largest subfamily of the transforming growth factor-beta (TGF-β) superfamily (Ashe H.L., 2005). BMPs are involved in many important cellular processes such as proliferation, differentiation, migration and apoptosis both during and after early development. The BMPs, particularly BMPs 2, 4, 5, 6, 7 and 10 are implicated in the heart and play an essential role for heart development (Lyons K.M. et al., 1995; Neuhaus H. et al., 1999).

BMP2 is initially expressed in the extraembryonic mesodermal cells and promyocardium. Later, its expression is detected in the outer myocardial cells of the antrioventricular (AV) canal and outflow tract (Zhang H. and Bradley A., 1996; Lee, K.Y. et al., 2007). BMP2 knockout mice show a displaced heart to the exocoelomic cavity (Zhang H. and Bradley A., 1996; Lee K.Y. et al., 2007) and BMP2 conditional knockout mice show severe defects in AV cushion morphogenesis since BMP2 is required for the induction of endocardial epithelial-mesenchymal transformation of the AV myocardium (Ma L. et al., 2005).

BMP4 is initially expressed in the extraembryonic ectoderm and later in the extraembryonic mesoderm (Fujiwara T. et al., 2002). BMP4 gene knockout in mice is lethal and leads to complete loss of mesoderm formation except a small portion of animals who manage to reach the beating heart stage (Winnier G. et al., 1995). During heart development, BMP4 is expressed in the sinus venosus, dorsal midline of the atrium and AV canal, splanchnic and branchial arch mesoderm (Liu W. et al., 2004). BMP4 is required for endocardial cushion development and for normal septation of the OFT. Conditional inactivation of BMP4 leads to atrioventricular canal defect which is one of the most common human congenital heart abnormalities (Jiao K. et al., 2003).

During heart development, the cardiac progenitor cells in the primitive streak reside together with BMP antagonist Chordin. Later these progenitor cells migrate into the anterior later plate mesoderm where another BMP antagonist Noggin is present (Streit A. et al., 1998; Yuasa S. et al., 2005). These colocalizations of cardiomyocyte progenitor cells and BMP antagonists suggest that BMPs inhibit cardiac development and that BMP antagonists promote cardiac development. Interestingly, this transient inhibition of BMP signaling in early developmental stage strongly induces cardiomyocyte induction from murine ES cells (Yuasa S. and Fukuda K., 2008; Yuasa S. et al., 2005). All these data collectively suggest that BMPs have dual role during cardiomyocyte development. The spatial and temporal control of BMPs and BMP antagonists are crucial for the proper development of cardiomyoyctes.

1.3.9.1.3 Wnt Signaling

Wnt proteins are encoded by Wnt genes that are defined by their sequence homology to *wingless* in *Drosophila* and *int-1* in the mouse. They are secreted lipid-modified glycoproteins which regulate crucial aspects of development, including cell-fate specification, proliferation, survival, migration and adhesion (MacDonald B.T. et al., 2009; Logan C.Y. and Nusse R., 2004). Many of these effects are mediated by the well characterized canonical Wnt/β catenin pathway. In the absence of Wnt, cytoplasmic β catenin is phosphorylated and subsequently degraded by the destruction complex consisting of the scaffolding protein axin, tumor suppressor protein adenomatosis polyposis coli (APC), and the serine/threonine kinase GSK-3β (Stamos J.L. and Weis W.I., 2013). However upon binding of Wnt to a co-receptor complex that consists of seven transmembrane receptors of the frizzled (Fzd) family and the lipoprotein receptor related 5/6 (Lrp5/6) proteins, cytoplasmic β catenin is stabilized, accumulates in the nucleus and activates its target genes through interaction with LEF/TCF family transcription factors (Angers S. and Moon R.T., 2009; MacDonald B.T. and He X., 2012).

Wnt ligands and receptors together with the Frizzled family of receptors have been detected in the mesoderm of the heart-forming fields, cardiac neural crest cells and adult heart. Early functional analysis in chicken and *Xenopus* embryos indicated an

inhibitory role of the canonical Wnt/β catenin pathway during myocardial specification. Whereas inhibition of canonical Wnt signaling pathway by Wnt inhibitor dickkopf (Dkk) or other Wnt inhibitors results in ectopic cardiomyocyte formation, overexpression of Wnt3a or Wnt8 in X blocks cardiogenesis in *Xenopus* (Schneider V. and Mercola M., 2001). Similarly, inhibition of Wnt/β catenin pathway is required for early cardiogenesis in chicken (Marvin M.J. et al., 2001; Tzahor E. and Lassar A.B., 2001). However recent publications in zebrafish, mouse embryos and mouse and human embryonic stem cells (hESCs) have revealed a dual role for Wnt/β-catenin signaling during vertebrate heart development. According to this model, Wnt/β-catenin pathway induces cardiac specification during early developmental stages and later it inhibits the cardiogenesis (Gessert S. and Kuhl M., 2010**;** Ueno S. et al., 2007; Klaus A. et al., 2007; Naito A.T. et al., 2006; Paige S.L. et al., 2010). In accordance with this model, early treatment of differentiating mouse or human ES cells with Wnt ligands enhances cardiomyoycte formation via promotion of mesoderm specification. On the other hand, later treatment of ES cells with the Wnt inhibitor Dickkopf1 (Dkk1) promotes cardiomyocyte differentiation. Likewise, the cardiomyocyte progenitor cell marker Mesp1 drives cardiac differentiation of ES cells via directly activating Dkk1 expression (Figure 11) (David R. et al., 2008).

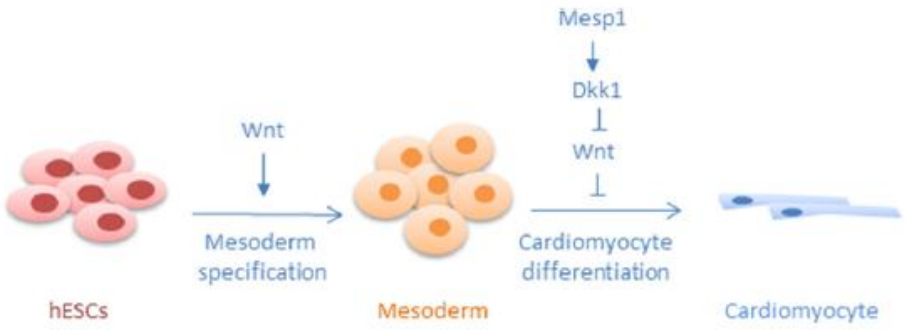

Figure 11. Roles of Wnt/β-catenin signaling during vertebrate heart development. Wnt/β-catenin signaling is required for heart development in a biphasic manner: while the activation of the pathway promotes mesoderm specification in early phases of hESC differentiation, it hampers cardiomyocyte differentiation at later stages. This late-stage suppression can act through the cardiac differentiation inducer Mesp1, which activates the Wnt inhibitor Dkk1 (Ozhan G. and Weidinger G., 2015).

1.3.9.1.4 FGF Signaling

Fibroblast growth factors (FGFs) are a large family of secreted polypeptides that regulate the establishment of cardiomyocyte number (Zaffran S. and Frasch M., 2002). They are thought to signal in a dose-dependent manner through receptor tyrosine kinases (Böttcher R.T. and Niehrs C., 2005). Studies in *FGFR* (*heartless*) mutant *Drosophila* reveals the critical roles of FGR in mesoderm migration and in cardiac fate assignment of FGFR both in mesoderm migration and in cardiac fate assignment (Michelson A.M. et al., 1998). Both key cardiogenic transcription factors Nkx2.5 and Gata4 are not expressed in FGF8 (acerebellar) mutant zebrafish (Reifers F. et al., 2000). FGF and BMP signals cooperate during cardiac induction. FGF8 is capable of inducing cardiac mesoderm together with BMP2 and mouse embryos lacking BMP4 also exhibit a loss of FGF8 expression (Fujiwara T. et al., 2002). Similarly, *in vitro* studies in FGFR1 knockout embryoid bodies confirm the roles of FGFs as the embryoid bodies fail to express cardiac genes and do not form contractile foci (Dell'Era P. et al., 2003).

1.3.9.2 TRANSCRIPTION FACTORS

1.3.9.2.1 Brachyury and Eomes

The T-box transcription factor Brachyury is a key regulator in formation of the mesoderm and the notochord in vertebrate embryos (Herrmann B.G. et al., 1990; Wilkinson D.G. et al., 1990; Evans A.L. et al., 2012). Upon induction by Wnt/β catenin signaling, Brachyury marks the mesodermal cells ingressing through the primitive streak (Showell T. et al., 2004). These mesodermal cells generate two distinct cell populations: Brachyury^{+}/ Flk-1^{+} and Brachyury^{+}/ Flk-1^{-}. After inhibition of canonical Wnt/β catenin signaling and activation of non-canonical Wnt signaling, Brachyury^{+} mesodermal progenitor cells are committed towards a cardiogenic fate (Gessert S. and Kuhl M., 2010). Brachyury^{+}/ Flk-1^{+} progenitors within the cardiogenic mesoderm down-regulates the Brachyury expression and activates T-box transcription factor Eomesodermin (Eomes). Brachyury (David R. et al., 2011) and Eomes (Costello I. et al., 2011) acting together induce the expression of Mesp1 which has been described as the ‘‘master regulator’’ of cardiac progenitor specification (Bondue A. et al., 2008).

1.3.9.2.2 Mesp1

Mesoderm posterior 1, Mesp1, is a basic helix-loop-helix transcription factor (Saga Y. et. al., 1996) which is established in high hierarchical regulator of cardiovascular system (Saga Y. et al., 1999; Kitajima S. et al, 2000; Saga Y. et al., 2000; Bondue A. et al., 2008; David R. et al., 2008; Lindsley R.C. et al., 2008). According to the cell fate mapping studies, Mesp1 first appears in both nascent and extraembryonic mesoderm within the primitive streak (Saga Y. et. al., 1996). Later its expression is detected in the common progenitors of myocardium, endocardium and the vascular system. Mesp1 is accepted as the earliest molecular marker for cardiac lineages. $Mesp1^{+}$ cells can generate major cardiovascular cell types including cariomyocytes, vascular smooth muscle cells and endothelial cells, and they contribute to the myocardium, endocardium and epicardium as well (Bondue A. et al., 2008; David R. et al., 2008; Lindsley R.C. et al., 2008; Bondue A. et al., 2010). Mesp1 knockout mice display a morphogenetic abnormality of the heart, cardia bifida due to delayed migration of cardiac progenitor cells. However initial inhibition of cell migration is rescued by the expression of Mesp1 orthologue Mesp2. Mesp1 and Mesp2 double knockout embryos die without developing heart. Moreover these embryos lack a clear embryonic mesodermal layer between the endoderm and ectoderm layers. Abnormal cell accumulation is observed in the primitive streak of double knockout embryos because mesodermal cells can't migrate from the primitive streak. These data indicate that Mesp1 and Mesp2 act together during early gastrulation and are essential for the mesoderm development (Kitajima S. et al., 2000; Saga Y. et al., 2000).

1.3.9.2.3 Nkx2.5

Nkx2.5/Csx is a homeodomain-containing transcriptional activator (Komuro I. and Izumo S., 1993; Lints T.J. et al., 1993) originally identified as a mammalian homolog of *Drosophila* "*tinman*" (Bodmer R. et al., 1993). A mutant version of this gene exhibits a complete loss of heart formation in *Drosophila* underlining the importance of *tinman* in heart development (Bodmer R. et al., 1993). Similarly in mice, loss of Nkx2.5 results in embryonic lethality with failure of cardiac looping and myocardial defects. Moreover the expression of several cardiac genes including *MLC2v*, *ANP*, *Mef2c*, and *Hand1* was reduced in the heart of Csx/Nkx2-5–deficient embryos (Lyons I. et al., 1995; Tanaka M.

et al., 1999). In humans, Nkx2.5 mutations have been linked to a variety of congenital heart diseases including septation, alignment, compaction and cardiac conduction defects (Schott J.J. et al., 1998; Goldmuntz E. et al., 2001; Elliott D.A. et al., 2003; Kasahara H. et al., 2004; Hirayama-Yamada K. et al., 2005; Sarkozy A. et al., 2005; Draus J.M. et al., 2009; Stallmeyer B.G. et al., 2010; Ouyang P. et al., 2011; Costa M.W. et al., 2013). During embryogenesis, Nkx2.5 expression is activated in the cardiac mesoderm by multiple inducing signals such as BMP, FGF and stage-specific canonical Wnt signaling (Zaffran S. et al., 2002), and its transcriptional activity is enhanced through physical interaction with other transcription factors such as Gata4 and Tbx5 (Durocher D. et al., 1997; Zhu W. et al., 2000; Hiroi Y. et al., 2001; Garg V. et al., 2003). Nkx2.5 can form multiprotein complex with Gata4 and Tbx5 to regulate a subset of downstream genes involved in cardiac development (Belaguli N.S. et al., 2000; Sepulveda J.L., et al., 1998).

1.3.9.2.4 Hand1 and Hand2

Hand1 (eHAND) and Hand2 (dHAND) are two basic helix-loop-helix transcription factors which are in the downstream of Nkx2.5. They are essential for the proper development of the left and right ventricular myocardium. Hand1 is highly expressed in left ventricle and Hand2 is highly expressed in right ventricle (McFadden D.G. et al., 2005). Targeted mutation of Hand2 in mice results in embryonic lethality caused by right ventricular hypoplasia and vascular malformations (Srivastava D. et al., 1997; Yamagishi H. et al., 2000). Hand1-null mice cause embryonic lethality along with a cardiac development arrest (Firulli A.B. et al., 1998). Overexpression of the same gene *in vivo* results in an extended heart tube (Risebro C.A. et al., 2006). It is also important to note that Hand1 expression and cardiac looping are abolished in Nkx2.5-null mice (Biben C. and Harvey R.P., 1997).

1.3.9.2.5 Tbx5

T-box transcription factor Tbx5, another interactor of Nkx2.5, is a critical transcription factor in formation of linear heart tube, cardiac looping, chamber specification, chamber septation, and cardiomyocyte differentiation (Bruneau B.G. et al., 2001; Hiroi Y. et al., 2001; Liberatore C.M. et al., 2000). Tbx5 expression is graded with the linear heart tube

formation and further restricted to the atria and left ventricle (Bruneau B.G. et al., 1999). Embryonic mice lacking Tbx5 have abnormal heart tube formation with hypoplastic atria. On contrary, overexpression of Tbx5 inhibits the ventricular maturation (Bruneau B.G. et al., 2001). Mice double heterozygous for Tbx5 and Gata4 die because of impaired ventricular myocardium and atrial septal defects (Maitra M. et al., 2009). Tbx5 physically interacts with Nkx2.5 in order to control gene expression in cells of the cardiac conduction system (Bruneau B.G. et al., 2001; Hiroi Y.et al., 2001)

1.3.9.2.6 Gata4

The zinc finger transcription factor Gata4 plays a critical role in the regulation of cardiac differentiation and morphogenesis in a dosage dependent manner. Disruption of Gata4 in mice result in failure of midline fusion of the heart primordia and abnormal ventral folding, which leads to embryonic lethality (Heikinheimo M. et al., 1994; Kuo C.T. et al., 1997; Molkentin J.D. et al., 1997). Interestingly, for normal heart development, Gata4 expression is required in the underlying endoderm rather than cardiac mesoderm itself (Molkentin J.D. et al., 1997; Charron F. and Nemer M., 1999; Watt A.J. et al., 2004; Zeisberg E.M. et al., 2005). Gata4 can directly regulate other transcription factors including Mef2c, Hand2 and Gata6 (Bruneau B.G. et al., 2001) and a wide spectrum of cardiac-specific genes such as myosin heavy chain, myosin light chain 1/3, cardiac troponin C, cardiac troponin I and atrial natriuretic peptide (Molkentin J.D., 2000; Kuo C.T. et al., 1997; Molkentin J.D. et al., 1997; Liang Q. and Molkentin J.D., 2002).

1.3.9.2.7 Isl1

Islet-1 (Isl-1) is a LIM homedomain contaning protein (Tanizawa Y. et al, 1994) that plays a critical role in the cell fate determination of second heart field (Roche P. et al. 2013). Isl-1 is initially suggested as a specific marker for only SHF and its derivatives, whereas recent findings suggest a common progenitor role for Isl-1 in heart development. Isl-1 is one of the first cardiac transcription factors to be expressed, and its expression is detected in the progenitors of both FHF and SHF lineages during development in chicken, *Xenopus* and mice (Yuan S. and Schoenwolf G.C., 2000; Brade T. et al., 2007; Abu-Issa R. and Kirby M.L., 2008; Prall O.W. et al., 2007). Isl-1^{+} progenitor cells contribute to cardiomyocyte, smooth muscle and endotheial cells in the

right ventricle, outflow tract, the right ventricle, parts of the atria and the inner curvature of the left ventricle (Cai C.L.. et al. 2003; Sun Y. et al. 2007; Bu L. et al.,2009). Additionally, Isl-1^{+} progenitors give rise to vascular smooth muscle cells and endothelial cells (Bu L. et al., 2009) and Isl1 can mark the cardiac neural crest derivatives as well (Engleka K.A. et al., 2012). Isl-1 knockout mice completely lose the outflow tract, right ventricle, and much of the atria. Disruption of Isl-1 negatively affects cell migration, proliferation and survival of the SHF progenitors (Cai C.L. et al., 2003).

1.3.9.2.8 MyocD

Myocardin (MyocD) is a muscle lineage–restricted transcriptional coactivator. MyocD expression is detected in the cardiac crescent and subsequently in the embryonic mesoderm and postnatal heart (Parmacek M.S., 2007). Knockdown of MyocD in *Xenopus* results in inhibition of cardiac development and the absence of expression of cardiac differentiation markers with disruption of expression of cardiac differentiation markers (Small E.M. et al., 2005). Deletion of MyocD in the adult mouse heart leads to dilated cardiomyopathy and heart failure (Huang J. et al., 2009). Recent studies suggest a potential regulatory mechanism for MyocD and BMP10 signaling pathway in cardiac growth, chamber maturation and embryonic survival (Huang J. et al., 2012).

1.3.10 *IN VITRO* DIFFERENTIATION OF EMBRYONIC STEM (ES) OR EMBRYONIC CARCINOMA (EC) CELLS

Embryonic stem cells (ESCs) hold great promises as they can differentiate into all types of cells in the body. Up to now, various methods using either 2D or 3D culture systems are described for ES cell differentiation towards all three germ layers. One of the classical way of ES cell differentiation is to use of so-called embryoid bodies (EBs). EBs are cellular aggregates of ES cells which can mimic morphogenic steps occurring in three dimension in the growing embryo. Differentiation of ES cells into EBs can be done in several different ways. The most common one is the withdrawal of LIF from the ES cell medium, and later culture of ES cells in suspension in bacterial grade petri dishes. Because ESCs can’t adhere to the petri dishes, they begin to form cell clusters consisting of differentiating cells. The drawback of this method is the generation of a heterogeneous EB population varying in both shape and size which have further impact

on cell lineage commitment. A second method of generating EBs is to culture ES cells in ‘hanging drops’. In this method, drops containing the same amount of ES cells are placed on the lid of a petri dish. Over time ES cells form similar size of EBs at the bottom of the each drop because of the gravity effect (Brickman J.M. and Serup P., 2016). Whether formed via suspension or hanging drop, culturing of embryoid bodies in suspension over 10 days leads to cell commitment towards ectoderm, mesoderm and endoderm lineages (Figure 12). As a consequence, they begin to exhibit the phenotypes of committed lineages. For example in the case of mesoderm lineage commitment and subsequent cardiomyocyte differentiation, they begin to beat spontaneously.

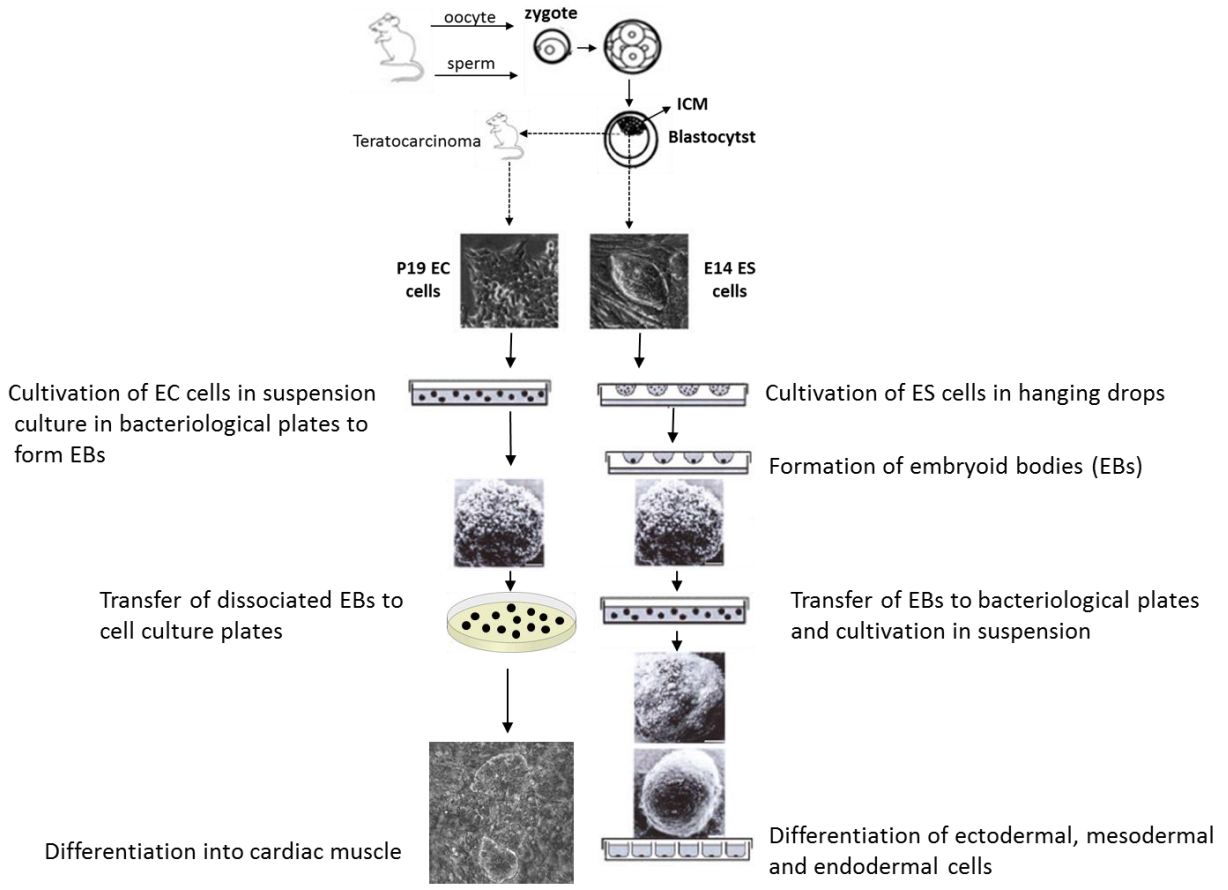

Figure 12. Summary of *in vitro* differentiation of ES cells and EC cells. Cultivation of either EC cells in suspension or ES cells in hanging drops leads to formation of EBs. Further maintenance of EBs results in commitment towards the three germ layers (Modified from Boheler K.R. 2002).

P19 cells represents one of the best model system to study early events of cardiogenesis. They are originated from a teratocarcinoma induced in C3H/HeHa mice and are capable of forming cardiac muscle cells efficiently upon 0.5-1 % DMSO treatment (Edwards M.K.S. et al., 1983; McBurney M.W. et al., 1982). Successful differentiation of P19 cells into cardiac myocytes requires initial aggregation of P19 cells into EBs (McBurney M.W. et al., 1982). Meanwhile the cells are exposed to DMSO which results in a transient increase in intracellular calcium levels that could trigger downstream signaling events essential for cardiac muscle differentiation (Morley P. and Whitfield J.F., 1993). Then EBs are dissociated into single cells, and the single cells are cultured under adherent conditions without DMSO treatment until they start to beat spontaneously (Figure 12). Characterization of the resulting cardiomyocytes is essential for the further studies. Typically the first sign of successful differentiation is the appearance of contractile foci in the culture. This phenotype requires further characterization of cardiac-specific contractile proteins such as cardiac troponin T (cTnT) by flow cytometry. RT-PCR evaluation of a variety of cardiac genes such as alpha myosin heavy chain (*α-MHC*), beta myosin heavy chain (*β-MHC*), myosin light chain 2a (*MYL2a*), myosin light chain 2v (*MYL2v*) or immunolabeling of myofilament proteins provide more evidence for the determination of faithful cardiomyocyte differentiation. With the assessment of the electrophysiological properties, the capacity to generate action potential and release intracellular Ca^{+2}, *in vitro* differentiated cardiomyocytes can be regarded as functional cardiomyocytes similar to the ones in the heart (Mummery C.L. et al., 2012).

1.4 ZRF1 AND ITS ROLE IN DIFFERENTIATION

The Zuotin-related factor 1, Zrf1 (also termed MPP11, MIDA1 and Dnajc2) has recently been identified as an epigenetic regulator of gene transcription in stem cells and cancer (Aloia L. et al., 2015). Upon differentiation signal, Zrf1 specifically binds to monoubiquitinated histone H2A, displaces PRC1 from the chromatin and facilitates the expression of its target genes in NT2 cells. ChIP-on-chip experiments conducted in the same cell line revealed that most of the target genes of Zrf1 are involved in development and differentiation, including genes in some signaling pathways such as

WNT, TGF and EGF; or transcription factors such as helix-loop-helix TFs, Pou-domain TFs and homeobox genes (Richly H. et al., 2010).

As a multifunctional protein, Zrf1 plays a crucial role in several processes, including stem cell maintenance, cell-fate decisions, differentiation, senescence and carcinogenesis In all these processes, Zrf1 functions as a chromatin-associated factor (Aloia L. et al., 2015). For example Zrf1 homologue GlsA is crucial for asymmetric cell division and germ cell specification in algae (Miller S.M. and Kirk D.L., 1999; Cheng Q. et al., 2005; Pappas V. Miller S.M., 2009). Zrf1 *C. elegans* ortholog dnj11 is involved in asymmetric cell division of it was shown that Zrf1 is required to establish neural progenitor cells (NPCs) from mESCs and to maintain NPC self-renewal (Aloia L. et al., 2014). Neuronal differentiation triggered by Zrf1 is partially regulated by Id1, which interacts with Zrf1 and blocks its recruitment to chromatin (Aloia L. et al., 2015).

2 AIM OF THE STUDY

Up to now, Zrf1 was described as a regulator of neuronal differentiation and was shown to contribute to the generation of ectoderm-derived lineages. However, not much is known about its involvement in the regulation of the other germ layers (endoderm and mesoderm). Given the high abundance of H2A-ubiquitylation and the genome-wide distribution of PRC1 complexes at genes of all three germ layers (Bracken A.P. and Helin K., 2009) we reasoned that Zrf1 might control the differentiation of the other germ layers. Previous studies pointed at a potential role of Zrf1 in the mesoderm-derived hematopoietic lineage as elevated Zrf1 expression was found in leukemic blasts (Greiner J. et al., 2003). Hence we sought to investigate the following:

1) Does ZRF1 have any impact on development of germ layers besides ectoderm?

2) If so, is there a specific phenotype that Zrf1 depletion might cause in this germ layer and what is the underlining molecular mechanism of the observed phenotype?

3 MATERIAL AND METHODS

3.1 CELL CULTURE

3.1.1 E14TG2A ES CELLS

E14Tg2A ES cells were cultured in feeder-free conditions in cell culture dishes coated with 0.1% gelatin. Gelatin solution was produced by overnight stirring of powder gelatin (Sigma) in MQ water at 75°C, followed by sterile filtering. Before plating of the cells, dishes were coated with the required volume of gelatin solution, enough to cover the dish surface (5 ml in 10 cm dishes), and incubated for at least 30 min at 37 °C in Forma™ Steri-Cult™ CO2 incubator (Thermo Scientific). Before plating of the cells, excess gelatin was removed from dishes and fresh medium was immediately added. Cells were cultured in Glasgow Minimum Essential Medium (Sigma) supplemented with 15% PanSera ES Bovine Serum (PAN-Biotech), Non-Essential Amino Acids (Gibco), Sodium Pyruvate (Gibco), L-Glutamine (Gibco), Penicillin/Streptomycin (Gibco), β-mercaptoethanol (Sigma) and Leukemia Inhibitory Factor (LIF). Cells were passaged every second day and their medium was exchanged on a daily basis. Depending on the cell line, the passage ratio varied from 1/8 to 1/4.

3.1.2 P19 TERATOCARCINOMA CELLS

The P19 cells were cultured in Dulbecco's Modified Eagle Medium (Gibco) supplemented with 10% Fetal Bovine Serum (Gibco), L-Glutamine (Gibco) and Penicillin/Streptomycin (Gibco). Cells were passaged in every 2nd to 3rd days and their medium was exchanged on a daily basis.

3.1.3 HEK293T CELLS

HEK293T cells were cultured in Dulbecco's Modified Eagle Medium (Gibco), supplemented with 10% Standard Fetal Bovine Serum (Gibco), L-glutamine and Penicillin/Streptomycin in 15 cm dishes. They were passaged in every 2nd to 3rd day.

3.1.4 GENERATION OF STABLE ES KNOCKDOWN AND RESCUE CELL LINES

For the production of lentiviruses containing shRNA, HEK293T cells were grown overnight in 10 cm dishes and the next day the medium was replaced with OPTIMEM

low serum medium (Gibco), two hours prior to transfection. For the transfection, 15 µg shRNA, 5 µg pMDLg/pRRe, 5 µg pRSV-Rev and 5 µg pMD2.G plasmids were mixed with 500 µl OPTIMEM and 43 µg lipofectamine 2000 (Life Technologies) with OPTIMEM. 5 min later plasmids were mixed with lipofectamine and 10 min later the mixture was added to the HEK293T cells. 9 hours post-transfection, the OPTIMEM was replaced with 6 ml complete stem cell medium and the day after, the medium containing the viral particles was collected and passed through a 0,45 µm filter (Millipore). 2 mL of filtered medium containing the viral particles was added for transduction to $2x10^5$ stem cells in a 6 well plate (pre-incubated with 8 µg/ml polybrene (Sigma) for 2 hours) and the plates were centrifuged for 90 min at 1200 rpm at room temperature. 2 ml fresh fresh medium was added per well and cells were incubated overnight. The same procedure was repeated 3 more times after which the cells were left to recover for 48 hrs. Knockdown cells were selected with 2 µg/mL puromycin (Sigma) for 3 days and then frozen or analyzed for RNA or protein expression. After thawing, cells were selected with up to 8 µg/mL puromycin. For rescue experiments, human Zrf1 cDNA cloned pCBA-3xFlag plasmid (Aloia L. et al 2014) was transfected into shZrf1 cells using Lipofectamine 2000. Prior to transfection, $3x10^5$ cells were seeded in 1 well of a 6 well plate with complete medium lacking antibiotic. Next day, medium was replaced with OPTIMEM low serum medium (Gibco) two hours before transfection. For the transfection, 5 µg plasmid and 15 µl lipofectamine 2000 (Life Technologies) were prepared in 500 µl OPTIMEM. After 5 min, plasmids and lipofectamine were mixed, and incubated 20 min at room temperature. Later the mixture was added to the Zrf1 knockdown cells. 5 hours later, cells were split in two 10 cm plates and left to recover overnight. Following day, the medium was changed and cells were selected with 500 µg/ml geneticin (Santa Cruz-G418). Cells were kept on selection during all experiments.

3.1.5 GENERATION OF STABLE ZRF1 KNOCKDOWN P19 CELL LINES

Stable Zrf1 knockdown and control cell lines was established using commercial shZrf1 plasmids “TRCN0000365853” and “TRCN0000365925” together with a non-mammalian control (shNMC) plasmid from Sigma. Transfection was performed according to the protocol established in E14 cells. 5 µg shRNA or shNMC plasmid and 15 µl

lipofectamine 2000 were used to transfect the cells and 4 µg/ml puromycin was used for selection.

Name	Company	Sequence
shNMC: Mission pLKO.1-puro	Sigma	
shZrf1: TRCN0000365853	Sigma	CCGGAGAAGATGATCTGCAATTATTCTCGAGAATA ATTGCAGATCATCTTCTTTTTTG
shZrf1: TRCN0000365925	Sigma	CCGGCAATGAGGCAGACCGTGTTAACTCGAGTTA ACACGGTCTGCCTCATTGTTTTTG

Table 2. shRNA plasmids used for the cell line generations.

3.2 *IN VITRO* DIFFERENTIATION

3.2.1 EMRBYOID BODIES

E14Tg2A embryoid bodies (EBs) were formed with the hanging-drop method, starting with 10^3 mESCs / 30 µL drop, in medium without LIF. 48 hours after the drop formation, EBs were collected and cultured in suspension in the bacteriological plates from that point. The medium was replaced every second day and the experiment is maintained until day 10 to day 16. In every two day starting from EB day 2, microscopy images were acquired with a Leica DM-IL microscope.

3.2.2 P19 CARDIOMYOCYTE DIFFERENTIATION

To induce cardiac differentiation, a total of $3x10^5$ P19 cells in 10 ml complete medium with 1 % DMSO (Sigma) were cultured in suspension in the bacteriological plates to form embryoid bodies for 4 days. The formed EBs were then transferred to gelatin coated 6-well tissue culture plates and maintained in complete medium free of DMSO for an additional 11 days. The medium was replenished every 48 hours and microscopy images were acquired either with Leica DM-IL or Leica AF7000 microscopes.

3.3 BEATING ASSAYS AND ANALYSIS

The numbers of spontaneously beating EBs derived from E14 shNMC and shZrf1 cell lines were counted in every 2 days under an inverted-light microscope starting from day 10 to day 16. For each experiment, at least 100 EBs from each cell type were counted.

The beating frequency was calculated as “Beating EB number/Total EB number” and represented in a time course.

The spontaneous beating areas formed in P19 control and Zrf1 knockdown cells were recorded with either a Leica DM-IL or Leica AF7000 microscope at day 12 and day 15. To quantify the beating areas, differences between the consecutive frames in each movie were calculated. The differences between images were smoothed with a Gaussian filter and the triangle method threshold was applied to segment into beating and not-beating parts. A maximum projection image was calculated to account for the beating areas from the entire movie. The resulting image was smoothed with a minimum filter and beating and not-beating areas were measured. The analysis was performed with ImageJ software. The percentage of beating area was calculated as “Beating area/Total measured area” and represented in a time course.

3.4 HISTOLOGICAL STAINING

3.4.1 FIXATION AND SECTIONING OF EBS

After 16 days of differentiation, EBs were collected in a 15 ml conical falcon and waited until they settled down with the gravity. After washing one time with 1xPBS, settled EBs were fixed for 30 min with freshly thawed 4 % paraformaldehyde (PFA) at room temperature. Fixed EBs were washed one more time with 1xPBS, and treated with 10 % and % 20 sucrose solutions in 1xPBS at room temperature for 30 min, respectively. Finally EBs were left in 30% sucrose in 1xPBS overnight at 4 ^{o}C. Next day sucrose solution was discarded, EBs were carefully embedded at the center of peel-a-way histology molds using OCT (VWR) compound and frozen slowly on dry ice. Cryomolds were stored at -86 ^{o}C until sectioning. Frozen blocks were sectioned at an 8 µm thickness with the cryostat machine (Leica CS3050 S) and sections were collected to ultra-attach histology glass slides. Then they were left for air dry at room temperature for 30 min and subsequently processed for further histological or immunostainings.

3.4.2 HEMATOXYLIN AND EOSIN STAINING

- Glass slides were placed into a staining jar and samples were brought to distilled water.

- Samples were stained with Mayers Hemalaun (Carl Roth) for 10 min.
- Slides were briefly rinsed with distilled water and treated with 0.2% ammonium hydroxide for 60 sec.
- After alkali differentiation, slides were rinsed in a running tap water for 10 min.
- Prior to Eosin staining, samples were differentiated through dipping into 95% ethanol 10 times and counterstained with Eosin Y for 60 sec.
- After rinsing in distilled water, samples were dehydrated prior to mounting: 70% ethanol for 5 min, 95 % ethanol for 5 min, 100 % ethanol for 5 min two times, Roticlear (Carl Roth) for 5 min two times.
- Slides were mounted with Roti-Mount (Carl Roth) and air dried overnight at fume hood.
- Staining images were with a Leica DM2500 microscope.

Receipts	
Eosin Y stock solutions (1 %)	10 g Eosin Y (Carl Roth) 200 ml H_2O 800 ml 95 % ethanol
Eosin Y working solutions (0.25 %)	250 ml Eosin Y working solution 750 ml 80 % ethanol 5 ml glacial acetic acid (Sigma)

Table 3. Receipts for the solutions used in Hematoxylen and Eosin staining.

3.4.3 ALCIAN BLUE AND HEMATOXYLIN STAINING

Alcian Blue and Hematoxylin counter staining was performed according to the protocol of University of Rochester Medical Center.

- Samples were brought to distilled water, differentiated in acid-alcohol for 20 sec. and stained with Alcian Blue Hematoxylin for 15 min.
- Slides were gently rinsed and samples were differentiated in acid-alcohol again for 3 sec.
- After rinsing gently in distilled water with 3 changes, slides were placed in 0.5 % ammonium water for 15 sec. and rinsed in distilled water with 2 changes.
- Prior to Eosin staining, samples were placed in in 95 % ethanol for 1 min and subsequently stained with Eosin Y for 1 min.

Receipts	
Alcian Blue Hematoxylin	1 g Alcian Blue (Sigma) 100 ml Mayers Hemalaun
Acid-alcohol	500 ml % 70 ethanol 5 ml Hydrochloric acid (36.5-38 %) (Sigma)
0.5 % Ammonium Water	2.5 ml Ammonium Hydroxide (28-30 %) (Sigma) 500 ml distilled water

Table 4. Receipts for the solutions used in Alcian Blue and Hematoxylen staining.

3.4.4 OIL RED O STAINING

- Samples were incubated in % 60 isopropanol: 40 % H_2O mix for 5 min and stained in Oil Red O staining solution for 20 min.
- After washing away excess staining, samples were incubated in 60 % isopropanol for 2 min.
- Slides were rinsed with 2 changes of distilled water for 2 min per change, mounted in aqueous mounting medium (homemade glycerol jelly) and left for air dry.
- Staining images were acquired with a Leica DM2500 microscope.

Receipts	
Oil Red O Stock Solution	0.5 g Oil O Red powder (Sigma) 100 ml isopropanol
Oil Red O Staining Solution	60 % Oil Red O Stock Solution 40 % H2O

Table 5. Receipts for the solutions used in Oil O Red staining.

3.5 IMMUNOFLUORESCENCE STAINING AND ANALYSIS

After initial cell aggregation, dissociated single P19 cells were seeded on gelatin coated coverslips in 6 well tissue culture plates and cultured until day 15. P19 cells grown on coverslips were washed with 1xPBS and fixed for 20 min with freshly thawed 4 % PFA. Afterwards, both P19 cells and cryosections of E14 derived EBs were immunostained with same protocol. They were washed twice with 1xPBS and incubated for 10 min in 0.5% Triton in 1xPBS for permeabilization. After permeabilization, cells were washed twice with 1x PBS and blocked for 1 hour at room temperature in 5%

FBS/0.1%Triton/1xPBS (blocking solution). The blocked cells were incubated over night at 4°C with primary antibodies diluted in blocking solution. After overnight incubation, stained cells were washed with 0.1 % Triton/1xPBS (wash buffer) three times and incubated with secondary antibodies prepared in wash buffer for 1.5 hour at room temperature in dark. Cells were washed with wash buffer three times for 10 min each in dark, mounted with VECTASHIELD Antifade Mounting Medium with DAPI (Vector) and sealed. Fluorescence images were acquired on a Leica SP5 microscope.

Quantification of Brachyury stainings in EBs is performed like this: As it was not possible to discern the individual nuclei to quantify the Brachyury staining per nucleus, the mean Brachyury staining intensity (intensity per area) in the entire EB nuclear area was measured instead. The DAPI staining image was smoothed with a Gaussian filter and the Nilblack local threshold was applied to segment the nuclei. The holes in the segmented image were filled, the outlines were smoothed with the binary open operation and objects smaller than 20 μm were excluded. The mean Brachyury staining intensity was measured inside the segmented nuclei.

Antibody Name	**Company**	**Dilution**
Brachyury (T)	SantaCruz (C19)	1:200
Cardiac Troponin I (cTnI)	Abcam (ab47003)	1:500
Anti-Rabbit Alexa Fluor 488	Invitrogen	1:500
Anti-Goat Alexa Fluor 488	Invitrogen	1:500

Table 6. Antibodies used in immunofluorescence staining.

3.6 RNA EXTRACTION, CDNA SYNTHESIS AND RT-QPCR

RNA was extracted by lysis with 1 mL Trizol Reagent (Ambion) for either E14 derived EBs or P19 cell pellets. Lysis was carried out by proper mixing and homogenization by passing the lysate through a syringe with a 0.9 x 40 mm 20G needle. Homogenized lysate was transferred in phase lock Heavy 2 mL tubes and incubated for 5 min at RT. 0.2 mL Chloroform (Sigma) was added and samples were shacked vigorously for 15 sec and incubated at RT for 3 min. Samples were centrifuged for 15 min at 4 °C, at 12.000 g and aqueous phase was transferred to a new tube. 0.5 mL analytical grade Isopropanol was added and RNA was precipitated by incubation at RT for 10 min

followed by centrifugation at 4 °C, 12.000 g for 10 min. The RNA pellet was washed once with 75% Ethanol and centrifuged for 5 min at 4 °C at 7500 g. After Ethanol removal the pellet was resuspended in 60 µL Nuclease Free Water (NFW) and incubated for 5 min at 57 °C. RNA was re-precipitated to remove any Trizol traces by adding 6 µL NaOAc 3M and 1 mL Ethanol. Precipitation was carried out at -80 °C from 1 hr to overnight. Samples were centrifuged for 20 min at max speed at 4 °C and washed twice with 1 mL ice-cold 75% Ethanol. Pellets were air-dried and resuspended in 20 µL NFW.

1 µg of RNA was used for cDNA synthesis by using the First Strand cDNA Synthesis Kit (Fermentas) with random hexamer primers. cDNA was diluted with NFW and 2 µL were used for qPCR. For each qPCR reaction, 2 µL cDNA and 2 µL NFW were combined with the following master mix at a final volume of 10 µL per reaction: Cyber Green Mix 2x (Life Technologies) 5 µL + Forward Primer (10 µM) 0.5 µL + Reverse Primer (10 µM) 0.5 µL.

qPCRs, were carried out using a Viia7 cycler (Life Technologies) at normal settings and expression was analyzed by using the ddCt method. The oligos (Table 7) were designed to span exon-exon junctions of transcripts and the results were normalized by using 18S or RPO oligos as reference.

Primer list for RT-qPCR			
Name	**Forward**	**Reverse**	**Ref.**
S18	GATCCATTGGAGGGCAAGTCT	CCAAGATCCAACTACGAGCTTTTT	
Pax3	CCGGGGCAGAATTACCCAC	GCCGTTGATAAATACTCCTCCG	
Otx2	GGCTGAGTCTGACCACTTCG	AATGTCGTCCTCTCCCTTCG	
Fgf8	TAATTGCCAAGAGCAACGGC	CGCCGTGTAGTTGTTCTCCA	
Runx1	AACGACCTCAGGTTTGTCGG	GCAACTTGTGGCGGATTTGT	
Mixl1	CGTCTTCCGACAGACCATGT	GTTCTGGAACCACACCTGGAT	
Flk1	GGCGGTGGTGACAGTATCTT	GTCACTGACAGAGGCGATGA	
Gata4	AAGACACCCCAATCTCGATATGTT	CATGGCCCCACAATTGACAC	
Gsc	GGAGACGAAGTACCCAGACG	AAACCAGACCTCCACCTTCTC	
Sox7	AGCAAGATGCTGGGAAAGTC	TCTGCCTCATCCACATAGGGT	

Nodal	TGGGGGAGGAGTTTCATCCT	CGGTGGGGTTGGTATCGTTT	
BMP4	TGAGCCTTTCCAGCAAGTTT	CTTCCCGGTCTCAGGTATCA	
Wnt3a	ACCGTCACAACAATGAGGCT	CCGTGGCATTTGCACTTGAG	
Brachyury	GCTCTAAGGAACCACCGGTCATC	ATGGACTGCAGCATGGACAG	Klattenhoff CA et al 2013
Eomes	TGTGACGGCCTACCAAAACA	AGCCGTGTACATGGAATCGT	
Mesp1	CCTCATCTCCGCTCTTCAG	ATCTACTCCCTCCGAAGGTG	
Nkx2.5	ACATTTTACCCGGGAGCCTA	CGCTCCAGCTCGTAGACC	Klattenhoff CA et al. 2013
Tbx5	ATCGCCGATACAGATGAGGG	TTCGTGGAACTTCAGCCACAG	Klattenhoff CA et al. 2013
Hand1	AAAGGGAGTTGCCTCAGC	CTGGTCTCACTGGTTTAGCTC	
Isl1	TCATCCGAGTGTGGTTTCAA	CCATCATGTCTCTCCGGACT	Klattenhoff CA et al. 2013
Hand2	ACCAGCTACATCGCCTACCT	GCTTTTCAAGATCTCATTCAGC	
MyocD	AGGGTGCGCACAGAACTCA	TTGGGACAAGGGTTGAGCC	Klattenhoff CA et al. 2013
RPO	TTCATTGTGGGAGCAGAC	CAGCAGTTTCTCCAGAGC	Morey L, Cell 2015
cTnT	GAGAGAAGGCCAAGGAGCTG	GGCACAGCTTTGACGAGAAC	
cTnI	CTCTGCCAACTACCGAGCCTA	CTCTTCTGCCTCTCGTTCCAT	
α-MHC	GCTGGGCTCCCTGGACATTGAC	CCTGGGCCTGGATTCTGGTGAT	
β-MHC	CATGGGATGGTAAGAAACGGG	TCCTCCAGTAAGTCGAAACGG	
MYL2	ATCGACAAGAATGACCTAAGGGA	ATTTTTCACGTTCACTCGTCCT	
MYL7	TCAGCTGCATTGACCAGAAC	CCCGAAGAGTGTGAGGAAGA	
Connexin43	ACAAGGTCCAAGCCTACTCCA	CCGGGTTGTTGAGTGTTACAG	
ANP	GCTTCCAGGCCATATTGGAG	GGGGGCATGACCTCATCTT	

Table 7. Primers used for RT-qPCR experiments.

3.7 WESTERN BLOT

P19 cell pellets were collected at time points mentioned and washed with 1xPBS. Samples were resuspended in 2xLaemmli buffer according to their pellet size and sonicated for 15 cycles (30 sec on/ 30 sec off) at high setting using a Diagenode Bioruptor plus. EBs were collected at time points mentioned, washed with 1xPBS and resuspended in 2xLaemmli buffer according to their total EB numbers. They were homogenized by passing the lysate through a syringe with a 0.9 x 40 mm 20G needle before sonication for 15 cycles (30 sec on/ 30 sec off) at high setting using a Diagenode Bioruptor plus. Both samples were boiled for 20 min at 95°C and centrifuged for 15 at room temperature at maximum speed. Boiled proteins were separated on 10 % SDS-PAGE for Western Blot analysis.

Antibody Name	Company	Dilution
Brachyury (T)	SantaCruz (C19)	1:500
Zrf1	Novus	1:500
Gata4	SantaCruz (C20)	1:500
H2A	Abcam (ab18255)	1:1000

Table 8. Antibodies used in western blot experiments.

3.8 CHROMATIN IMMUNOPRECIPITATION

Chromatin immunoprecipitation (ChIP) experiments for EBs were carried out as described in (Mazzoni et al., 2013) with a few modifications. Stably FLAG-tagged Zrf1 or control plasmid expressing E14 cells derived EBs were differentiated for 2 and 4 days. Differentiated EBs were collected in 50 ml conical tubes and washed two times with 1xPBS. During washes EBs were let to settle down at the bottom of the tubes by gravity. After washes, EBs were dissociated with 3 ml Accutase (Gibco-StemPro Accutase) enzyme for 3 min at water bath, and subsequently centrifuged at 600 rpm for 4 min. Dissociated EBs were washed one more time with 1xPBS and centrifuged at 600 rpm for 2 min. Cells were fixed in fixation buffer containing 1% formaldehyde for 15 min at room temperature and quenched with 0.125M Glycine for additional 5 min at room temperature. Fixed and crosslinked cells were centrifuged at 2000 rpm for 3 min and were resuspended in 5 ml Lysis Buffer A and 5 ml Lysis Buffer B, respectively. For each lysis step, samples were incubated for 10 min at 4 °C on a rotating wheel and were

pelleted with centrifugation at 4 °C, at 1350 g for 5 min. Finally nuclear extracts were resuspended in 2.4 ml Sonication Buffer and sonicated for 3 x 10 cycles (30 sec ON/ 30 sec OFF) at high setting. After each cycle the samples were incubated for 5 min on ice. Debris were removed by centrifugation at max speed at 4 °C for 15 min and clear supernatants were transferred into new tubes. After measurement with Bradford (Pierce Coomassie, Thermo Scientific), protein concentrations were normalized to each other. 1 mg of protein from each sample was used for immunoprecipitations (IPs) and 1% of total protein was kept as input that was stored at -20°C until next day. Samples were diluted 3 fold in ChIP Buffer and Triton X-100 at a final concentration of 1% in the sample. Protein A/G magnetic beads (Milipore-Magna ChIP™ Protein A+G Magnetic Beads) were washed with ChIP buffer three times. Finally 20 µl of washed beads and 5 µl Zrf1 (Novus)/ 5 µl anti- FLAG M2 (Sigma-F1804) or 1 µl mouse IgG were added per IP. IPs were carried out overnight at 4°C on a rotating wheel. After overnight incubation, bead-captured immunocomplexes were washed with 1 ml of each buffer respectively: 2x instant wash with ChIP Buffer; 1x instant wash with ChIP Buffer+ 500 mM NaCl; 2x 5 min wash with RIPA buffer; 1x 5 min wash with TE buffer. Elution of the immunocomplexes from the magnetic beads was carried out by the addition of 100 µL 2x STOP Buffer and incubation of samples in a thermomixer at 65 °C for 15 min. Elution was carried out two times and eluates were combined in new tubes. 2x STOP Buffer was also added to input samples and all samples were incubated overnight at 65 °C, at 1000 rpm to revert crosslinking. After crosslinking reversal, 1 µL RNaseA (100 mg/ mL stock, Qiagen) was added to the samples and they were incubated at 37 °C for 1hr. Proteins were degraded by the incubation of the samples with 20 µg of Proteinase K (Sigma-P2308) at 56 °C for 1hr. The DNA was purified with phenol: chlorophorm: isoamyl alcohol (Carl Roth) in phase lock tubes and chloroform. The purified DNA was precipitated overnight at – 80 °C by adding 1 µL Glycogen (Sigma), 10% of sample volume NaOAc 3M and 1 mL Ethanol. Precipitated DNA pellets were acquired by centrifugation at max speed at 4 °C for 20 min. Pellets were washed twice with cold 75% Ethanol and after they were air dried, resuspended in 200 µL NFW. 2 µL of the DNA was used for qPCR reactions. Reactions were carried out as described for the RT-

qPCR, using oligos specifically designed to amplify promoter, E-box or transcription start sites (TSSs) of genes (Table 10).

Receipts	
Fixation Buffer	0.1 M NaCl 1 mM EDTA 50 mM HEPES-KOH pH 7.6 11% freshly added formaldehyde
Lysis Buffer A	50 mM HEPES-KOH pH 7.6 140 mM NaCl 1 Mm EDTA 10% v/v Glycerol 0.5% NP-40 0.25% Triton X-100 Freshly added protease inhibitors (Roche- C0mplete™ ULTRA Tablets, Mini, EDTA-free, EASYpack Protease Inhibitors)
Lysis Buffer B	10 mM Tris-HCl pH 8 200 Mm NaCl 1 mM EDTA 0.5 mM EGTA Freshly added protease inhibitors
Sonication Buffer	10 mM Tris-HCl pH 8 100 mM NaCl 1 mM EDTA 0.5 mM EGTA 0.1% Na-deoxycholate 0.5% N-lauroylsarcosine Freshly added protease inhibitors
ChIP Buffer	20 mM Tris-HCl pH 8 150 mM NaCl 2 mM EDTA Freshly added protease inhibitors
ChIP Buffer + 500 mM NaCl	20 mM Tris-HCl pH 8 2 mM EDTA 500 mM NaCl
RIPA Buffer	10 mM Tris-HCl pH 8 0.25 M LiCl

	1 mM EDTA 0.5 % NP-40 0.5% Na-deoxycholate
TE Buffer	10 mM Tris-HCl pH 8.1 1 mM EDTA
2x STOP Buffer	20 mM Tris-HCl pH 8 100 mM NaCl 20 mM EDTA 1% SDS

Table 9. Receipts for the buffers used in ChIP experiments.

Primer List for ChIP-qPCR			
Name	**Forward**	**Reverse**	**Reference**
Nkx2.5 TSS	CCACATCCAGGGCAGAGA	CCAGGTGGGTAGCAGAGAGT	
Hand1 TSS	TAAAACTTGGGACCGCCACC	ACGTCCAAAGACCGGGTTTA	
Hand2 TSS	ATGGAGATCTTGCTGGGAAA	GGGTGTGCTCAGACAGTGG	
Tbx5 TSS	CTGGCTCAGAGCAGTCAACA	CCCCAAACTCTTGAACCACT	
Mesp1 promoter	GATGTAATACCAGACACCAGG	GGATAACTTAGTGACTCCCCG	David R. et al 2011
Brachyury E-box	CGCGCTGGAGCCCATTGT	GACACCCTTTGAAGTACCGAGCAG	

Table 10. Primers used in ChiP-qPCR experiments.

3.9 FLOW CYTOMETRY

After 13 days of differentiation, EBs from control, Zrf1 knockdown and rescue mESCs were collected and washed twice with PBS. Following the washes, EBs were incubated in %0.25 Trypsin-EDTA for 5 minutes at 37 °C. Enzymatic activity was stopped using 50% FBS in 1xPBS and dissociation was completed employing mechanical force with a 0.9 x 40 mm 20G needle. After spinning down at 900 rpm for 4 min, dissociated EBs were fixed and permeabilized for 20 minutes on ice using a BD Cytofix/Cytoperm kit. Cells were centrifuged at 1500 rpm for 4 min and washed twice with wash buffer

contained in the aforementioned kit. Prior to staining, cells were blocked with 1%BSA in 1xPBS for 15 minutes and washed twice with wash buffer. Later cells were stained with 5 µL cTnT-PE (BD-Pharmingen-564767) antibody prepared in blocking buffer on ice for 2 hours in the dark. After staining, cells were washed twice with wash buffer and resuspended in staining buffer (1% FBS in 1xPBS) and analyzed with an LSRFortessa cell analyzer (BD Biosciences). The cTnT positive cells (cTnT+) sorted from the three cell lines (control, Zrf1 knockdown and rescue) are represented as a relative ratio. cTnT+ cells from Zrf1 knockdown and rescue cells are normalized to cTnT+ cells in control cells and the values were calculated as fold change.

4 RESULTS

4.1 KNOCKDOWN OF ZRF1 IN MESC PROVOKES DEFORMATION OF THE MESODERM

To assess a potential function for Zrf1 during differentiation, we generated E14 mESCs either expressing a non-specific shRNA (Control) or shRNA targeting Zrf1 (shZrf1) by viral infection (Figure 1A and 1B). Employing hanging drop method, we differentiated both cell lines during 6 days and collected EB samples every two days. Then we analyzed the mRNA levels of selected marker genes of three germ layers: for ectoderm *Pax3*, *Otx2*, *Fgf8*; for mesoderm *Runx1*, *Mixl1*, *Flk1*; for endoderm *Gata4*, *Gsc* and *Sox7* (Figure 1C). We observed that depletion of Zrf1 had an impact on the expression of ectodermal and endodermal genes but a more pronounced effect on mesodermal marker genes. Remarkably, we noted that the expression of mesodermal marker genes was affected drastically by Zrf1 knockdown.

During early differentiation, spatiotemporal control of germ layer related genes is quite essential. Because aberrant gene expression can cause congenital problems in later life. To investigate whether aberrant gene expression seen in Zrf1 knockdown cells might affect the further differentiation of EBs, we differentiated both cell lines for longer time. After 16 days of differentiation, control cells outgrew and differentiated properly into the EBs with structures including cystic cavities similar to the yolk-sac and an outer endodermal layer analogous to primitive endoderm (white arrows in Figure 2A). In contrast, Zrf1 depleted cells displayed an accumulated cell mass in the center, failed to outgrow and develop structures like yolk sac and endoderm. To gain a better understanding of the structural impairments observed in shZrf1 cells, we sectioned control and knockdown cells which differentiated for 16 days at 8 µm thickness and performed Hematoxylin and Eosin (H&E) staining (Figure 2B). H&E staining of control EBs confirmed our previous observations. These EBs managed to form important features of the three germ layers such as neural rosette for ectoderm layer, fibrous connective tissue for mesoderm and gut like epithelium for endoderm (Black arrows in Figure 2B). Conversely, Zrf1 knockdown cells failed to form these tissues. In particular,

we noticed that the generation of connective tissue, which is indicative of mesoderm development, was impaired in Zrf1 depleted cells.

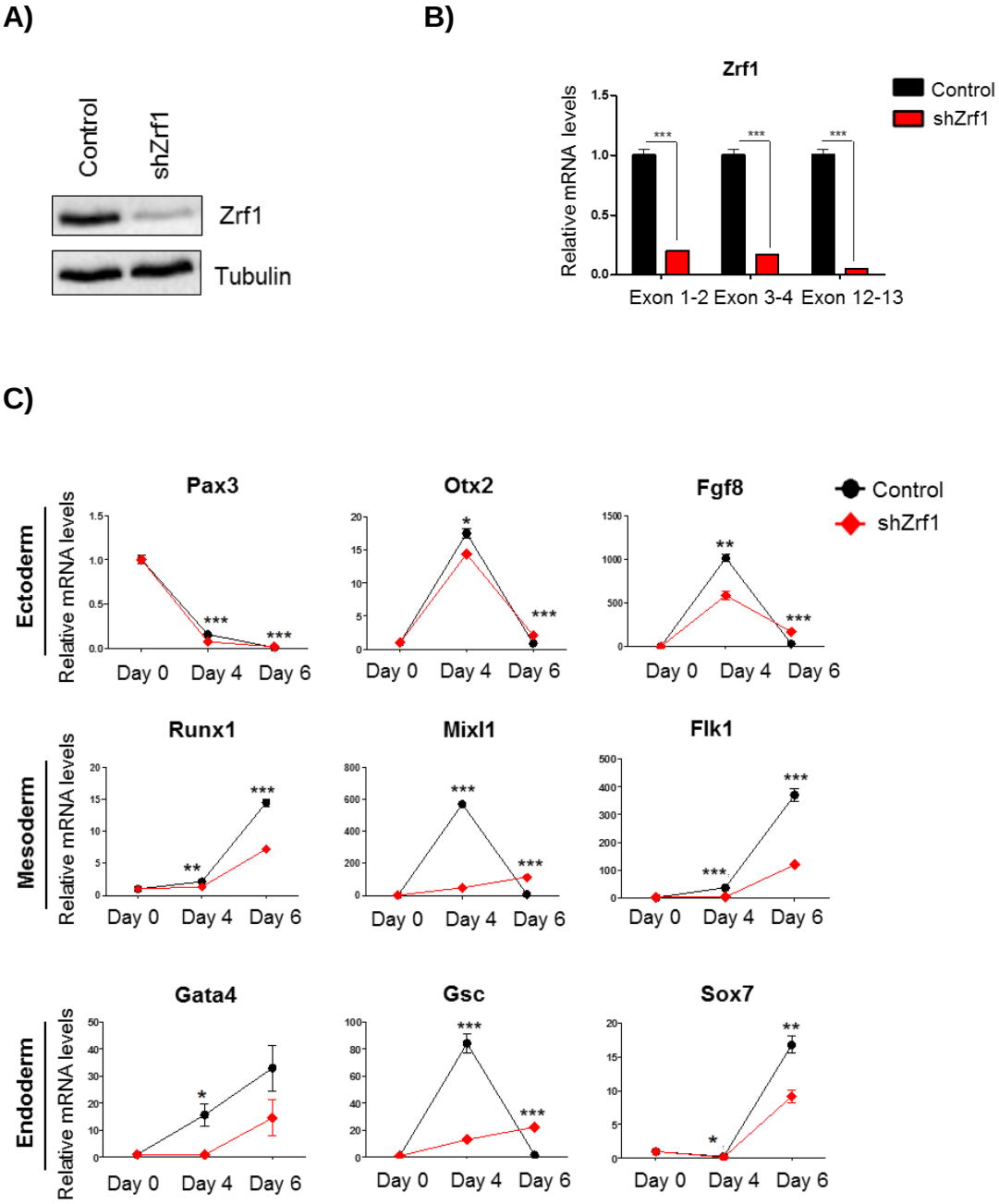

Figure 1. Zrf1 knockdown cells have abnormal gene expression for the germ layer related genes. (A) Western blot for Zrf1 after transfection of E14 cells with control and shRNA. Alpha tubulin was used as a loading control. (B) Real-time qPCR of control and shZrf1 cells for the expression of the different exons of Zrf1. Expression was normalized to the housekeeping gene beta actin. Data represent the average of three experiments, +/- S.E.M. *** $p<0.001$ as calculated by two-tailed unpaired t test. (C) Real-time qPCR of marker genes from the three germ layers at days 0, 4 and 6 of EB differentiation. Expression was normalized to the housekeeping gene S18. Data represent the average of three experiments, +/- S.E.M. *$p<0.5$, **$p<0.01$, *** $p<0.001$ as calculated by two-tailed unpaired t test.

A)

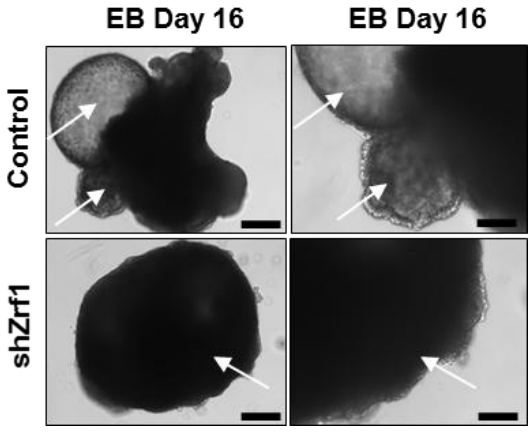

B)

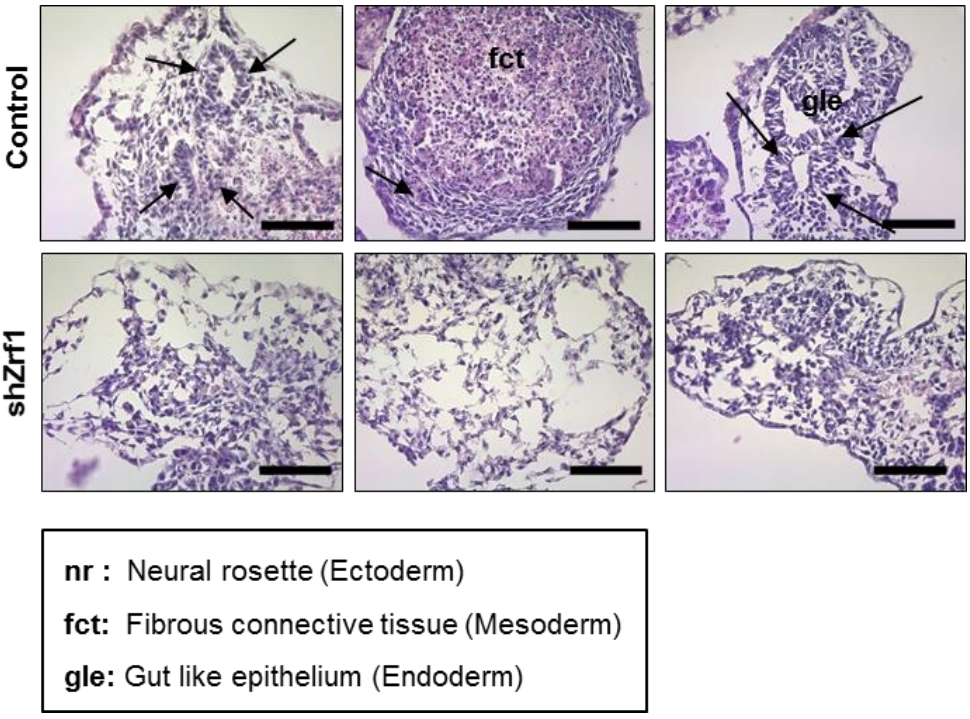

Figure 2. Zrf1 knockdown derived EBs can't properly differentiate into structures important for germ layers. (A) Brightfield images of control and shZrf1 derived EBs were taken at 10x (left panel) and 20x (right panel) magnification after 16 days of differentiation. White arrows indicate the presence or absence of structures similar to yolk-sac and external primitive endoderm in control EBs or Zrf1 depleted EBs, respectively. Scale bars: 200 μm (left panel) and 100 μm (right panel). (B) Representative images of hematoxylin and eosin stainings of control and Zrf1 knockdown EBs were taken at 40X magnification after 16 days of differentiation. Black arrows in the upper panel indicate the neural rosette, fibrous connective tissue and gut like epithelium, respectively. Scale bar, 50 μm.

Previous findings regarding the particular mesoderm impairment in Zrf1 depleted cells prompted us to check early *Brachyury* expression. As mentioned before Brachyury is one of the transcription factors capable of marking the mesoderm derived progenitors. For this purpose, we differentiated both cell lines until day 4 which is the peak point for the expression of *Brachyury*. After sectioning of EBs, we stained the cells with Brachyury antibody (Figure 3A). We observed a drastic reduction of nuclear *Brachyury* consistent with its diminished protein levels in Zrf1 knockdown cells (Figure 3B). Taken together, our data point at a critical function for Zrf1 in mesoderm development during EB formation.

A)

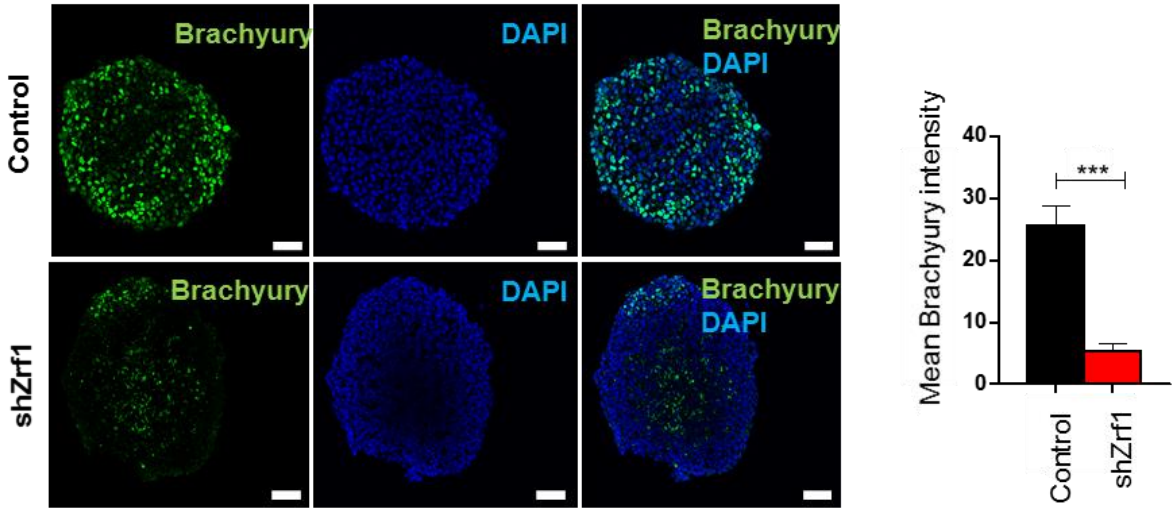

B)

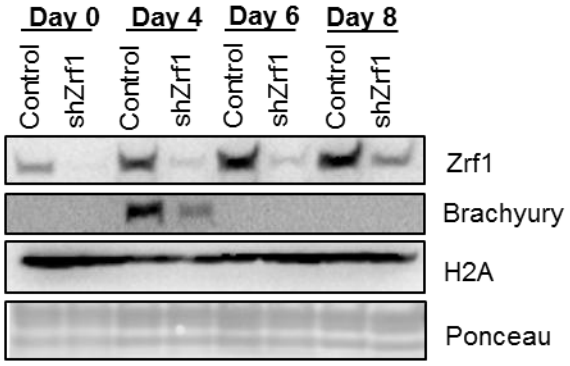

Figure 3. Mesoderm is particularly effected at early differentiation of Zrf1 depleted cells. (A) Representative immunofluorescence images and analyses of control and Zrf1 knockdown EBs using Brachyury antibody (mesoderm marker) after 4 days of differentiation. Data represent the mean Brachyury (green) intensity of three independent experiments. *** $p<0.001$ as calculated by two-tailed unpaired t test. Scale bars, 50 µm. (B) Protein level changes of Zrf1, Brachyury in control and Zrf1 knockdown EBs during 8 days of differentiation. H2A and ponceau were used as a loading control.

4.2 RE-ESTABLISHING ZRF1 EXPRESSION IN ZRF1 KNOCKDOWN CELLS RESCUES THE MESODERM PHENOTYPE

To ensure that the observed phenotype was due to the knockdown of Zrf1 we conducted functional rescue experiments. We restored Zrf1 expression in shZrf1 cells by transfecting plasmids encoding for human FLAG-tagged Zrf1. After antibiotic selection we established mESCs stably expressing FLAG-Zrf1 (Rescue) (Figure 4A). We generated EBs from the three cell lines (control, shZrf1 and rescue) and monitored their phenotypes during 8 days (Figure 4C). At day 2, control cells already formed an uniform EB population as expected from the hanging drop differentiation method. These cells are differentiated into proper sphere structures with an accumulated cell mass (darkness in the middle) at the center of the spheres. Their population behavior was confirmed by the measurement of their respective diameters as well (Figure 4B). Neither shZrf1 nor rescue derived EBs manage to form these structures at this time point (Figure 4C-Day 2) and they exhibited a completely heterogeneous population judged by their diameter size measurement (Figure 4B). At day 4, control cells continued to increase their EB size due to proliferating cell population within the EBs. Whereas shZrf1 cells failed to display any of these properties, rescue cells started to exhibit spherical structures similar to the control cells (Figure 4C-Day 4) and constituted a homogenous population (Figure 4B). Starting from day 6, control and rescue cells continued to outgrow forming cystic cavities which can be distinguished as light and hollow parts within EBs (Figure 4C-white arrows). On contrast, shZrf1 cells weren't able to outgrow and increase their EB size (Figure 4B). Moreover they were unsuccessful at further differentiation (Figure 4C-Day 6 and Day 8). During development, mesoderm gives rise to the chondrocytes (cartilage, bone), adipose tissue and cardiomyoctes. To analyze whether the previously observed mesoderm phenotypes were rescued by re-expression of Zrf1, we performed specific stainings for chondrogenesis and adipogenesis (Figure 5). To visualize chondrocytes, we stained sections of control and Zrf1 knockdown cells with Alcian Blue. Whereas tissues like cartilage is stained as blue/purple, tissues like bone marrow is stained as dark blue after alcian blue treatment. After 16 days of differentiation, control cells developed into cartilage, bone and bone

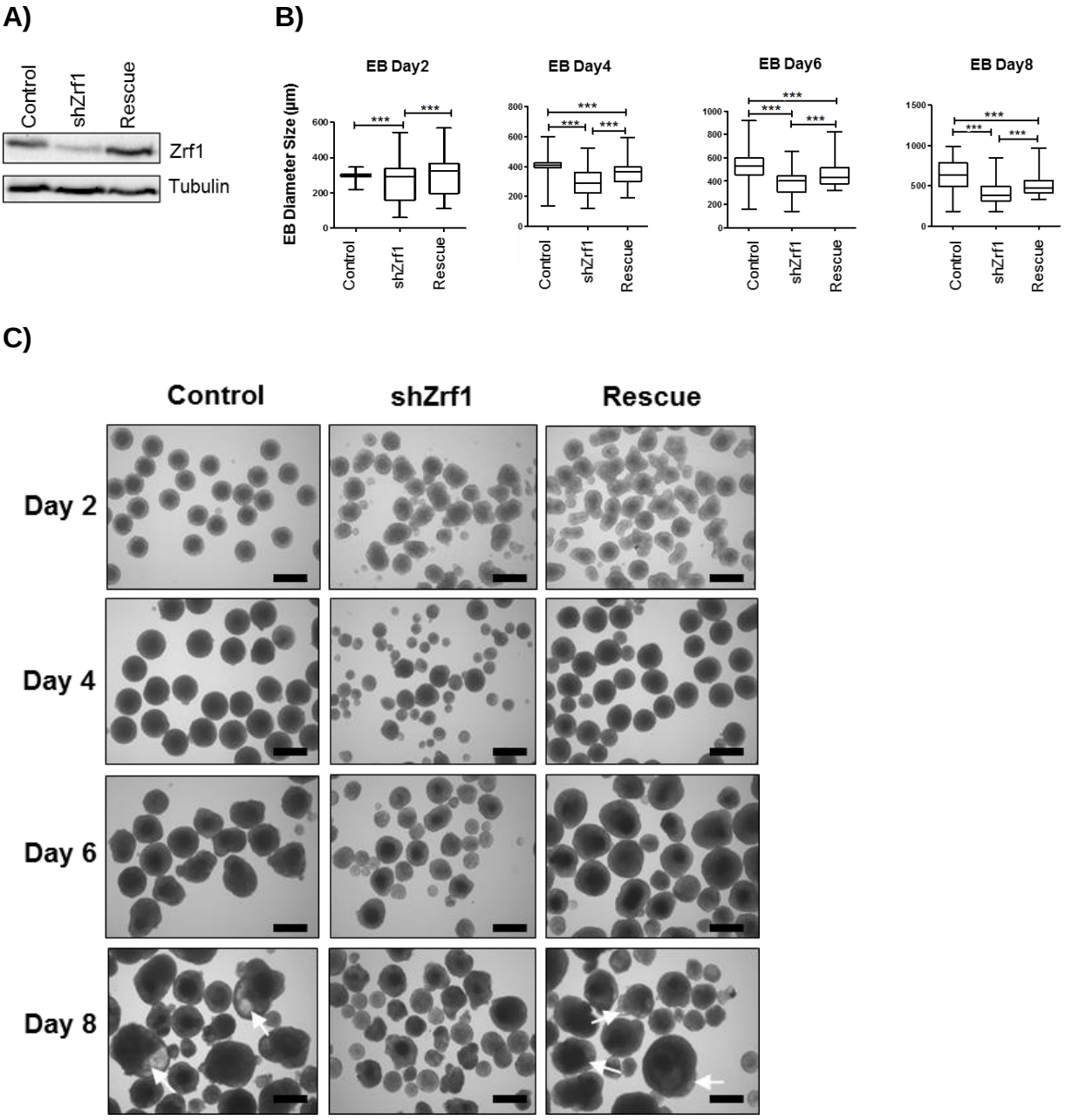

Figure 4. Zrf1 re-expression partially restores the differentiation properties of knockdown cells. (A) Western blot analyzing Zrf1 levels in control, shZrf1 and rescue cells. Alpha tubulin was used as a loading control. (B) Brightfield images of control, shZrf1 and rescue cells derived EBs were taken at 4x magnification at days 0, 4, 6 and 8. White arrows indicate the cystic cavities in control and rescue cell derived EBs. Scale bars, 500 µm. (C) Average diameters of EBs derived from control, Zrf1 knockdown and rescue cell lines. Feret diameter's of each EB was calculated using the ImageJ program. The whiskers of the plots represent the minimum and maximum values of the population of counted EBs. ***p<0.001 as calculated by two-tailed unpaired t test.

marrow tissues. Zrf1 knockdown cells failed to develop these tissues and mostly exhibited apoptotic cells at the center which are stained as dark pink. However restoring

Zrf1 levels caused a partial re-establishment of chondrogenic cells in agreement with our previous findings (Figure 5A, black arrows). To further support a specific function for Zrf1 in mesoderm formation we analyzed its impact on the generation of adipocytes by performing Oil Red O staining. Whereas control cells have intense big red lipid droplets, as a marker of differentiated adipocytes, Zrf1 knockdown cells have significantly less lipid droplets with a comparably smaller size. Rescue cells, on the other hand, partially restored this defect exhibiting a more pronounced Oil Red O staining (Figure 5B, black arrows).

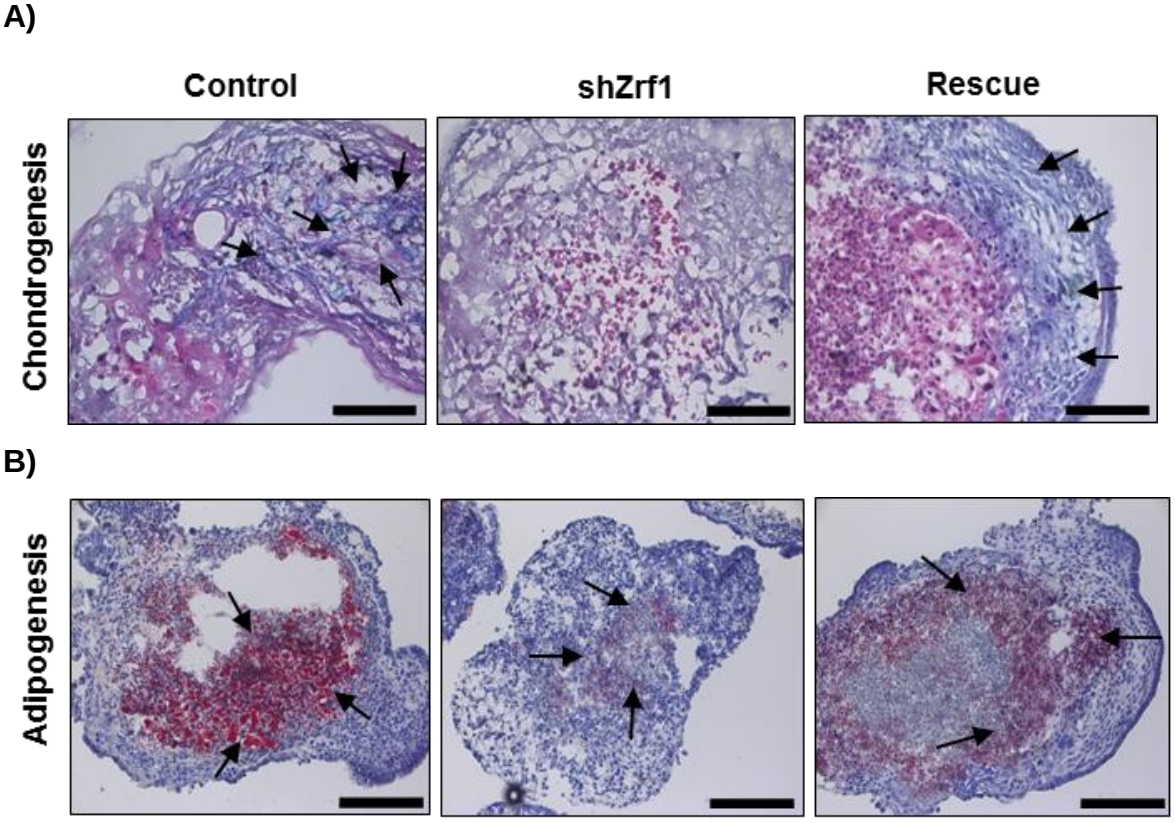

Figure 5. Restoration of Zrf1 expression in Zrf1 knockdown ES cells rescues the mesoderm phenotype. (A) Representative images of alcian blue stainings of control, Zrf1 knockdown and rescue EBs were taken at 40x magnification after 16 days of differentiation. Black arrows indicate mesoderm derived tissues in alcian blue staining. Cartilage: blue, purple. Bone marrow: dark blue. Scale bar, 50 µm. (B) Representative images of Oil Red O stainings of control, Zrf1 knockdown and rescue EBs were taken at 20x magnifications. Black arrows indicate mesoderm derived lipid droplets in Oil Red O staining. Scale bar, 100 µm.

One of the essential sign of successful differentiation into mesoderm is the appearance of cardiomyocytes which spontaneously start to beat in culture over 10 days. To explore

Zrf1 depletion had an effect on cardiomyocyte differentiation, we monitored both cells for the beating phenotype from day 10 to day 16, and plotted the beating frequencies into a time course (Figure 6A). Control EBs began to beat around day 10 and continued to increase the number of beating EBs until day 16. Although there were a few beating EBs exist, there was a drastic reduction of beating cell clusters in Zrf1 depleted EBs. Rescue cells, on the other hand, managed to restore this phenotype. To demonstrate that observed beating cell clusters are actually derived from cardiac cells not randomly beating cell clusters, we performed FACS analysis of cardiac troponin T (cTnT: contractile protein of cardiac muscles) of control, shZrf1 and rescue cells (Figure 6B). Relative ratio of CTnT+ cells of three cell lines confirmed that beating cells are cardiomyoyctes and Zrf1 depletion is responsible for the impaired cardimyoyctes. Collectively, our data implies that Zrf1 is important for chondrogenesis, adipogenesis and cardiogenesis, moreover it fulfills an essential function during mesoderm development.

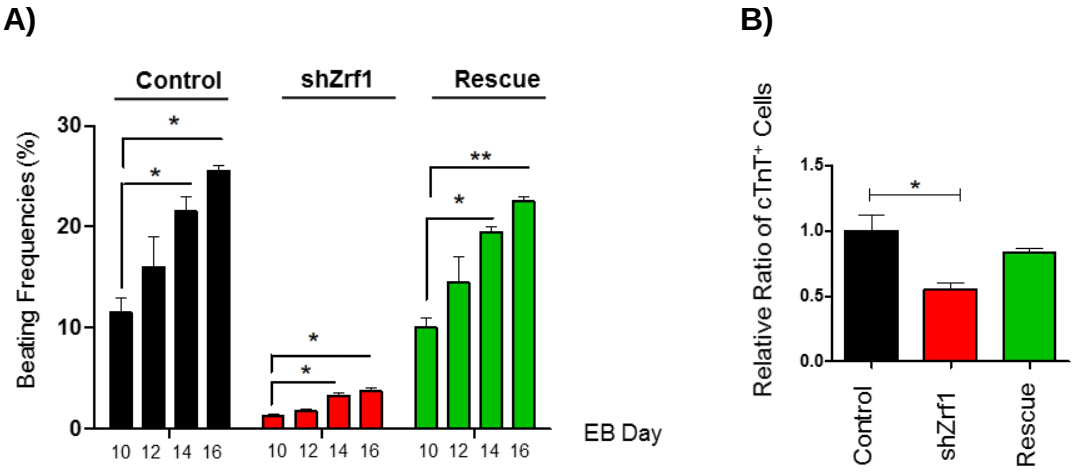

Figure 6. Zrf1 knockdown cells can't properly differentiate into cardiomyoyctes during *in vitro* development. (A) The numbers of spontaneously beating EBs were counted under an inverted-light microscope on Day 10, 12, 14 and 16 of the culture. Data represent the average of three experiments, +/- S.E.M. *p<0.5, **p<0.01, as calculated by two-tailed unpaired t test. (B) FACS analysis using cTnT-PE antibody in control, Zrf1 knockdown and rescue mES cells after 13 days of differentiation. The relative ratio of cTnT+ cells from Zrf1 knockdown and rescue EBs were calculated as fold change compared to cTnT+ cells in control mES cells. Data represent the average of three experiments, +/- S.E.M. *p<0.5.

4.3 ZRF1 DEPLETION LEADS TO ABERRANT GENE EXPRESSION IN CARDIOMYOGENESIS RELATED GENES AND IMPAIRS THE EXPRESSION OF GENES SPECIFIC FOR CARDIAC SUBTYPES

Polycomb complexes are essential regulators of epigenetic gene silencing in embryonic and adult stem cells. They are required for the maintenance of pluripotency and for further differentiation. A previously published report revealed that PRC1 subunit Mel18 is involved in the regulation of mesoderm cell fate specification and early cardiac mesoderm formation in embryonic stem cells (Morey L. et al., 2015). Zrf1 was shown to exhibit opposite functions on target genes of PRC1 subunit Ring1b (Richly H. et al., 2010). Based on the interplay between Zrf1 and PRC1 complex together with our previous findings, we reasoned that Zrf1 might be involved in the regulation of cardiomyogenesis. Hence we aimed to focus on Zrf1's role in cardiac differentiation.

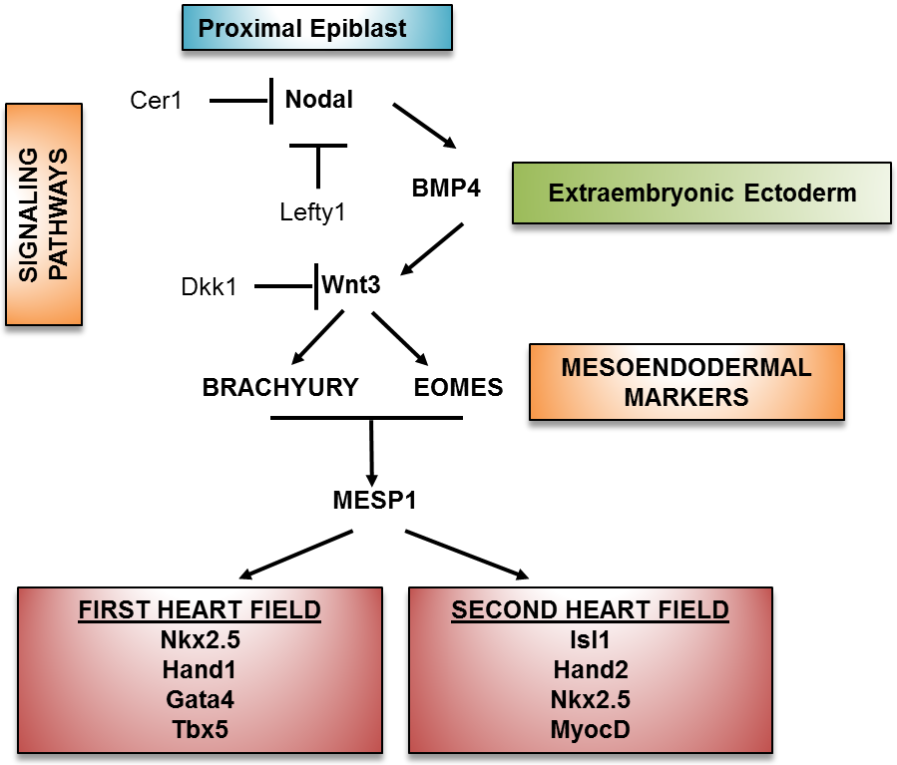

Figure 7. Schematic illustration of cardiomyogenesis. Cardiomyogenesis begins with mesoderm induction which is triggered by Nodal signaling in the proximal epiblast. Nodal signaling maintains BMP4 expression in the extraembryonic ectoderm. BMP4 acts by inducing Wnt3 expression in the proximal epiblast. Nodal and Wnt signaling are restricted to the posterior epiblast by specific antagonists (*Lefty1* and *Cer1*; *Dkk1*, respectively). Wnt induces the expression of mesoendodermal markers *Brachyury* and *Eomes*. Then Brachyury and Eomes together induce the expression of *Mesp1*. Downstream of Mesp1, a complex network of transcription factors, which belong to first and second heart fields, tightly control the proper development of cardiac tissues (Summarized from Dyer L.A. et al., 2009).

Cardiomyogenesis is a very complex process in which a variety of signaling pathways and transcription factors are involved. Context- and stage-specific control of the process is very critical for the development of functional cardiomyocytes. Therefore, we differentiated control and shZrf1 cells for 6 days and investigated the expression profiles of cardiomyogenesis related genes starting from the mesoderm induction to heart field specification (Figure 7).

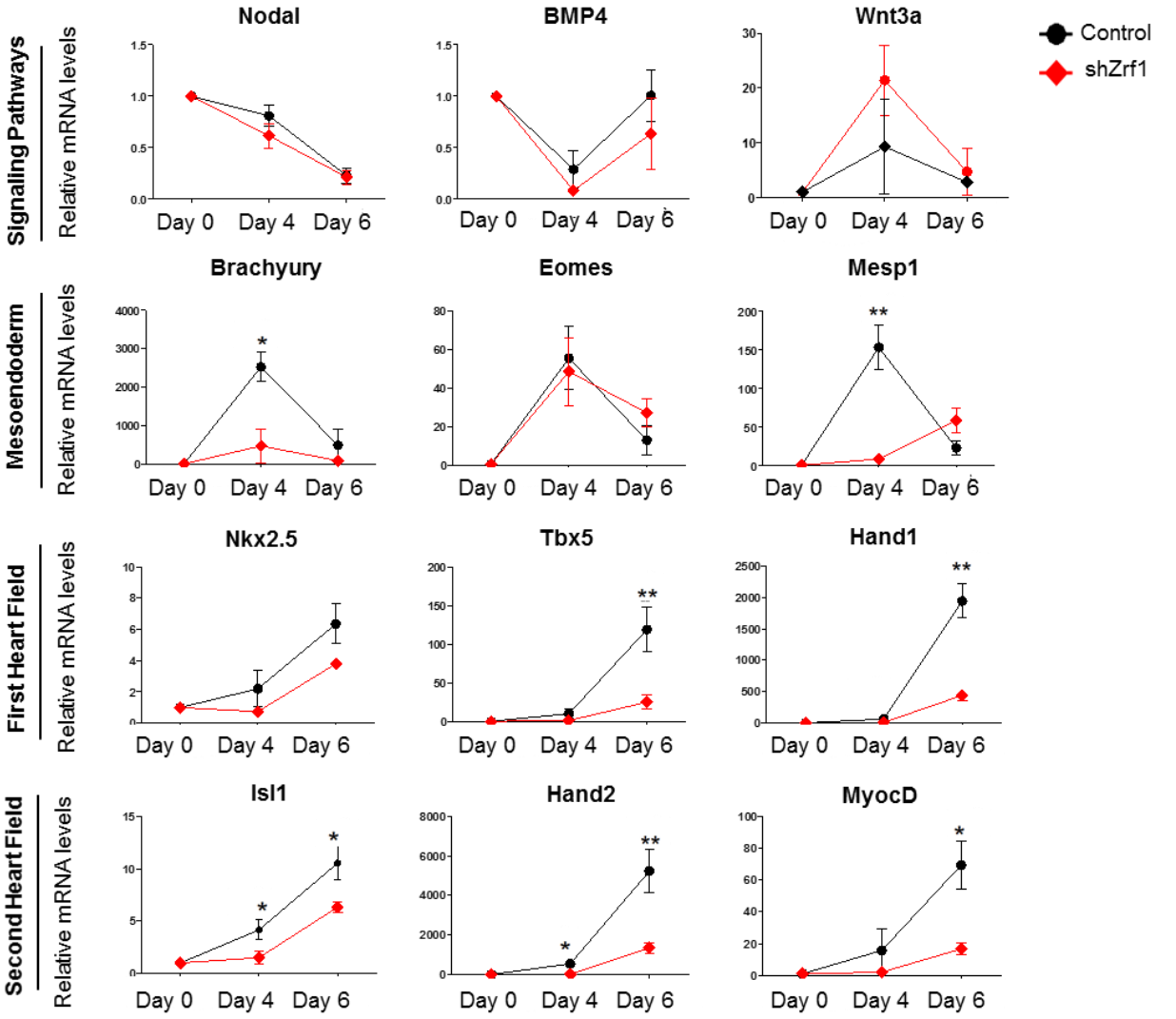

Figure 8. Zrf1 controls the temporal expression of the genes related to cardiomyogenesis. Real-time qPCR of signaling pathway, mesoendoderm, Mesp1, first and second heart field related genes at days 0, 4 and 6 of EB differentiation. Expression was normalized to the housekeeping gene S18. Data represent the average of five experiments, +/- S.E.M. *p<0.5, **p<0.01, *** p<0.001 as calculated by two-tailed unpaired t test.

First we analyzed the genes important for cardiogenic mesoderm formation, which represents the first step of cardiomyogenesis. Signaling pathways, particularly Nodal, Wnt and BMP4 play a regulatory role in the mesoderm formation. According to our RT-PCR data, both cell lines exhibited similar expression patterns for the signaling pathway related genes. Although the expression of Nodal and BMP4 were slightly decreased in Zrf1 knockdown cells, Wnt3a expression levels were not drastically affected (Figure 8). Next we analyzed the following three genes in the pathway: *Brachyury*, *Eomes* and *Mesp1*. We observed a dramatic and specific reduction of Brachyury and Mesp1 expression upon Zrf1 depletion, whereas Eomes levels did not significantly change. Even though the levels were decreased, shZrf1 cells displayed similar expression patterns for Brachyury and Eomes. Interestingly, the peak point of Mesp1 expression was shifted from day 4 to day 6 in Zrf1 knockdown cells (Figure 8). Later we continued to examine the expression levels of important transcription factors of both heart fields. We noticed that almost all of them were affected by Zrf1 depletion. Whereas the expression patterns stayed same in both cell line, shZrf1 cells weren't able to upregulate the gene expressions to the same level with control cells, particularly for day 6 (Figure 8).

Adult heart consists of muscle (atrium and ventricle) and non-muscle structures (nodal conduction system). We hypothesized that such a strong effect of Zrf1 depletion on cardiomyogenesis related genes might lead an aberrant expression of the genes which encode the aforementioned structures. To explore this hypothesis, we analyzed specific gene groups for atrium, ventricle and the nodal conduction system at later time points of differentiation, day 8 and day 10, respectively (Ng S.Y. et al., 2010; Liang X. et al., 2015) (Figure 9). We observed that the expression of nearly all the genes tested were affected upon Zrf1 knockdown cells. Especially the genes encoding the contractile proteins such as atrium specific α-MHC, MLC2a and ventricle specific β-MHC, MLC2v, and the gap junction proteins of conduction system such as Cx40, Cx43 were significantly down-regulated in shZrf1 cells. These findings were in accordance with the previous beating deficiency observed in shZrf1 derived EBs. Taken together our data suggest that Zrf1 is essential for the proper expression of genes that drive

cardiomyogenesis, and thereby the successful development of heart tissue without showing any bias towards cardiac subtypes.

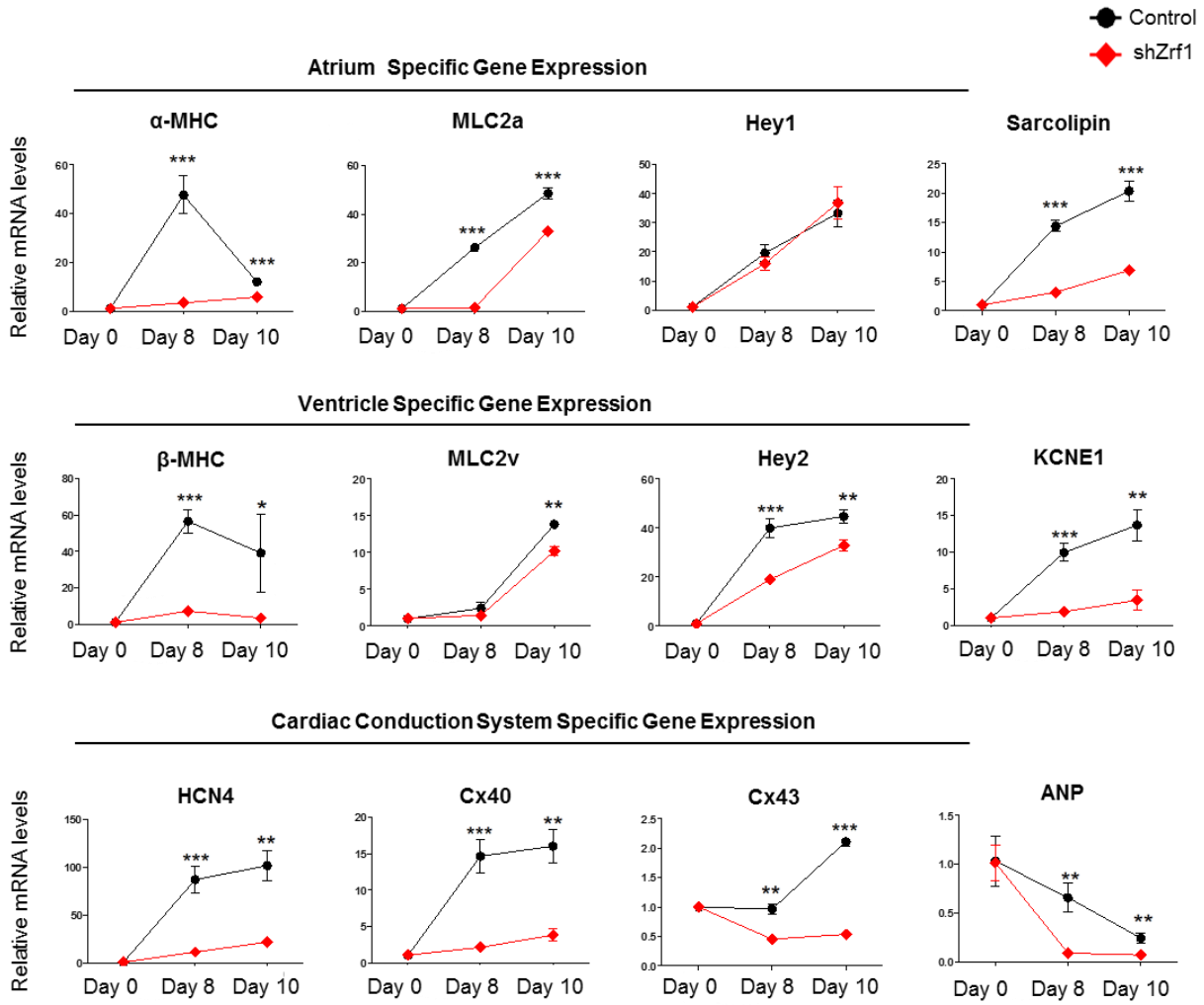

Figure 9. Zrf1 depletion affects the genes essential for the generation of atrium, ventricle and the nodal conduction system. Real-time qPCR of atrium, ventricle and nodal conduction system specific genes at days 0, 8 and 10 of EB differentiation. Expression was normalized to the housekeeping gene S18. Data represent the average of three experiments, +/- S.E.M. *p<0.5, **p<0.01, *** p<0.001 as calculated by two-tailed unpaired t test.

4.4 ZRF1 CONTROLS THE TEMPORAL EXPRESSION OF CARDIOMYOGENESIS SPECIFIC GENES

To further ensure that the aberrant gene expression profile seen in shZrf1 cells was a consequence of Zrf1 depletion, we assessed the expression of selected genes starting from the mesoderm formation to heart field specification in the rescue cell line (Figure

10). Genes involved in the signaling pathways, *Brachyury* or *Mesp1* (data not shown) were either not affected by Zrf1 depletion or showed enhanced expression in rescue cells. On contrast, we noticed a partial or complete restoration of the expression of first and second heart field related genes. Particularly the expression of *Nkx2.5*, *Hand1*, *Hand2* and *Tbx5* were almost at the same levels with the control cells at day 6. Collectively, these data indicate that re-expression of Zrf1 is not sufficient to rescue the expression of signaling genes, yet it plays a direct role in the transcriptional activation of genes essential for the formation of the heart fields.

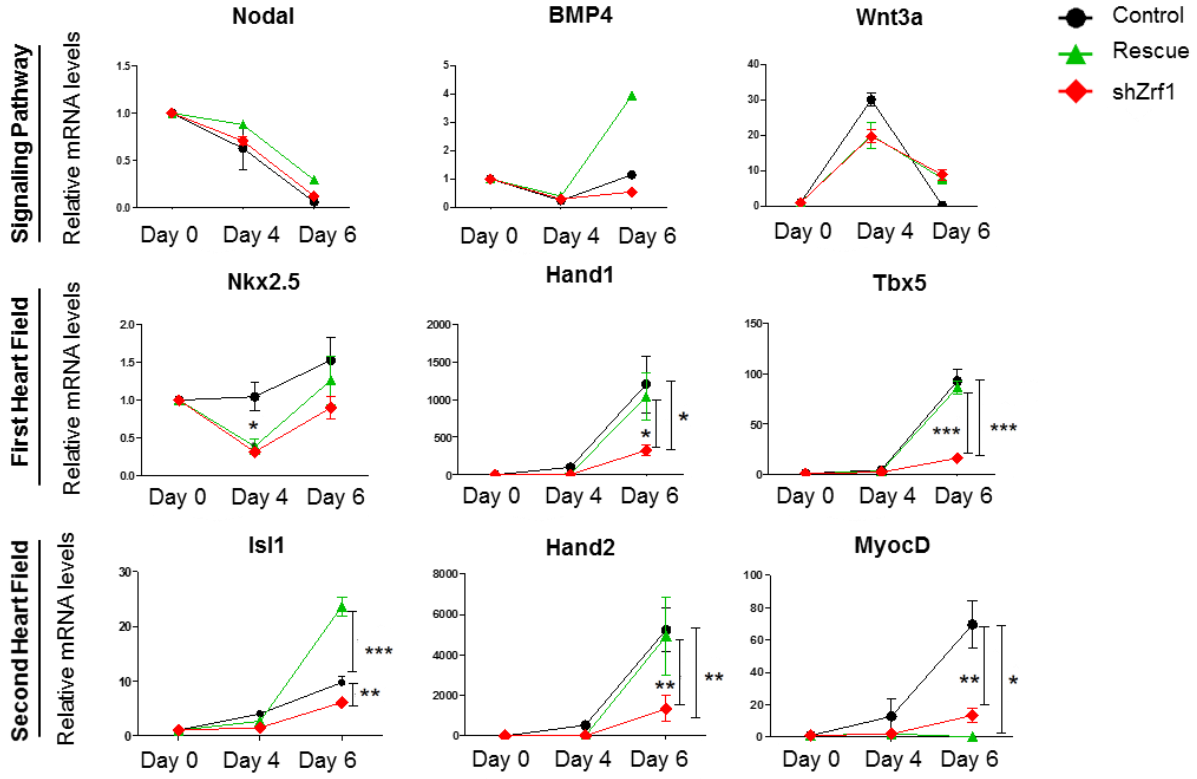

Figure 10. Zrf1 plays a direct role in the transcriptional activation of some cardiomyogenesis specific genes. Real-time qPCR of control, shZrf1 and rescue EBs for cardiomyogenesis specific genes at days 0, 4 and 6 of EB differentiation. Expression was normalized to the housekeeping gene S18. Data represent the average of three experiments, +/- S.E.M. *p<0.5, **p<0.01, *** p<0.001 as calculated by two-tailed unpaired t test.

To investigate the direct relationship between Zrf1 and heart field related genes, we carried out ChIP experiments utilizing a mESC line expressing a FLAG-tagged Zrf1 fusion protein. First we differentiated this cell line for 6 days and collected EB samples at day 2, 4 and 6. Then we performed a ChIP-qPCR with specific primers designed to

clarify Zrf1 occupancy on a set of selected cardiomyogenesis specific genes (*Brachyury, Mesp1, Hand1, Hand2* and *Tbx5*) over a time course (Figure 11A). In line with the mRNA expression data, we observed that Zrf1 particularly occupies the transcription start sites (TSSs) of *Nkx2.5*, *Hand1*, *Hand2* and *Tbx5* genes compared to the promoter of *Mesp1* and E-box of *Brachyury*.

A)

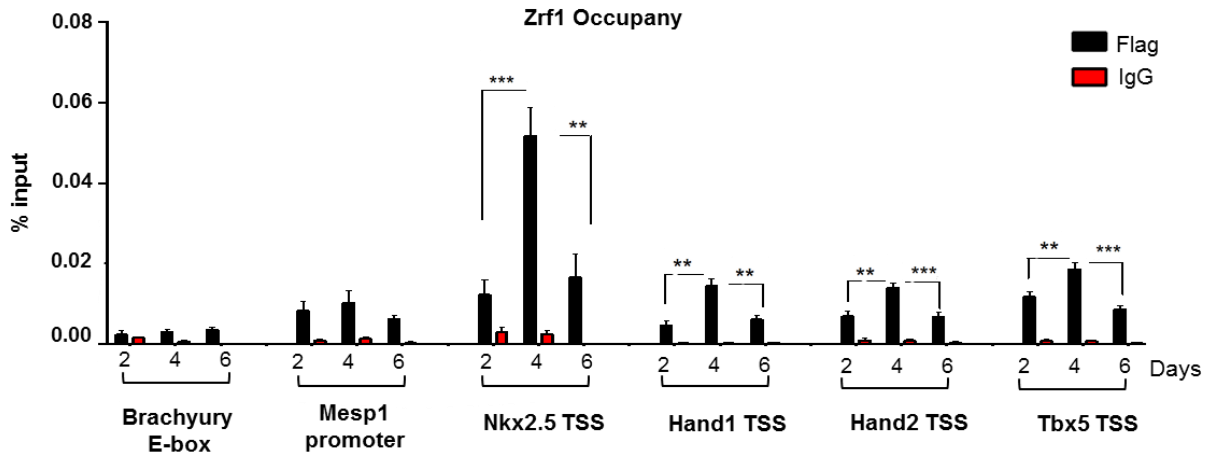

B)

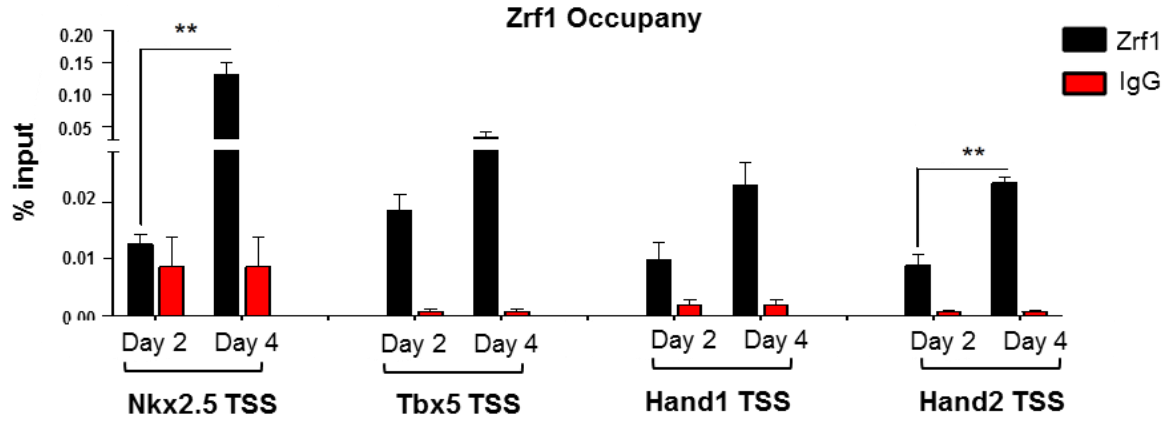

Figure 11. Zrf1 is specifically recruited the TSSs of its target genes at day 4 of differentiation. (A) Flag ChIP-qPCR of selected genes (Brachyury, Mesp1, Nkx2.5, Tbx5, Hand1, and Hand2) in flag tagged Zrf1 cells derived EBs after 2, 4 and 6 days of differentiation. Values are expressed as percentage of input. Data represent the average of three experiments, +/- S.E.M. **p<0.01, ***p<0.001 as calculated by two-tailed unpaired t test. (B) Zrf1 ChIP-qPCR of selected genes (*Nkx2.5*, *Tbx5*, *Hand1* and *Hand2*) in FLAG-tagged Zrf1 cells derived EBs after 2 and 4 days of differentiation. Values are expressed as percentage of input. Data represent the average of three experiments, +/- S.E.M. **p<0.01, as calculated by two-tailed unpaired t test.

Interestingly, Zrf1 is highly enriched at TSSs of these selected genes at day 4, which seems to be a critical time point in Zrf1 mediated gene expression. Likewise in ChIP experiments employing Zrf1 antibodies we found Zrf1 specifically occupying the TSSs of *Nkx2.5*, *Tbx5*, *Hand1* and *Hand 2* pointing at a function in activating these genes, similar to the Zrf1 dependent activation of neuronal lineage genes as previously reported (Figure 11B) (Richly H. et al., 2010).

Taken together, our data implies that Zrf1 binds the promoters of cardiomyogenesis specific genes early during development. Zrf1 dependent activation of its target genes causes the temporal expression of genes and thereby contributes to faithful cardiomyocyte formation.

4.5 ZRF1 IS ESSENTIAL FOR CARDIOMYOCYTE DIFFERENTIATION IN P19 CELLS

We have shown that Zrf1 plays a role in regulating genes that contribute to the generation of the first and second heart fields during murine embryonic development employing the hanging drop method. However this type of differentiation method has some drawbacks since the growth factors present in the serum that used in culture medium might cause some artefacts. To circumvent any possible misinterpretation of our previous findings based on this approach in E14 cells, we confirmed our data using P19 cell line which is an excellent model to study the early events of cardiac differentiation.

We generated P19 cell lines by stably integrating plasmids encoding short hairpin RNAs targeting Zrf1 (shZrf1) or a non-specific sequence (shControl) and ensured that the control cells are capable of generating functional cardiomyoyctes. First we determined the presence of cardiac specific contractile protein cardiac troponin I (cTnI) with immunostaining (Figure 12A). Further we analyzed the electrophysiological features of beating clusters with cell motion imaging system (Figure 12B). This system allows to the detection of beating frequency measurement, beating velocity magnitude and the motion directions in 2D videos with a method called “block matching”. In this method, beating signals generated from cells in each video frame is divided into analysis regions. A degree of similarity, or difference, between these regions in the video frames

A)

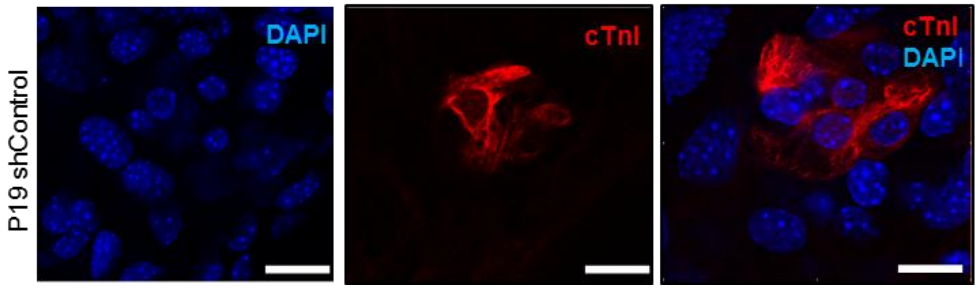

B)

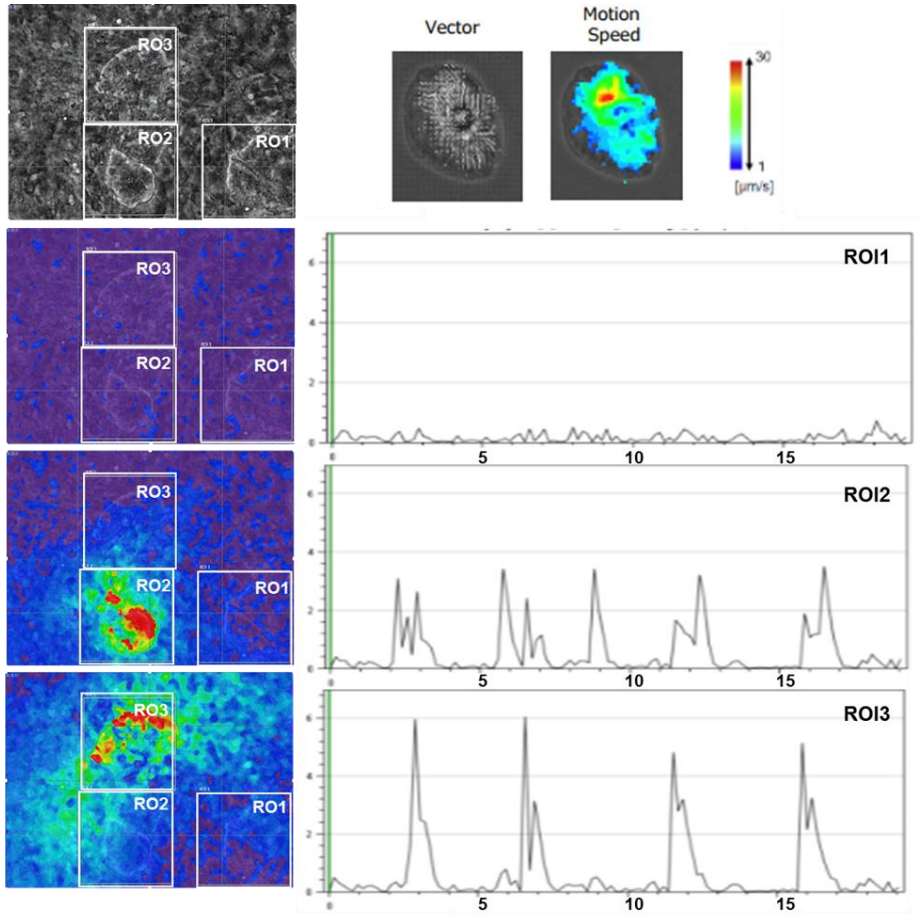

Figure 12. P19 cells are capable of generating functional cardiomyoyctes. (A) Representative immunofluorescence images of cardiac troponin I in control P19 cells after 15 days of cardiac differentiation. Scale bars, 10 µm. (B) Screen shots of the videos of beating areas in control P19 cells after processing them with cell motion imaging system, and the graphs which are showing the beating frequency and amplitude of the beating clusters in control cells. ROI1 (region of interest 1): control area, ROI2 (region of interest 2): beating cluster, ROI3 (region of interest 3): beating cluster. Color code from blue to red represent the motion speed of the contraction.

is calculated (Eeva L. et al, 2016). After differentiation of control cells for 15 days, we recorded different videos of the beating areas for 20 seconds. We adjusted the non-

beating area in the video as a threshold (RO1) and used the differences between the video frames to calculate a velocity vector with a color code reflecting the contractility of the area. Both of the selected areas displayed proper electrophysiology with contraction and relaxation periods. Whereas the beating frequency of RO2 was higher compared to RO3, the contraction amplitude of RO3 was stronger than RO2 which can be seen as sharper peaks in the diagram (Figure 12B RO2 and RO3). After verifying the success of differentiation system and knockdown of Zrf1 in two different clones (Figure 13A), we assessed the Zrf1 protein levels after supplementing the cells with 1% DMSO, which causes spontaneous differentiation. In line with our previous data, we observed that Zrf1 expression was increasing until day 4 after DMSO treatment (Figure 13B and 13C). Beyond this time point Zrf1 expression was decreasing stepwise suggesting a function early during P19 differentiation comparable to the Zrf1 function during stem cell differentiation.

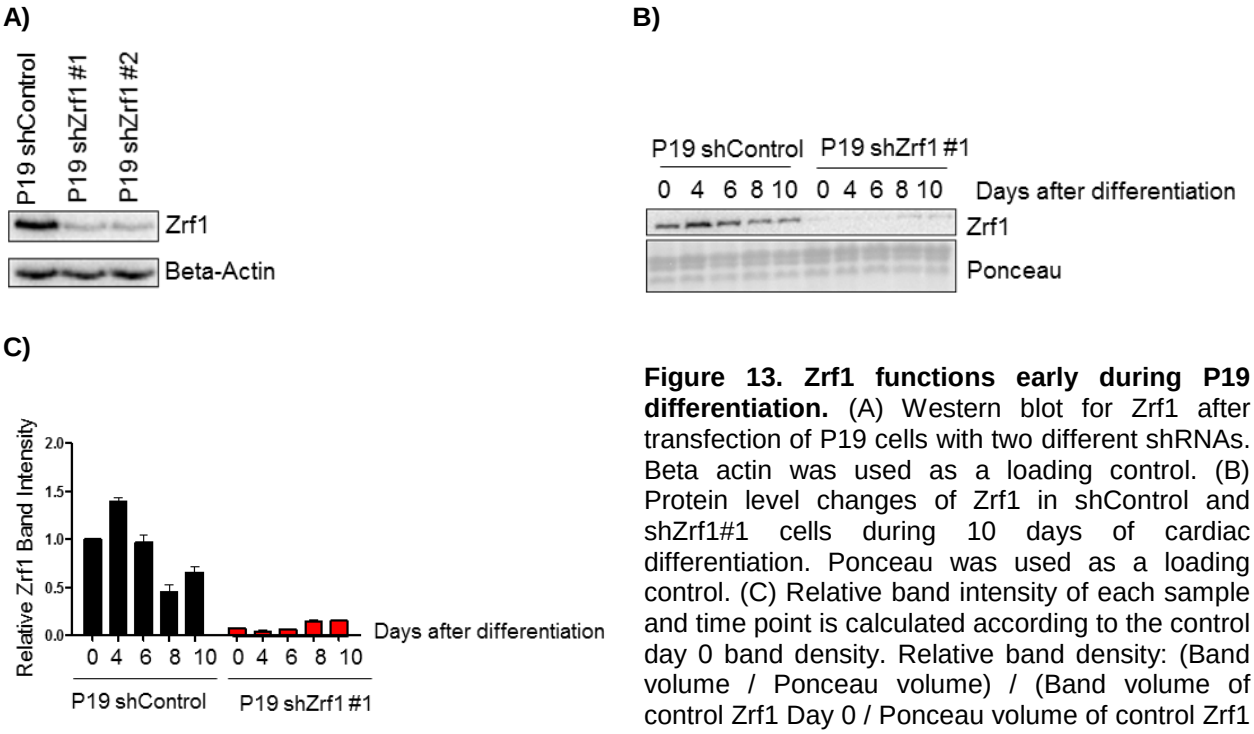

Figure 13. Zrf1 functions early during P19 differentiation. (A) Western blot for Zrf1 after transfection of P19 cells with two different shRNAs. Beta actin was used as a loading control. (B) Protein level changes of Zrf1 in shControl and shZrf1#1 cells during 10 days of cardiac differentiation. Ponceau was used as a loading control. (C) Relative band intensity of each sample and time point is calculated according to the control day 0 band density. Relative band density: (Band volume / Ponceau volume) / (Band volume of control Zrf1 Day 0 / Ponceau volume of control Zrf1 Day 0).

To further investigate the effect of Zrf1 depletion in adult cardiomyocytes, we analyzed the expression of genes, which are present in functional cardiomyocytes (Figure 14). Similar to E14 cells, the expression of cardiac troponins (*cTnT* and *cTnI*), myosin heavy

chains (*α-MHC* and *β-MHC*) and myosin light chains (*MYL2a* and *MYL2v*) were significantly reduced in Zrf1 knockdown cells. Moreover, the expression levels of genes encoding for gap junction proteins (Cx40 and Cx43) and genes that are responsible for the pacemaker activity of the heart (HCN4 and ANP) were drastically affected by Zrf1 depletion.

To further support our RT-PCR data with physiological findings, we examined the beating rate of control and Zrf1 knockdown cell lines at days 12 and 15 of cardiac differentiation. When analyzing areas of both monolayer cultures we observed in control conditions about 14% (Day 12) and 26 % (Day 15) beating activity (Figure 15). In contrast, when analyzing comparable monolayer regions of Zrf1 knockdown cells we nearly did not detect any beating activity. Collectively, these data show that Zrf1 is essential for the proper development of cardiac tissue.

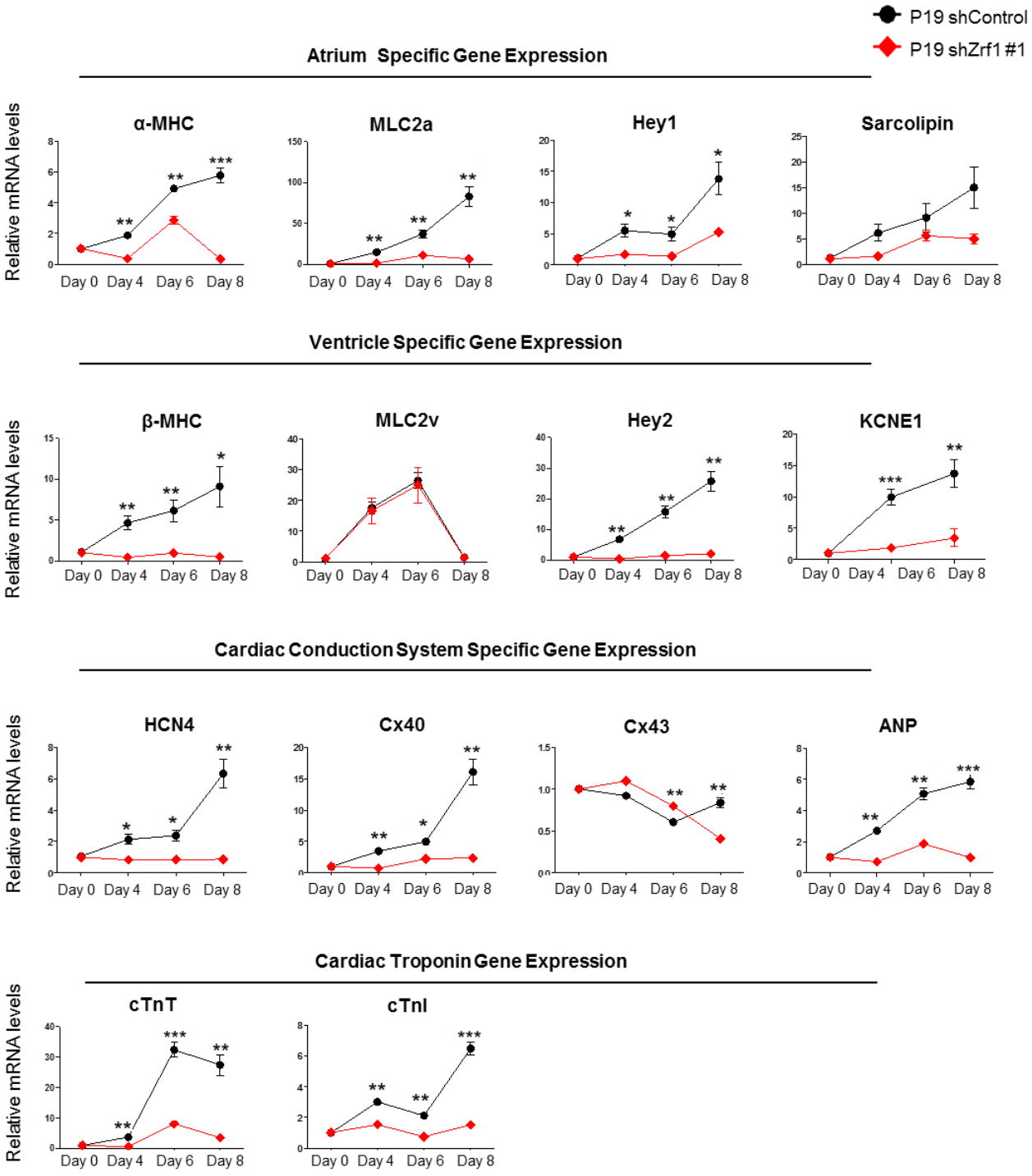

Figure 14: Zrf1 is essential for the cardiomyocyte differentiation in P19 cells. Real-time qPCR of atrium, ventricle, nodal conduction system specific genes together with cardiac troponin genes at days 0, 4, 6 and 8 days of cardiac differentiation. Expression was normalized to the housekeeping gene RPO. Data represent the average of three experiments, +/- S.E.M. *p<0.5, **p<0.01, *** p<0.001 as calculated by two-tailed unpaired t test.

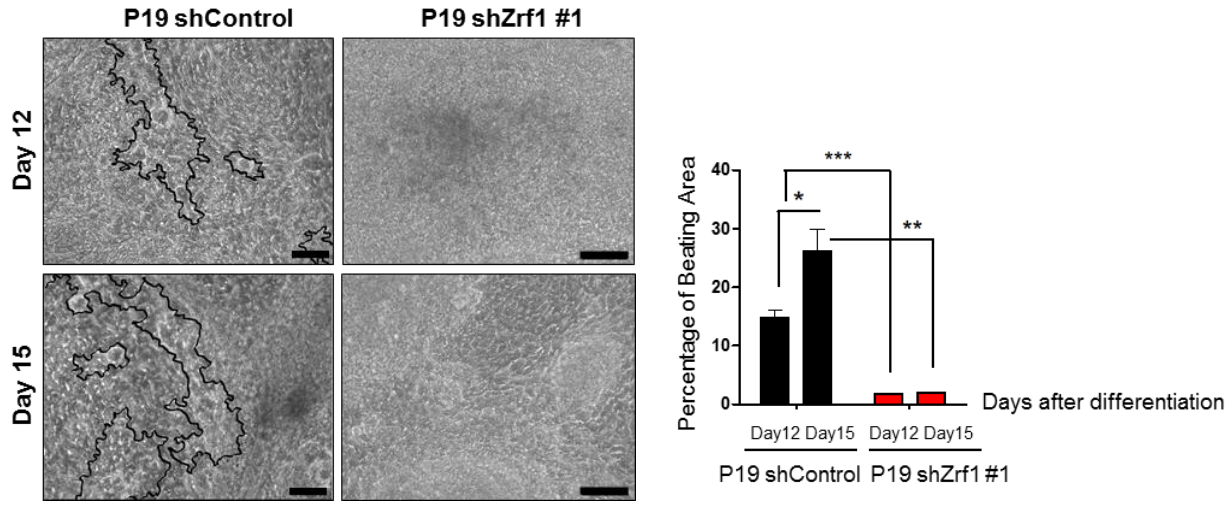

Figure 15. Zrf1 is essential for cardiomyocyte differentiation in P19 cells. Representative images and quantifications of beating areas of control and Zrf1 knockdown P19 cells after 12 and 15 days of cardiac differentiation. The spontaneous beating areas in P19 cells were recorded with either a Leica DM-IL or Leica AF7000 microscope and quantified by using ImageJ program. Scale bars, 100 μm. Data represent the average of three experiments, +/- S.E.M. *p<0.5, **p<0.01, *** p<0.001 as calculated by two-tailed unpaired t test.

5 DISCUSSION

Cardiovascular diseases (CVDs) are the leading cause of death worldwide. Whether caused by congenital defects or acquired injuries, CVDs usually result in loss of terminally differentiated cardiomyocytes. Adult human cardiomyocytes have limited self-renewal capacity. For this reason, stem cell-based regenerative therapy emerges as one of the most promising approaches to fight CVDs. Regenerative therapy aims at the replacement of injured or defective cardiac tissues by healthy ones making use of various cell sources (Aguirre A. et al., 2013). Still, faithful cardiac regenerative therapy will rely on understanding the underlying molecular mechanisms of cardiac development (Alexander J.M. and Bruneau B.G., 2010). The transcriptional regulation of cardiac development requires precise spatiotemporal control of gene expression. Hence, epigenetic regulators play an essential role by establishing a cell-type specific chromatin pattern which is essential for cell commitment and differentiation (Dobreva G. and Braun T., 2012). Among many epigenetic players, Trithorax and Polycomb group proteins have attracted particular attention for their ability to activate and repress transcription. Recently, Mel18, a subunit of PRC1 was shown to impact on mesoderm differentiation by directly controlling the expression of transcription factors essential for early cardiac mesoderm cell specification (Morey L. et al., 2015). Still, many open questions remain as to how PRCs regulate transcription during cardiomyogenesis.

In the present study, we elucidated a specific function of Zrf1 during the early stages of mesoderm development. The H2A-ubiquitin binding Zrf1 protein replaces PRC1 from promoters of its targets genes thereby contributing to transcriptional activation (Richly H. et al. 2010; Richly H. and Di Croce L., 2011). So far, Zrf1 was shown to primarily operate during differentiation into the neuronal lineage (Richly H. et al., 2010; Aloia L. et al., 2014; Aloia L. et al., 2015). Notably, PRC1 silences a wide range of genes generating the three germ layers during development (Bracken A.P. and Helin K., 2010). Hence, taking into account the broad spectrum of PRC1 target genes and the high abundance of H2A-ubiquitylation, we speculated that Zrf1 played additional roles in the formation of other germ layers. The phenotype of Zrf1 depleted EBs and the deregulation of key genes from the three germ layers during *in vitro* development

suggest a broader role of Zrf1 during development. We observed a particularly pronounced effect during the generation of mesoderm as the expression of one of the key factors, Brachyury, was drastically impaired in Zrf1 knockdown cells. Moreover, we noticed a significant reduction of the expression of *Flk1*, *Runx1* and *Mixl1* genes, which are important mesodermal markers for hematopoiesis. In agreement with these data it was previously shown that expression of Zrf1 is upregulated in acute and chronic myeloid leukemia (Greiner J. et al., 2003). Analyzing Zrf1 knockdown derived EBs we observed malformation of three different mesoderm derived tissues (adipocytes, cartilage and cardiac tissue). Importantly, re-establishing Zrf1 expression in the knockdown cells led to a significant rescue of the phenotypes. Taken together, these results point at an essential regulatory role for Zrf1 in the generation of mesoderm derived tissues.

Focusing on differentiation of mESC and P19 cells we found that Zrf1 plays a prominent role in cardiomyocyte differentiation. Analyzing the transcription of selected cardiac-specific genes in control and Zrf1 depleted EBs, we provide evidence that Zrf1 affects the expression of almost every tested gene. However, rescue experiments indicated a specific involvement of Zrf1 only in the transcriptional activation of first and second heart field related genes. Hand1, Hand2, Tbx5 are essential transcription factors for left-right patterning of the heart. Their expression is influenced by the transcription factor Nkx2.5, which represents a critical regulator of cardiomyogenesis. Notably, Zrf1 shows the strongest enrichment at the TSS of Nkx2.5 thereby controlling the main transcriptional regulator driving the development of both heart fields. Hence, the restoration of gene expression of other target genes (*Hand1*, *Hand2* and *Tbx5*) in the rescue cell line could partially be a consequence of Zrf1 dependent Nkx2.5 expression.

At the physiological level we observed a marked decrease of the beating activity in E14 derived Zrf1 knockdown cells, which was partially rescued by re-establishing Zrf1 expression. Since differentiation of E14 cells establishes a mixed population of differentiated cells we used a well-characterized model system of cardiac differentiation. Employing P19 cells we confirmed that Zrf1 is essential for the proper development of cardiomyocytes, which exhibit contractile units of reminiscent of heart muscles and

rhythmic beating activities as judged by RT-PCR, microscopy and beating assay results of control and Zrf1 knockdown cells.

In conclusion, Zrf1 contributes to the generation of the mesoderm layer but in particular it promotes the generation of the cardiac lineage during *in vitro* development. Hence, the function of Zrf1 needs to be considered when addressing molecular mechanisms of cardiovascular diseases.

6 REFERENCES

Abu-Issa R, Kirby ML. Patterning of the heart field in the chick. Dev Biol 2008 319(2):223–233

Aguirre A, Sancho-Martinez I, Izpisua Belmonte JC. Reprogramming toward heart regeneration: stem cells and beyond. Cell Stem Cell. 2013 Mar 7;12(3):275-84.

Akazawa H. Mechanisms of Cardiovascular Homeostasis and Pathophysiology–From Gene Expression, Signal Transduction to Cellular Communication. Circ J. 2015; 79: 2529 – 2536.

Alberts B, Johnson A, Lewis J, Raff M, Roberts K , Walter P. Molecular Biology of the Cell. 4th edition. 2002 New York: Garland Science.

Alexander JM, Bruneau BG. Lessons for cardiac regeneration and repair through development. Trends Mol Med 2010 16, 426-434.

Aloia L, Di Stefano B, Sessa A, Morey L, Santanach A, Gutierrez A, Cozzuto L, Benitah SA, Graf T, Broccoli V, Di Croce L. Zrf1 is required to establish and maintain neural progenitor identity. Genes Dev. 2014 Jan 15;28(2):182-97.

Aloia L, Gutierrez A, Caballero JM, Di Croce, L. Direct interaction between Id1 and Zrf1 controls neural differentiation of embryonic stem cells. EMBO reports 2015 16, 63-70.

Angers S, Moon RT. Proximal events in Wnt signal transduction. Nat Rev Mol Cell Biol. 2009;10(7):468–77. 2.

Ashe, HL. BMP signalling: synergy and feedback create a step gradient. Curr. Biol. 2005 15, R375–R377

Atit R, Sgaier S.K, Mohamed O.A, Taketo M.M, Dufort D, Joyner A.L, Niswander L, Conlon R.A. Beta-catenin activation is necessary and sufficient to specify the dorsal dermal fate in the mouse. Dev Biol. 2006;296:164–176

Bantignies F, Roure V, Comet I, Leblanc B, Schuettengruber B, Bonnet J, Tixier V, Mas A, Cavalli G. Polycomb-dependent regulatory contacts between distant Hox loci in Drosophila. Cell. 2011 Jan 21;144(2):214-26.

Barnes RM, Black BL. Nodal Signaling and Congenital Heart Defects. Chapter Etiology and Morphogenesis of Congenital Heart Disease 2016 pp 183-192.

Beisel C, Paro R. Silencing chromatin: comparing modes and mechanisms. Nat Rev Genet. 2011 Feb;12(2):123-35.

Belaguli NS, Sepulveda JL, Nigam V, Charron F, Nemer M, Schwartz RJ. Cardiac tissue enriched factors serum response factor and GATA-4 are mutual coregulators. Mol Cell Biol. 2000 Oct;20(20):7550-8.

Bernstein BE, Mikkelsen TS, Xie X, Kamal M, Huebert DJ, Cuff J, Fry B, Meissner A, Wernig M, Plath K, Jaenisch R, Wagschal A, Feil R, Schreiber SL, Lander ES. A bivalent chromatin structure marks key developmental genes in embryonic stem cells. Cell. 2006 Apr 21;125(2):315-26.

Biben C, Harvey RP. Homeodomain factor Nk2–5 controls left/right asymmetric expression of bHLH gene eHand during murine heart development. Genes Dev 1997; 11: 1357–1369

Billon N, Iannarelli P, Monteiro M.C, Glavieux-Pardanaud C, Richardson WD, Kessaris N, Dani C, Dupin E. The generation of adipocytes by the neural crest. Development. 2007;134:2283–2292.

Blackledge NP, Farcas AM, Kondo T, King HW, McGouran JF, Hanssen LL, Ito S, Cooper S, Kondo K, Koseki Y, Ishikura T, Long HK, Sheahan TW, Brockdorff N, Kessler BM, Koseki H, Klose RJ. Variant PRC1 complex-dependent H2A ubiquitylation drives PRC2 recruitment and polycomb domain formation. Cell. 2014 Jun 5;157(6):1445-59.

Bodmer R. The gene tinman is required for specification of the heart and visceral muscles in Drosophila. Development 1993; 118:719-729

Boheler KR, Czyz J, Tweedie D, Yang HT, Anisimov SV, Wobus AM. Differentiation of pluripotent embryonic stem cells into cardiomyocytes. Circ Res. 2002 Aug 9;91(3):189-201.

Boklage, CE. How New Humans Are Made: Cells and Embryos, Twins and Chimeras, Left and Right, Mind/Self/Soul, Sex, and Schizophrenia. World Scientific, 2010.

Bondue A, Lapouge G, Paulissen C, Semeraro C, Iacovino M, Kyba M, Blanpain C. Mesp1 acts as a master regulator of multipotent cardiovascular progenitor specification. Cell Stem Cell. 2008 Jul 3;3(1):69-84.

Böttcher RT, Niehrs C. Fibroblast growth factor signaling during early vertebrate development. Endocr Rev 2005;26:63–77

Boyer LA, Lee TI, Cole MF, Johnstone SE, Levine SS, Zucker JP, Guenther MG, Kumar RM, Murray HL, Jenner RG, Gifford DK, Melton DA, Jaenisch R, Young RA. Core transcriptional regulatory circuitry in human embryonic stem cells. Cell. 2005 Sep 23;122(6):947-56.

Bracken AP, Helin K. Polycomb group proteins: navigators of lineage pathways led astray in cancer. Nat Rev Cancer. 2009 Nov;9(11):773-84.

Bracken AP, Helin K. Polycomb group proteins: navigators of lineage pathways led astray in cancer. Nat Rev Cancer. 2009 Nov;9(11):773-84.

Brade T, Gessert S, Kuhl M, Pandur P. The amphibian second heart field: Xenopus islet-1 is required for cardiovascular development. Dev Biol. 2007 Nov 15;311(2):297-310.

Brade T, Pane LS, Moretti A, Chien KR, Laugwitz KL. Embryonic heart progenitors and cardiogenesis. Cold Spring Harb Perspect Med. 2013 Oct 1;3(10):a013847.

Brennan J, Norris DP, Robertson EJ. Nodal activity in the node governs left-right asymmetry Genes Dev. 2002;16:2339–44.

Brickman JM, Serup P. Properties of embryoid bodies. Wiley Interdiscip Rev Dev Biol. 2016 Dec 2.

Bruneau BG, Logan M, Davis N, Levi T, Tabin CJ, Seidman JG, Seidman CE. Chamber-specific cardiac expression of Tbx5 and heart defects in Holt-Oram syndrome. Dev Biol 1999; 211:100–108

Bruneau BG, Nemer G, Schmitt JP, Charron F, Robitaille L, Caron S, Conner DA, Gessler M, Nemer M, Seidman CE, Seidman JG. A murine model of Holt-Oram syndrome defines roles of the T-box transcription factor Tbx5 in cardiogenesis and disease. Cell. 2001; 106:709–721

Bu L, Jiang X, Martin-Puig S, Caron L, Zhu S, Shao Y, Roberts DJ, Huang PL, Domian IJ, Chien KR. Human ISL1 heart progenitors generate diverse multipotent cardiovascular cell lineages. Nature. 2009 Jul 2;460(7251):113-7.

Buckingham M, Meilhac S, Zaffran S. Building the mammalian heart from two sources of myocardial cells. Nat Rev Genet. 2005 Nov;6(11):826-35.

Burridge PW, Keller G, Gold JD, Wu JC. Production of de novo cardiomyocytes: human pluripotent stem cell differentiation and direct reprogramming. Cell Stem Cell. 2012 Jan 6;10(1):16-28.

Cai CL, Liang X, Shi Y, Chu PH, Pfaff SL, Chen J, Evans S. Isl1 identifies a cardiac progenitor population that proliferates prior to differentiation and contributes a majority of cells to the heart. Dev Cell. 2003 Dec;5(6):877-89.

Cao R, Tsukada Y, Zhang Y. Role of Bmi-1 and Ring1A in H2A ubiquitylation and Hox gene silencing. Mol Cell. 2005 Dec 22;20(6):845-54.

Cao R, Wang H, He J, Erdjument-Bromage H, Tempst P, Zhang Y. Role of hPHF1 in H3K27 methylation and Hox gene silencing. Mol Cell Biol. 2008 Mar;28(5):1862-72.

Cao R, Zhang Y. The functions of E(Z)/EZH2-mediated methylation of lysine 27 in histone H3. Curr Opin Genet Dev. 2004 Apr;14(2):155-64.

Chambers I, Silva J, Colby D, Nichols J, Nijmeijer B, Robertson M, Vrana J, Jones K, Grotewold L, Smith A. Nanog safeguards pluripotency and mediates germline development. Nature. 2007 Dec 20;450(7173):1230-4.

Charron F, Nemer M. GATA transcription factors and cardiac development. Semin Cell Dev Biol. 1999 Feb;10(1):85-91.

Chen C, Shen MM. Two modes by which Lefty proteins inhibit nodal signaling. Curr Biol. 2004;14:618–24.

Cheng Q, Pappas V, Hallmann A, Miller SM. Hsp70A and GlsA interact as partner chaperones to regulateasymmetric division in Volvox. Dev Biol 2005;286:537-48.

Comet I, Helin K. Revolution in the Polycomb hierarchy. Nat Struct Mol Biol. 2014 Jul;21(7):573-5.

Conlon FL, Lyons KM, Takaesu N, Barth KS, Kispert A, Herrmann B, Robertson EJ. A primary requirement for nodal in the formation and maintenance of the primitive streak in the mouse. Development. 1994;120:1919–28.

Cooper S, Dienstbier M, Hassan R, Schermelleh L, Sharif J, Blackledge NP, De Marco V, Elderkin S, Koseki H, Klose R, Heger A, Brockdorff N. Targeting polycomb to pericentric heterochromatin in embryonic stem cells reveals a role for H2AK119u1 in PRC2 recruitment. Cell Rep. 2014 Jun 12;7(5):1456-70.

Costa MW, Guo G, Wolstein O, Vale M, Castro ML, Wang L, Otway R, Riek P, Cochrane N, Furtado M, Semsarian C, Weintraub RG, Yeoh T, Hayward C, Keogh A, Macdonald P, Feneley M, Graham RM, Seidman JG, Seidman CE, Rosenthal N, Fatkin D, Harvey RP. Functional characterization of a novel mutation in NKX2-5 associated with congenital heart disease and adult-onset cardiomyopathy. Circ CardiovascGenet. 2013; 6(3):238–247.30

Costello I, Pimeisl IM, Drager S, Bikoff EK, Robertson EJ, Arnold SJ. The T-box transcription factor Eomesodermin acts upstream of Mesp1 to specify cardiac mesoderm during mouse gastrulation. Nat Cell Biol 2011 13:1084–1091.

Czermin B, Melfi R, McCabe D, Seitz V, Imhof A, Pirrotta V. Drosophila enhancer of Zeste/ESC complexes have a histone H3 methyltransferase activity that marks chromosomal Polycomb sites. Cell. 2002 Oct 18;111(2):185-96.

David R, Brenner C, Stieber J, Schwarz F, Brunner S, Vollmer M, Mentele E, Muller-Hocker J, Kitajima S, Lickert H, Rupp R, Franz WM (2008) MesP1 drives vertebrate cardiovascular differentiation through Dkk-1-mediated blockade of Wnt-signalling. Nat Cell Biol 10(3):338–345

David R, Jarsch VB, Schwarz F, Nathan P, Gegg M, Lickert H, Franz WM. Induction of MesP1 by Brachyury(T) generates the common multipotent cardiovascular stem cell. Cardiovasc Res. 2011 Oct 1;92(1):115-22.

Dell'Era P, Ronca R, Coco L, Nicoli S, Metra M, Presta M. Fibroblast growth factor receptor-1 is essential for in vitro cardiomyocyte development. Circ Res. 2003 Sep 5;93(5):414-20.

Di Croce L, Helin K. Transcriptional regulation by Polycomb group proteins. Nat Struct Mol Biol. 2013 Oct;20(10):1147-55.

Dobreva G, Braun T. When silence is broken: polycomb group proteins in heart development. Circ Res. 2012 Feb 3;110(3):372-4.

Draus JM, Hauck MA, Goetsch M, Austin EH, Tomita-Mitchell A, Mitchell ME. Investigation ofsomatic NKX2-5 mutations in congenital heart disease. J Med Genet. 2009; 46(2):115–122

Duncan DM, Burgess EA, Duncan I. Control of distal antennal identity and tarsal development in Drosophila by spineless-aristapedia, a homolog of the mammalian dioxin receptor. Genes Dev. 1998 May 1;12(9):1290-303.

Durocher D, Charron F, Warren R, Schwartz RJ, Nemer M. The cardiac transcription factors Nkx2-5 and GATA-4 are mutual cofactors. EMBO J. 1997 Sep 15;16(18):5687-96.

Dyer LA, Kirby ML. The role of secondary heart field in cardiac development. Dev Biol. 2009 Dec 15;336(2):137-44.

Edwards MKS, Harris JF, McBurney MW. Induced muscle differentiation in an embryonal carcinoma cell line. Mol Cell Biol 1983;3:2280–2286.

Elliott DA, Kirk EP, Yeoh T, Chandar S, McKenzie F, Taylor P, Grossfeld P, Fatkin D, Jones O, Hayes P, Feneley M, Harvey RP. Cardiac Homeobox gene NKX2-5 mutations and congenital heart disease: associations with atrial septal defect and hypoplastic left heart syndrome. J Am Coll Cardiol. 2003; 41(11):4–8

Engleka KA1, Manderfield LJ, Brust RD, Li L, Cohen A, Dymecki SM, Epstein JA. Islet1 derivatives in the heart are of both neural crest and second heart field origin. Circ Res. 2012 Mar 30;110(7):922-6.

Evans AL, Faial T, Gilchrist MJ, Down T, Vallier L, Pedersen RA, Wardle FC, Smith JC. Genomic targets of Brachyury (T) in differentiating mouse embryonic stem cells. PLoS One. 2012;7(3):e33346.

Evans MJ, Kaufman MH. Establishment in culture of pluripotential cells from mouse embryos. Nature. 1981 Jul 9;292(5819):154-6.

Firulli, AB, McFadden DG, Lin Q, Srivastava D and Olson EN. Heart and extra-embryonic mesodermal defects in mouse embryos lacking the bHLH Transcription factor Hand1. Nat. Genet. 1998; 18, 266-270

Francis NJ, Kingston RE, Woodcock CL. Chromatin compaction by a polycomb group protein complex. Science. 2004 Nov 26;306(5701):1574-7.

Fujiwara T, Dehart DB, Sulik KK, Hogan BL. Distinct requirements for extra-embryonic and embryonic bone morphogenetic protein 4 in the formation of the node and primitive streak and coordination of left–right asymmetry in the mouse. Development. 2002 Oct;129(20):4685-96.

Garg V, Kathiriya IS, Barnes R, Schluterman MK, King IN, Butler CA, Rothrock CR, Eapen RS, Hirayama-Yamada K, Joo K, Matsuoka R, Cohen JC, Srivastava D. GATA4 mutations cause human congenital heart defects and reveal an interaction with TBX5. Nature. 2003; 424 (6947): 443–7

Gessert S, Kuhl M. The multiple phases and faces of wnt signaling during cardiac differentiation and development. Circ Res. 2010 Jul 23;107(2):186-99.

Gesta S, Tseng YH, Kahn CR. Developmental origin of fat: tracking obesity to its source. Cell. 2007;131:242–256.

Gilbert S. Developmental biology 9th edition. 2010 USA: Sinauer Associates.

Goldmuntz E, Geiger E, Benson DW. NKX2.5 mutations in patients with tetralogy of fallot. Circulation. 2001; 104(21):2565–2 568.

Greiner J, Ringhoffer M, Taniguchi M, Hauser T, Schmitt A, Döhner H, Schmitt M. Characterization of several leukemia-associated antigens inducing humoral immune responses in acute and chronic myeloid leukemia. Int J Cancer. 2003 Aug 20;106(2):224-31.

Gritsman K, Zhang J, Cheng S, Heckscher E, Talbot WS, Schier AF. The EGF-CFC protein one-eyed pinhead is essential for nodal signaling. Cell. 1999;97:121–32.

Hatzold J, Conradt B. Control of apoptosis by asymmetric cell division. PLoS Biol 2008; 6:e84.

Hay DC, Sutherland L, Clark J, Burdon T. Oct-4 knockdown induces similar patterns of endoderm and trophoblast differentiation markers in human and mouse embryonic stem cells. Stem Cells. 2004;22:225–235.

He S, Nakada D, Morrison SJ.Mechanisms of stem cell self-renewal. Annu Rev Cell Dev Biol. 2009;25:377-406.

Heikinheimo M, Scandrett JM, Wilson DB. Localization of transcription factor GATA-4 to regions of the mouse embryo involved in cardiac development. Dev Biol. 1994 Aug;164(2):361-73.

Herrmann BG, Labeit S, Poustka A, King TR, Lehrach H. Cloning of the T gene required in mesoderm formation in the mouse. Nature. 1990 Feb 15;343(6259):617-22.

Hirai H, Karian P, Kikyo N. Regulation of embryonic stem cell self-renewal and pluripotency by leukaemia inhibitory factor. *Biochem J. 2011 Aug 15;438(1):11-23.*

Hirayama-Yamada K, Kamisago M, Akimoto K, Aotsuka H, Nakamura Y, Tomita H, Furutani M, Imamura S, Takao A, Nakazawa M, Matsuoka R. Phenotypes with GATA4 or NKX2.5 mutations in familial atrial septal defect. Am J MedGenet A. 2005; 135(1):47–52

Hiroi Y, Kudoh S, Monzen K, Ikeda Y, Yazaki Y, Nagai R, Komuro I. Tbx5 associates with Nkx2-5 and synergistically promotes cardiomyocyte differentiation. Nature Genetics. 2001; 28 (3): 276–80

Huang J, Elicker J, Bowens N, Liu X, Cheng L, Cappola TP, Zhu X, Parmacek MS. Myocardin regulates BMP10 expression and is required for heart development. J Clin Invest. 2012 Oct;122(10):3678-91

Huang J, Min Lu M, Cheng L, Yuan LJ, Zhu X, Stout AL, Chen M, Li J, Parmacek MS. Myocardin is required for cardiomyocyte survival and maintenance of heart function. Proc Natl Acad Sci U S A. 2009 Nov 3;106(44):18734-9.

Jaenisch R, Young R. Stem cells, the molecular circuitry of pluripotency and nuclear reprogramming. Cell. 2008 Feb 22;132(4):567-82.

Jiao K, Kulessa H, Tompkins K, Zhou Y, Batts L, Baldwin HS, Hogan BL. An essential role of Bmp4 in the atrioventricular septation of the mouse heart. Genes Dev. 2003 Oct 1;17(19):2362-7.

Jürgens G. A group of genes controlling the spatial expression of the bithorax complex in Drosophila. Nature. 1985 316, 153-155.

Kasahara H, Benson DW. Biochemical analyses of eight NKX2.5 homeodomain missense mutations causing atrioventricular block and cardiac anomalies. Cardiovasc Res. 2004; 64(1):40–51

Keller GM. In vitro differentiation of embryonic stem cells. Curr Opin Cell Biol 1985 7, 862–869.

Kelly RG. The second heart field. Curr Top Dev Biol 2012 100: 33–65.

Kimelman D. Mesoderm induction: From caps to chips. Nat Rev Genet. 2006 May;7(5):360-72.

Kitajima S, Takagi A, Inoue T, Saga Y. MesP1 and MesP2 are essential for the development of cardiac mesoderm. Development. 2000 Aug;127(15):3215-26.

Klattenhoff CA, Scheuermann JC, Surface LE, Bradley RK, Fields PA, Steinhauser ML, Ding H, Butty VL, Torrey L, Haas S, Abo R, Tabebordbar M, Lee RT, Burge CB, Boyer LA. Braveheart, a long noncoding RNA required for cardiovascular lineage commitment. Cell. 2013 Jan 31;152(3):570-83

Komuro I, Izumo S. Csx: a murine homeobox-containing gene specifically expressed in the developing heart. Proc Natl Acad Sci U S A. 1993;90:8145–8149.

Kouzarides T. Chromatin modifications and their function. Cell. 2007 Feb 23;128(4):693-705.

Ku M, Koche RP, Rheinbay E, Mendenhall EM, Endoh M, Mikkelsen TS, Presser A, Nusbaum C, Xie X, Chi AS, Adli M, Kasif S, Ptaszek LM, Cowan CA, Lander ES, Koseki H, Bernstein BE. Genomewide analysis of PRC1 and PRC2 occupancy identifies two classes of bivalent domains. PLoS Genet. 2008 Oct;4(10):e1000242.

Kumar A, Lualdi M, Lewandoski M, Kuehn MR. Broad mesodermal and endodermal deletion of Nodal at postgastrulation stages results solely in left/right axial defects. Dev Dyn. 2008;237:3591–601.

Kuo CT, Morrisey EE, Anandappa R, Sigrist K, Lu MM, Parmacek MS, Soudais C, Leiden JM. GATA4 transcription factor is required for ventral morphogenesis and heart tube formation. Genes Dev. 1997;11:1048–1060.

Kuzmichev A, Nishioka K, Erdjument-Bromage H, Tempst P, Reinberg D. Histone methyltransferase activity associated with a human multiprotein complex containing the Enhancer of Zeste protein. Genes Dev. 2002 Nov 15;16(22):2893-905.

Kwon SM, Alev C, Asahara T. The role of notch signaling in endothelial progenitor cell biology. Trends Cardiovasc Med. 2009 Jul;19(5):170-3.

Laugesen A, Helin K. Chromatin repressive complexes in stem cells, development, and cancer. Cell Stem Cell. 2014 Jun 5;14(6):735-51.

Laugwitz KL, Moretti A, Caron L, Nakano A, Chien KR. Islet1 cardiovascular progenitors: a single source for heart lineages? Development. 2008 Jan;135(2):193-205.

Laurila E, Ahola A, Hyttinen J, Aalto-Setälä K. Methods for in vitro functional analysis of iPSC derived cardiomyocytes - Special focus on analyzing the mechanical beating behavior. Biochim Biophys Acta. 2016 Jul;1863(7 Pt B):1864-72.

laus A, Saga Y, Taketo MM, Tzahor E, Birchmeier W. Distinct roles of Wnt/beta-catenin and Bmp signaling during early cardiogenesis. Proc Natl Acad Sci U S A. 2007;104(47):18531–6.

Lawson KA, Meneses JJ, Pedersen RA. Clonal analysis of epiblast fate during germ layer formation in the mouse embryo. Development. 1991 Nov;113(3):891-911.

Lee KY, Jeong JW, Wang J, Ma L, Martin JF, Tsai SY, Lydon JP, DeMayo FJ. Bmp2 is critical for the murine uterine decidual response. Mol Cell Biol. 2007 Aug;27(15):5468-78.

Lewis EB. A gene complex controlling segmentation in reading of the manuscript. Drosophila. Nature. 1978 Dec 7;276(5688):565-70.

Liang Q, Molkentin JD. Divergent signaling pathways converge on GATA4 to regulate cardiac hypertrophic gene expression. J Mol Cell Cardiol. 2002;34:611–616

Liang X, Evans SM, Sun Y. Insights into cardiac conduction system formation provided by HCN4 expression. Trends Cardiovasc Med. 2015 Jan;25(1):1-9.

Liberatore CM1, Searcy-Schrick RD, Yutzey KE. Ventricular expression of Tbx5 inhibits normal heart chamber development. Dev Biol. 2000 Jul 1;223(1):169-80.

Lindsley RC, Gill JG, Murphy TL, Langer EM, Cai M, Mashayekhi M, Wang W, Niwa N, Nerbonne JM, Kyba M, Murphy KM. Mesp1 coordinately regulates cardiovascular fate restriction and epithelial-mesenchymal transition in differentiating ESCs. Cell Stem Cell. 2008 Jul 3;3(1):55-68.

Lints TJ, Parsons LM, Hartley L, Lyons I, Harvey RP. Nkx-2.5: a novel murine homeobox gene expressed in early heart progenitor cells and their myogenic descendants. Development. 1993;119:419–431.

Liu W, Selever J, Wang D, Lu MF, Moses KA, Schwartz RJ, Martin JF. Bmp4 signaling is required for outflow-tract septation and branchial-arch artery remodelling. Proc. Natl. Acad. Sci. U. S. A. 101, 4489–4494

Loden M, van Steensel B. Whole-genome views of chromatin structure. Chromosome Res. 2005;13:289–298.

Logan CY, Nusse R. The Wnt signaling pathway in development and disease. Annu Rev Cell Dev Biol. 2004;20:781–810.).

Loh KM, Lim B. A precarious balance: pluripotency factors as lineage specifiers. Cell Stem Cell. 2011 Apr 8;8(4):363-9.

Loh YH, Wu Q, Chew JL, Vega VB, Zhang W, Chen X, Bourque G, George J, Leong B, Liu J, Wong KY, Sung KW, Lee CW, Zhao XD, Chiu KP, Lipovich L, Kuznetsov VA, Robson P, Stanton LW, Wei CL, Ruan Y, Lim B, Ng HH. The Oct4 and Nanog transcription network regulates pluripotency in mouse embryonic stem cells. Nat Genet. 2006 Apr;38(4):431-40.

Lyons I, Parsons LM, Hartley L, Li R, Andrews JE, Robb L, Harvey RP. Myogenic and morphogenetic defects in the heart tubes of murine embryos lacking the homeo box gene Nkx2-5. Genes Dev. 1995 Jul 1;9(13):1654-66.

Lyons KM, Hogan BL, Robertson EJ. Colocalization of BMP 7 and BMP 2 RNAs suggests that these factors cooperatively mediate tissue interactions during murine development. Mech Dev. 1995 Mar;50(1):71-83.

Ma L, Lu MF, Schwartz RJ, Martin JF. Bmp2 is essential for cardiac cushion epithelial– mesenchymal transition and myocardial patterning. Development. 2005 Dec;132(24):5601-11.

MacDonald BT, He X. Frizzled and LRP5/6 receptors for Wnt/beta-catenin signaling. Cold Spring Harb Perspect Biol. 2012;4(12):a007880.

MacDonald BT, Tamai K, He X. Wnt/beta-catenin signaling: components,mechanisms, and diseases. Dev Cell. 2009;17(1):9–26.

Maitra M, Schluterman MK, Nichols HA, Richardson JA, Lo CW, Srivastava D, Garg V. Interaction of Gata4 and Gata6 with Tbx5 is critical for normal cardiac development. Dev Biol. 2009; 326:368–377

Margueron R, Reinberg D. The Polycomb complex PRC2 and its mark in life. Nature. 2011 Jan 20;469(7330):343-9.

Martin GR. Isolation of a pluripotent cell line from early mouse embryos cultured in medium conditioned by teratocarcinoma stem cells. Proc Natl Acad Sci U S A. 1981 Dec;78(12):7634-8.

Marvin MJ, Di Rocco G, Gardiner A, Bush SM, Lassar AB. Inhibition of Wnt activity induces heart formation from posterior mesoderm. Genes Dev 2001;15:316–27.; 2.

Masui S, Nakatake Y, Toyooka Y, Shimosato D, Yagi R, Takahashi K, Okochi H, Okuda A, Matoba R, Sharov AA, Ko MS, Niwa H. Pluripotency governed by Sox2 via regulation of Oct3/4 expression in mouse embryonic stem cells. Nat Cell Biol. 2007 Jun;9(6):625-35.

Matin MM, Walsh JR, Gokhale PJ, Draper JS, Bahrami AR, Morton I, Moore HD, Andrews PW. Specific knockdown of Oct4 and beta2-microglobulin expression by RNA interference in human embryonic stem cells and embryonic carcinoma cells. Stem Cells. 2004;22:659–668.

Mazzoni EO, Mahony S, Closser M, Morrison CA, Nedelec S, Williams DJ, An D, Gifford DK, Wichterle H. Synergistic binding of transcription factors to cell-specific enhancers programs motor neuron identity. Nat Neurosci. 2013 Sep;16(9):1219-27.

McBurney MW, Jones-Villeneuve EMV, Edwards MKS, Anderson PJ. Control of muscle and neuronal differentiation in a cultured embryonal carcinoma cell line. Nature 1982;299:165–167.

McFadden DG, Barbosa AC, Richardson JA, Schneider MD, Srivastava D, Olson ED. The Hand1 and Hand2 transcription factors regulate expansion of the embryonic cardiac ventricles in a gene dosage-dependent manner. Development 2005; 132: 189-201

Mendenhall EM, Koche RP, Truong T, Zhou VW, Issac B, Chi AS, Ku M, Bernstein BE. GC-rich sequence elements recruit PRC2 in mammalian ES cells. PLoS Genet. 2010 Dec 9;6(12):e1001244.

Meshorer E, Misteli T. Chromatin in pluripotent embryonic stem cells and differentiation. Nat Rev Mol Cell Biol. 2006 Jul;7(7):540-6.

Michelson AM, Gisselbrecht S, Zhou Y, Baek KH, Buff EM. Dual functions of the heartless fibroblast growth factor receptor in development of the Drosophila embryonic mesoderm. Dev Genet 1998;22:212–29.

Miller SM, Kirk DL. glsA, a Volvox gene required for asymmetric division and germ cell specification, encodes a chaperone-like protein. Development 1999;126:649-58.

Mitsui K, Tokuzawa Y, Itoh H, Segawa K, Murakami M, Takahashi K, Maruyama M, Maeda M, Yamanaka S. The homeoprotein Nanog is required for maintenance of pluripotency in mouse epiblast and ES cells. Cell. 2003;113:631–642.

Mjaatvedt CH, Nakaoka T, Moreno-Rodriguez R, Norris RA, Kern MJ, Eisenberg CA, Turner D, Markwald RR. The outflow tract of the heart is recruited from a novel heart-forming field. Dev Biol. 2001 Oct 1;238(1):97-109.

Molkentin JD, Lin Q, Duncan SA, Olson EN. Requirement of the transcription factor GATA4 for heart tube formation and ventral morphogenesis. Genes Dev. 1997;11:1061–1072.

Molkentin JD. The zinc finger-containing transcription factors GATA-4, -5, and -6: ubiquitously expressed regulators of tissue-specific gene expression. J Biol Chem. 2000;275:38949–38952.

Moorman A. Heart fields and cardiac morphogenesis. 2013 Cold Spring Harb Perspect Med 10.1101/cshperspect.a015750.

Morey L, Santanach A, Blanco E, Aloia L, Nora EP, Bruneau BG, Di Croce L. Polycomb Regulates Mesoderm Cell Fate-Specification in Embryonic Stem Cells through Activation and Repression Mechanisms. Cell Stem Cell. 2015 Sep 3;17(3):300-15

Morey L, Santanach A, Blanco E, Aloia L, Nora EP, Bruneau BG, Di Croce L. Polycomb Regulates Mesoderm Cell Fate-Specification in Embryonic Stem Cells through Activation and Repression Mechanisms. Cell Stem Cell. 2015 Sep 3;17(3):300-15.

Morley P, Whitfield JF. The differentiation inducer, dimethyl sulfoxide, transiently increases the intracellular calcium ion concentration in various cell types. J Cell Physiol 1993;156:219–225.

Morrison SJ, Shah NM, Anderson DJ. Regulatory mechanisms in stem cell biology. Cell. 1997 Feb 7;88(3):287-98.

Müller J, Hart CM, Francis NJ, Vargas ML, Sengupta A, Wild B, Miller EL, O'Connor MB, Kingston RE, Simon JA. Histone methyltransferase activity of a Drosophila Polycomb group repressor complex. Cell. 2002 Oct 18;111(2):197-208.

Mummery CL, Zhang J, Ng ES, Elliott DA, Elefanty AG, Kamp TJ. Differentiation of Human ES and iPS Cells to Cardiomyocytes: A Methods Overview Circ Res. 2012 Jul 20;111(3):344-58.

Naito AT, Shiojima I, Akazawa H, Hidaka K, Morisaki T, Kikuchi A, Komuro I. Developmental stage-specific biphasic roles of Wnt/betacatenin signaling in cardiomyogenesis and hematopoiesis. Proc Natl Acad Sci U S A. 2006;103(52):19812–7.

Neuhaus H, Rosen V, Thies RS. Heart specific expression of mouse BMP-10 a novel member of the TGF-[beta] superfamily. Mech Dev. 1999 Feb;80(2):181-4.

Ng SY, Wong CK, Tsang SY. Differential gene expressions in atrial and ventricular myocytes: insights into the road of applying embryonic stem cell-derived cardiomyocytes for future therapies. Am J Physiol Cell Physiol. 2010 Dec;299(6):C1234-49.

Nichols J, Zevnik B, Anastassiadis K, Niwa H, Klewe-Nebenius D, Chambers I, Scholer H, Smith A. Formation of pluripotent stem cells in the mammalian embryo depends on the POU transcription factor Oct4. Cell. 1998;95:379–391.

Niwa H, Burdon T, Chambers I, Smith A. Self-renewal of pluripotent embryonic stem cells is mediated via activation of STAT3. Genes Dev. 1998 Jul 1;12(13):2048-60.

Noseda M, Peterkin T, Simoes FC, Patient R, Schneider MD. Cardiopoietic factors: Extracellular signals for cardiac lineage commitment. Circ Res. 2011 Jan 7;108(1):129-52.

O'Connor TP, Crystal RG. Genetic medicines: treatment strategies for hereditary disorders. Nat Rev Genet. 2006 Apr;7(4):261-76.

Okumura-Nakanishi S, Saito M, Niwa H, Ishikawa F. Oct-3/4 and Sox2 regulate Oct-3/4 gene in embryonic stem cells. J Biol Chem. 2005;280:5307–5317.

Ouyang P, Saarel E, Bai Y, Luo C, Lv Q, Xu Y, Wang F, Fan C, Younoszai A, Chen Q, Tu X, Wang QK. A de novo mutation in NKX2.5 associated with atrial septal defects, ventricular noncompaction, syncope and suddendeath. Clin Chim Acta. 2011 Jan 14;412(1-2):170-5.

Ozhan G, Weidinger G. Wnt/β-catenin signaling in heart regeneration. Cell Regen (Lond). 2015 Jul 8;4(1):3.

Paige SL, Osugi T, Afanasiev OK, Pabon L, Reinecke H, Murry CE. Endogenous Wnt/beta-catenin signaling is required for cardiac differentiation in human embryonic stem cells. PLoS One. 2010 Jun 15;5(6):e11134.

Pansky B. Review of Medical Embryology Book. Macmillan USA (December 1, 1982)

Pappas V, Miller SM. Functional analysis of the Volvox carteri asymmetric division protein GlsA. Mech Dev 2009; 126:842-51.

Parmacek MS. Myocardin-related transcription factors: critical coactivators regulating cardiovascular development and adaptation. Circ Res. 2007; 100(5):633–644.

Prall OW, Menon MK, Solloway MJ,Watanabe Y, Zaffran S, Bajolle F, Biben C, McBride JJ, Robertson BR, Chaulet H, Stennard FA, Wise N, Schaft D, Wolstein O, Furtado MB, Shiratori H, ChienKR, Hamada H, Black BL, Saga Y, Robertson EJ, Buckingham ME, Harvey RP. An Nkx2-5/Bmp2/Smad1 negative feedback loop controls heart progenitor specification and proliferation. Cell 2007 128(5):947–959.

Pray-Grant MG, Daniel JA, Schieltz D, Yates JR 3rd, Grant PA. Chd1 chromodomain links histone H3 methylation with SAGA- and SLIK-dependent acetylation. Nature. 2005 Jan 27;433(7024):434-8.

Reifers F, Walsh EC, Léger S, Stainier DY, Brand M. Induction and differentiation of the zebrafish heart requires fibroblast growth factor 8 (fgf8/acerebellar). Development. 2000 Jan;127(2):225-35.

Ringrose L, Ehret H, Paro R. Distinct contributions of histone H3 lysine 9 and 27 methylation to locus-specific stability of polycomb complexes. Mol Cell. 2004 Nov 19;16(4):641-53.

Ringrose L, Paro R. Epigenetic regulation of cellular memory by the Polycomb and Trithorax group proteins. Annu Rev Genet. 2004;38:413-43.

Risebro CA, Smart N, Dupays L, Breckenridge R, Mohun TJ, Riley PR. Hand1 regulates cardiomyocyte proliferation versus differentiation in the developing heart. Development. 2006; 133, 4595-4606

Robertson EJ. Embryo-derived stem cell lines. In Robertson, E.J. (ed.), Teratocarcinomas and Embryonic Stem Cells: A Practical Approach, IRL Press, . Oxford, 1987 pp. 71-l 12.

Roche P, Czubryt MP, Wigle JT. Molecular Mechanisms of Cardiac Development: Chapter 1. Advances in Biochemistry in Health and Disease 4. Springer Science and Business Media New York 2013. pp:19-34.

Romito A, Cobellis G. Pluripotent Stem Cells: Current Understanding and Future Directions. Stem Cells Int. 2016;2016:9451492.

Ruppert EE, Fox RS, Barnes RD. Introduction to Bilateria. Invertebrate Zoology (7th ed.). 2004 Brooks/Cole. pp. 217–218

Saga Y, Hata N, Kobayashi S, Magnuson T, Seldin MF, Taketo MM (1996) MesP1: a novel basic helix–loop–helix protein expressed in the nascent mesodermal cells during mouse gastrulation. Development 122 (9):2769–2778

Saga Y, Kitajima S, Miyagawa-Tomita S. Mesp1 expression is the earliest sign of cardiovascular development. Trends Cardiovasc Med 2000 10(8):345–352

Saga Y, Miyagawa-Tomita S, Takagi A, Kitajima S, Miyazaki J, Inoue T. MesP1 is expressed in the heart precursor cells and required for the formation of a single heart tube. Development 1999 126 (15):3437–3447

Santos-Rosa H, Schneider R, Bernstein BE, Karabetsou N, Morillon A, Weise C, Schreiber SL, Mellor J, Kouzarides T. Methylation of histone H3 K4 mediates association of the Isw1p ATPase with chromatin. Mol Cell. 2003 Nov;12(5):1325-32.

Sarkozy A, Conti E, Neri C, D'Agostino R, Digilio MC, Esposito G, Toscano A, Marino B, Pizzuti A, Dallapiccola B. Spectrum of atrial septal defects associated with mutations of NKX2.5 and GATA4 transcription factors. J Med Genet. 2005 Feb;42(2):e16.

Saurin AJ, Shao Z, Erdjument-Bromage H, Tempst P, Kingston RE. A Drosophila Polycomb group complex includes Zeste and dTAFII proteins. Nature. 2001 Aug 9;412(6847):655-60.

Sauvageau M, Sauvageau G. Polycomb group proteins: multi-faceted regulators of somatic stem cells and cancer. Cell Stem Cell. 2010 Sep 3;7(3):299-313.

Schneider V, Mercola M. Wnt antagonism initiates cardiogenesis in Xenopus laevis. Genes Dev 2001;15:304–15

Schott JJ, Benson DW, Basson CT, Pease W, Silberbach GM, Moak JP, Maron BJ, Seidman CE, Seidman JG. Con-genital heart disease caused by mutations in the transcription factor NKX2-5. Science. 1998; 281(5373):108–111.

Schuettengruber B, Cavalli G. Recruitment of polycomb group complexes and their role in the dynamic regulation of cell fate choice. Development. 2009 Nov;136(21):3531-42.

Schwartz YB, Pirrotta V. Polycomb silencing mechanisms and the management of genomic programmes. Nat Rev Genet. 2007 Jan;8(1):9-22.

Sengupta AK, Kuhrs A, Müller J. General transcriptional silencing by a Polycomb response element in Drosophila. Development. 2004 May;131(9):1959-65.

Sepulveda JL, Belaguli N, Nigam V, Chen CY, Nemer M, Schwartz RJ. GATA-4 and Nkx-2.5 coactivate Nkx-2 DNA binding targets: role for regulating early cardiac gene expression. Mol Cell Biol. 1998 Jun;18(6):3405-15.

Sexton T, Yaffe E, Kenigsberg E, Bantignies F, Leblanc B, Hoichman M, Parrinello H, Tanay A, Cavalli G. Three-dimensional folding and functional organization principles of the Drosophila genome. Cell. 2012 Feb 3;148(3):458-72.

Sha K, Boyer LA. The chromatin signature of pluripotent cells. StemBook [Internet]. Cambridge (MA): Harvard Stem Cell Institute; 2008-.2009 May 31.

Shah S, Gnanasegaran G, Sundberg-Cohon J, Buscombe JR. The Heart: Anatomy, Physiology and Exercise Physiology. Integrating Cardiology for Nuclear Medicine Physicians 2009; pp 3-22

Shao Z, Raible F, Mollaaghababa R, Guyon JR, Wu CT, Bender W, Kingston RE. Stabilization of chromatin structure by PRC1, a Polycomb complex. Cell. 1999 Jul 9;98(1):37-46.

Shen MM, Schier AF. The EGF-CFC gene family in vertebrate development. Trends Genet. 2002;16:303–9).

Shen MM. Nodal signaling: developmental roles and regulation. Development. 2007;134:1023–34).

Showell C, Binder O, Conlon FL. T-box genes in early embryogenesis. Dev Dyn 2004 229: 201–218.

Simon JA, Kingston RE. Mechanisms of polycomb gene silencing: knowns and unknowns. Nat Rev Mol Cell Biol. 2009 Oct;10(10):697-708.

Simon JA, Kingston RE. Occupying chromatin: Polycomb mechanisms for getting to genomic targets, stopping transcriptional traffic, and staying put. Mol Cell. 2013 Mar 7;49(5):808-24.

Small EM, Warkman AS, Wang DZ, Sutherland LB,Olson EN, Krieg PA. Myocardin is sufficient and necessary for cardiac gene expression in Xenopus. Development. 2005;132(5):987–997.

Smith AG, Heath JK, Donaldson DD, Wong GG, Moreau J, Stahl M, Rogers D. Inhibition of pluripotential embryonic stem cell differentiation by purified polypeptides. Nature. 1988 Dec 15;336(6200):688-90.

Smith AG, Hooper ML. Buffalo rat liver cells produce a diffusible activity which inhibits the differentiation of murine embryonal carcinoma and embryonic stem cells. Dev Biol 1987 121, 1–9.

Smith AG. Embryo-derived stem cells: of mice and men. Annu Rev Cell Dev Biol. 2001;17:435-62.

Squazzo SL, O'Geen H, Komashko VM, Krig SR, Jin VX, Jang SW, Margueron R, Reinberg D, Green R, Farnham PJ. Suz12 binds to silenced regions of the genome in a cell-type-specific manner. Genome Res. 2006 Jul;16(7):890-900.

Srivastava D, Thomas T, Lin Q., Kirby ML, Brown D. and Olson EN. Regulation of cardiac mesodermal and neural crest development by the bHLH transcription factor, dHAND. Nat. Genet. 1997;16, 154-160

Stallmeyer B, Fenge H, Nowak-Göttl U, Schulze-Bahr E. Mutational spectrum in the cardiac transcription factor gene NKX2.5 (CSX) associated with congenital heart disease. ClinGenet. 2010; 78(6):533–540

Stamos JL, Weis WI. The beta-catenin destruction complex. Cold Spring Harb Perspect Biol. 2013;5(1):a007898.

Streit A, Lee KJ, Woo I, Roberts C, Jessell TM, Stern CD. Chordin regulates primitive streak development and the stability of induced neural cells, but is not sufficient for neural induction in the chick embryo. Development. 1998 Feb;125(3):507-19.

Sun Y, Liang X, Najafi N, Cass M, Lin L, Cai CL, Chen J, Evans SM. Islet 1 is expressed in distinct cardiovascular lineages, including pacemaker and coronary vascular cells. Dev Biol. 2007 Apr 1;304(1):286-96.

Tam PP, Behringer RR. Mouse gastrulation: the formation of a mammalian body plan. Mech Dev. 1997 Nov;68(1-2):3-25.

Tanaka M, Chen Z, Bartunkova S, Yamasaki N, Izumo S. The cardiac homeobox gene Csx/Nkx2.5 lies genetically upstream of multiple genes essential for heart development. Development. 1999 Mar;126(6):1269-80.

Tanizawa Y, Riggs AC, Dagogo-Jack S, Vaxillaire M, Froguel P, Liu L, Donis-Keller H, Permutt MA. Isolation of the human LIM/ homeodomain gene islet-1 and

identification of a simple sequence repeat polymorphism. Diabetes. 1994 Jul;43(7):935-41.

Thomson JA, Itskovitz-Eldor J, Shapiro SS, Waknitz MA, Swiergiel JJ, Marshall VS, Jones JM. Embryonic stem cell lines derived from human blastocysts. Science. 1998 Nov 6;282(5391):1145-7.

Thomson M, Liu SJ, Zou LN, Smith Z, Meissner A, Ramanathan S. Pluripotency factors in embryonic stem cells regulate differentiation into germ layers. Cell. 2011 Jun 10;145(6):875-89.

Till JE, McCulloch EA. A direct measurement of the radiation sensitivity of normal mouse bone marrow cells. Radiat Res. 1961 Feb;14:213-22.

Till JE, McCulloch EA. Hemopoietic stem cell differentiation. Biochim Biophys Acta 1980 605, 431–459.

Tzahor E, Lassar AB. Wnt signals from the neural tube block ectopic cardiogenesis. Genes Dev 2001;15:255–60.

Ueno S, Weidinger G, Osugi T, Kohn AD, Golob JL, Pabon L, Reinecke H, Moon RT, Murry CE. Biphasic role for Wnt/beta-catenin signaling in cardiac specification in zebrafish and embryonic stem cells. Proc Natl Acad Sci U S A. 2007 Jun 5;104(23):9685-90.

Waldo KL, Kumiski DH, Wallis KT, Stadt HA, Hutson MR, Platt DH, Kirby ML. Conotruncal myocardium arises from a secondary heart field. Development 2001 128: 3179–3188

Wang H, Wang H, Powell SN, Iliakis G, Wang Y. ATR affecting cell radiosensitivity is dependent on homologous recombination repair but independent of nonhomologous end joining. Cancer Res. 2004 Oct 1;64(19):7139-43.

Watt AJ, Battle MA, Li J, Duncan SA. GATA4 is essential for formation of the proepicardium and regulates cardiogenesis. Proc Natl Acad Sci U S A. 2004 Aug 24;101(34):12573-8.

Weissman IL. Stem cells: units of development, units of regeneration, and units in evolution. Cell 2000 100, 157–168.

Wilkinson DG, Bhatt S, Herrmann BG. Expression pattern of the mouse T gene and its role in mesoderm formation. Nature 1990 343: 657–659.

Williams RL, Hilton DJ, Pease S, Willson TA, Stewart CL, Gearing DP, Wagner EF, Metcalf D, Nicola NA, Gough NM. Myeloid leukaemia inhibitory factor maintains the developmental potential of embryonic stem cells. Nature. 1988 Dec 15;336(6200):684-7.

Winnier G, Blessing M, Labosky PA, Hogan BL. Bone morphogenetic protein-4 is required for mesoderm formation and patterning in the mouse. G Genes Dev. 1995 Sep 1;9(17):2105-16.

Wobus AM, Boheler KR. Embryonic stem cells: prospects for developmental biology and cell therapy. Physiol Rev. 2005 Apr;85(2):635-78.

Wrage PC, Tran T, To K, Keefer EW, Ruhn KA, Hong J, Hattangadi S, Treviño I, Tansey MG. The Neuro-Glial Properties of Adipose-Derived Adult Stromal (ADAS) Cells Are Not Regulated by Notch 1 and Are Not Derived from Neural Crest Lineage. PLoS ONE. 2008;3:e1453.

Wysocka J, Swigut T, Milne TA, Dou Y, Zhang X, Burlingame AL, Roeder RG, Brivanlou AH, Allis CD. WDR5 associates with histone H3 methylated at K4 and is essential for H3 K4 methylation and vertebrate development. Cell. 2005 Jun 17;121(6):859-72.

Yamagishi H, Olson EN, Srivastava D. The basic helix-loop-helix transcription factor, dHAND, is required for vascular development. J.Clin. Invest. 2000; 105, 261-270

Ying QL, Nichols J, Chambers I, Smith A. BMP induction of Id proteins suppresses differentiation and sustains embryonic stem cell self-renewal in collaboration with STAT3. Cell. 2003 Oct 31;115(3):281-92.

Ying QL, Nichols J, Chambers I, Smith A. BMP induction of Id proteins suppresses differentiation and sustains embryonic stem cell self-renewal in collaboration with STAT3. Cell. 2003 Oct 31;115(3):281-92.

Yuan S, Schoenwolf GC. Islet-1 marks the early heart rudiments and is asymmetrically expressed during early rotation of the foregut in the chick embryo. Anat Rec 2000 260(2):204–207

Yuasa S, Fukuda K. Cardiac regenerative medicine. Circ J. 2008;72 Suppl A:A49-55.

Yuasa S, Itabashi Y, Koshimizu U, Tanaka T, Sugimura K, Kinoshita M, Hattori F, Fukami S, Shimazaki T, Ogawa S, Okano H, Fukuda K. Transient inhibition of BMP signaling by Noggin induces cardiomyocyte differentiation of mouse embryonic stem cells. Nat Biotechnol. 2005 May;23(5):607-11

Zaehres H, Lensch MW, Daheron L, Stewart SA, Itskovitz-Eldor J, Daley GQ. High-efficiency RNA interference in human embryonic stem cells. Stem Cells. 2005;23:299–305.

Zaffran S, Frasch M. Early signals in cardiac development. Circ Res 2002;91:457–69.

Zeisberg EM, Ma Q, Juraszek AL, Moses K, Schwartz RJ, Izumo S, Pu WT. Morphogenesis of the right ventricle requires myocardial expression of Gata4. J Clin Invest. 2005 Jun;115(6):1522-31.

Zhang H, Bradley A. Mice deficient for BMP2 are nonviable and have defects in amnion/chorion and cardiac development. Development 1996 122, 2977–2986;

Zhu W, Shiojima I, Hiroi Y, Zou Y, Akazawa H, Mizukami M, Toko H, Yazaki Y, Nagai R, Komuro I. Functional analyses of three Csx/Nkx-2.5 mutations that cause human congenital heart disease. The Journal of Biological Chemistry. 2000; 275 (45): 35291–6

Zrf1 depletion causes an aggressive cancer phenotype and favors cell survival

INDEX OF CONTENT

1 INTRODUCTION 107

1.1 BREAST CANCER 107

1.1.1 BASIC FACTS 107

1.1.2 RISK FACTORS 107

1.1.3 HISTOPATHOLOGICAL CLASSIFICATION 109

1.1.4 MOLECULAR CLASSIFICATION 110

1.1.5 TREATMENT 112

1.2 APOPTOSIS 119

1.2.1 THE INTRINSIC (MITOCHONDRIAL) PATHWAY FOR APOPTOSIS 120

1.2.2 REGULATION OF APOPTOSIS 121

1.3 RELATIONSHIP OF ZRF1 AND CANCER 124

2 AIM OF THE STUDY 125

3 MATERIAL AND METHODS 126

3.1 CBIOPORTAL SOFTWARE ANALYSIS 126

3.2 CELL CULTURE 126

3.3 GENERATION OF STABLE ZRF1 KNOCKDOWN CELL LINES 126

3.4 CELL GROWTH EXPERIMENT 127

3.5 PREPARATION AND USAGE OF CHEMICAL STOCKS 127

3.6 MTT CELL PROLIFERATION ASSAY 127

3.7 KI67 STAINING 128

3.8 WOUND HEALING ASSAY 128

3.9 TRANSWELL CELL MIGRATION ASSAY 128

3.10 CELL ADHESION EXPERIMENT 129

3.11 ORGANOID LIKE STRUCTURE GENERATION IN SUSPENSION CULTURE 129

3.12 DETECTION OF APOPTOSIS 130

3.13 CELL CYCLE ANALYSIS 130

3.14 WESTERN BLOT 131

3.15 RNA EXTRACTION, CDNA SYNTHESIS AND RT-QPCR 131

4 RESULTS 134

4.1 ZRF1 IS OVEREXPRESSED IN BREAST INVASIVE DUCTAL CARCINOMA 134

4.2 ZRF1 DISPLAYS A DUAL ROLE ON CELL PROLIFERATION IN MICROENVIRONMENT CONTEXT 138

4.3 ZRF1 KNOCKDOWN CELLS EXHIBIT MORE AGGRESSIVE CANCER PHENOTYPE 142

4.4 ZRF1 KNOCKDOWN CELLS ARE RESISTANT TO ENDOCRINE THERAPY 145

5 DISCUSSION 149

6 REFERENCES 153

INDEX OF FIGURES

INTRODUCTION

Figure 1. Histological classification of breast cancer subtypes. 110
Figure 2. Molecular classification of breast cancer. 112
Figure 3. Schematic representation of the common structural and functional domains of ERα and ERβ. 114
Figure 4. Mechanisms of estrogen receptor (ER) action in breast cancer. 115
Figure 5. Mechanism of Tamoxifen. 117
Figure 6. The molecular mechanism for the pure anti-estrogen fulvestrant (ICI 185,780). 119
Figure 7. The molecular mechanism of the mitochondrial (intrinsic) pathway. 121
Figure 8. The Bcl-2 family of proteins. 122
Figure 9. Proteins of the IAP family. 123

RESULTS

Figure 1. Representative pie chart of the breast cancer type distribution in the TCGA dataset.. 134
Figure 2. CNA analysis of Zrf1. 135
Figure 3. Somatic mutation rate and types of Zrf1. 136
Figure 4. mRNA expression profile of Zrf1. 137
Figure 5. Zrf1 knockdown cells grow significantly less compared to control cells in normal conditions. 138
Figure 6. Zrf1 depletion stimulates S phase transition of cells. 140
Figure 7. Zrf1 depleted cells proliferated significantly more upon growth factor withdrawal. 141
Figure 8. Zrf1 knockdown cells migrate significantly more compared to control cells. 143
Figure 9. Zrf1 depletion results in the decrease of cellular adhesion properties. 144
Figure 10. Zrf1 knockdown cells are resistant to endocrine therapy. 147
Figure 11. Zrf1 regulates the expression of anti-apoptotic genes. 148
Figure 12. Summary of Zrf1's role in breast invasive ductal carcinoma. 150

INDEX OF TABLES

Table 1. shRNA plasmids used for the cell line generation. 127
Table 2. Antibodies used in western blot experiments. 131
Table 3. Primers used in RT-qPCR experiments.. 133

INDEX OF ABBREVIATIONS

BC: Breast cancer

BRCA1: Breast cancer 1, early onset

BRCA2: Breast cancer 2, early onset

ER: Estrogen receptor

DCIS: Ductal carcinoma *in situ*

LCIS: Lobular carcinoma *in situ*

Her2: Human epidermal growth factor receptor 2

PR: Progesterone receptor

TN: Triple negative

EGFR: Epidermal growth factor receptor

CSC: Cancer stem cell

OS: Overian suppression

SERMs: Selective estrogen receptor modulators

SERDs: Selective estrogen receptor down-regulators

AIs: Aromatase inhibitors

E1: Estrone

E2: Estradiol

E3: Estriol

DBD: DANN binding domain

LBD: Ligand binding domain

ERE: Estrogen response element

Hsp: Heat shock protein

AF: Activation function

AP-1: Activator protein-1

SP-1: Specificity protein-1

IGF1R: Insulin like growth factor receptor 1

PI3K/Akt: Phosphatidylinositol 3-kinase/Akt

TAM: Tamoxifen

4-OHT: 4-OH Tamoxifen

ICI: ICI 182,780

MPT: Mitochondrial permeability transition

MOMP: Mitochondrial outer membrane permeabilization

cyt c: Cythochrome C

SMAC: Second mitochondria-derived activator of caspases

AIF: Apoptosis inducing factor

EndoG: Endonuclease G

Apaf-1: Apoptotic protease activating factor 1

BH: Bcl-2 homolog

OMM: Outer mitochondria membrane

IAPs: Inhibitors of apoptosis proteins

c-IAP1: Cellular IAP1

c-IAP2: Cellular IAP2

NAIP: Neuronal apoptosis inhibitory protein

XIAP: X-linked inhibitor of apoptosis

BRUCE: BIR-containing ubiquitin conjugating enzyme

Ts-IAP: Testis-specific IAP

1 INTRODUCTION

1.1 BREAST CANCER

1.1.1 BASIC FACTS

Breast cancer (BC) is defined as an uncontrolled growth of breast cells. The majority of breast cancers begin either in the lobules of the breast tissue, which are the responsible part for milk production or in the ducts of the breast tissue, which connect the lobules to the nipple. Less commonly, BC can arise from the stromal tissues, which include the fatty and fibrous connective tissues of the breast (Society, AC, 2015-2016).

BC is one of the most diagnosed cancer worldwide. According to the American Cancer Society data, invasive breast cancer would be diagnosed in about 246,660 women and 2,600 men. In addition, 61,000 new cases of *in situ* breast cancer were diagnosed in women at the end of 2016 (Society, AC, 2016).

The most common symptom of breast cancer is the presence of a lump or mass in the breast. In rare situations, symptoms like changing in the size or shape of the breast, dimpling of the skin, fluid coming from the nipple, or a red scaly patch of skin can be observed. In cancer with distant spread of the disease, there might even be bone pain, swollen lymph nodes, shortness of breath, or yellow skin (NCI, 2016).

Due to improvement in early detection and treatment, the overall breast cancer death rates declined from 1989 to 2012. However, breast cancer still ranks second as a cause of cancer death in women. At the end of 2016, 40,450 women were estimated to lose their life because of BC (Society, AC, 2016).

1.1.2 RISK FACTORS

Sex is one of the most important determinants for developing breast cancer. Women have higher risks compared to men. Approximately every 1 in 8 women and every 1 in 870 men develop breast cancer during their lifetime.

Breast cancer incidence and death rates generally increase with age. The median age of diagnosis for black women is 58 and for white women is 62 (Howlader N. et al., 2015).

Family history of breast cancer particularly in a first-degree relative increases the risk of developing breast cancer proportionally. For example, a woman with a family history of breast cancer in a first degree relative has 2 fold more chance to develop breast cancer compared to a woman without a family history (Collaborative group, 2001).

Genetic alterations in either tumor suppressor genes or oncogenes generally predispose to develop cancers. *BRCA1* (Breast Cancer 1, early onset) and *BRCA2* (Breast Cancer 2, early onset) are well-studied tumor suppressor genes, which are correlated with breast cancer progression. BRCA genes are critical in DNA repair and their inactivation leads to the accumulation of errors and genetic instability favoring the growth of tumors. The average risk of developing a breast cancer by the age of 70 in the general population is 7%. However, this ratio increases up to 57%-65% and 45%-%55 for BRCA1 and BRCA2 mutation carriers, respectively (Antoniou A. et al., 2003; Chen S. and Parmigiani G., 2007; Mavaddat N. et al., 2013).

Duration of menstrual cycles is one of the main risk factors for breast cancer. Early menstruation or late menopause increases the lifetime exposure to reproductive hormones, and thereby can increase the risk of developing breast cancer. It has been shown that longer menstrual cycles are strongly linked to estrogen receptor positive (ER+) breast cancer subtypes (Anderson K.N. et al., 2014).

Pregnancy and breastfeeding are risk factors which are also related to the reproductive hormone exposure. Multiple pregnancies and having the first child at a younger age decreases the risk of breast cancer. For example, the risk of developing breast cancer is 50% less for a woman who had her first child before the age of 20 compared to a woman who did not have her first child at this age (Albrektsen G. et al., 2005). In line with this data, longer breastfeeding reduces the lifetime exposure to reproductive hormones (Britt K. et al., 2007) and stimulates the further differentiation of breast tissue, thereby decreases the risk of developing breast cancer (Faupel-Badger J.M. et al., 2013).

Obesity and low physical activity are other parameters increasing the breast cancer risk. Excess weight and a less active life style are increasing the fat tissue in the body which represents the largest source of estrogen, particularly in postmenopausal women.

Hence, increased exposure to estrogen are again promoting the cancer risk (WCRF, 2007; Neilson H.K. et al., 2009).

1.1.3 HISTOPATHOLOGICAL CLASSIFICATION

Breast cancer is a genetically and clinically heterogeneous disease including many different subtypes (Stingl J. and Caldas C., 2007). The right classification of the subtype is very important to select the best treatment regimen for the patient to benefit most. Because some breast cancers are less aggressive they can be treated with a surgical removal of a discrete portion or "lump" of breast (lumpectomy). Other breast cancers are more aggressive and life-threatening, and require to be treated with aggressive therapies that have major adverse effects.

The most adopted histopathological classification of breast cancer is based on the classification suggested by the WHO (Lakhani S. et al., 2012). Based on this classification, breast cancer can be broadly categorized into two major groups: *in situ* carcinoma and invasive (infiltrating) carcinoma.

In situ carcinoma is used to describe non-invasive, pre-cancerous breast cancer which shows abnormal cells that have not moved out from their original tissue or moved into surrounding breast tissues (Lakhani S. et al., 2012). Breast carcinoma *in situ* is further sub-classified as ductal or lobular depending on where cancerous cells arise from. Ductal carcinoma *in situ* (DCIS) is more common than lobular carcinoma *in situ* (LCIS) and usually diagnosed as stage 0. Based on the architectural features of the tumor, DCIS is further classified into 5 subtypes: Comedo, Cribiform, Micropapillary, Papillary and Solid (Connoly J. et al., 2004) (Figure 1).

Invasive or infiltrating carcinoma is used to describe tumors which are spread or invaded into surrounding breast tissue. Similar to *in situ* carcinomas, invasive carcinomas also represent a heterogeneous group of tumors with different histological subtypes. The major subtypes are invasive ductal, invasive lobular, ductal/lobular, mucinous (colloid), tubular, medullary and papillary carcinomas (Figure 1). Invasive ductal carcinoma (IDC) is, by far, the most common type of invasive lesions. Whereas 70–80% of all invasive lesions are invasive ductal carcinoma, only 10% are invasive

lobular carcinoma (Li C.L. et al., 2005). IDC is further sub-classified as either well-differentiated (grade 1), moderately differentiated (grade 2) or poorly differentiated (grade 3) (Figure1) (Malhotra G.K et al., 2010).

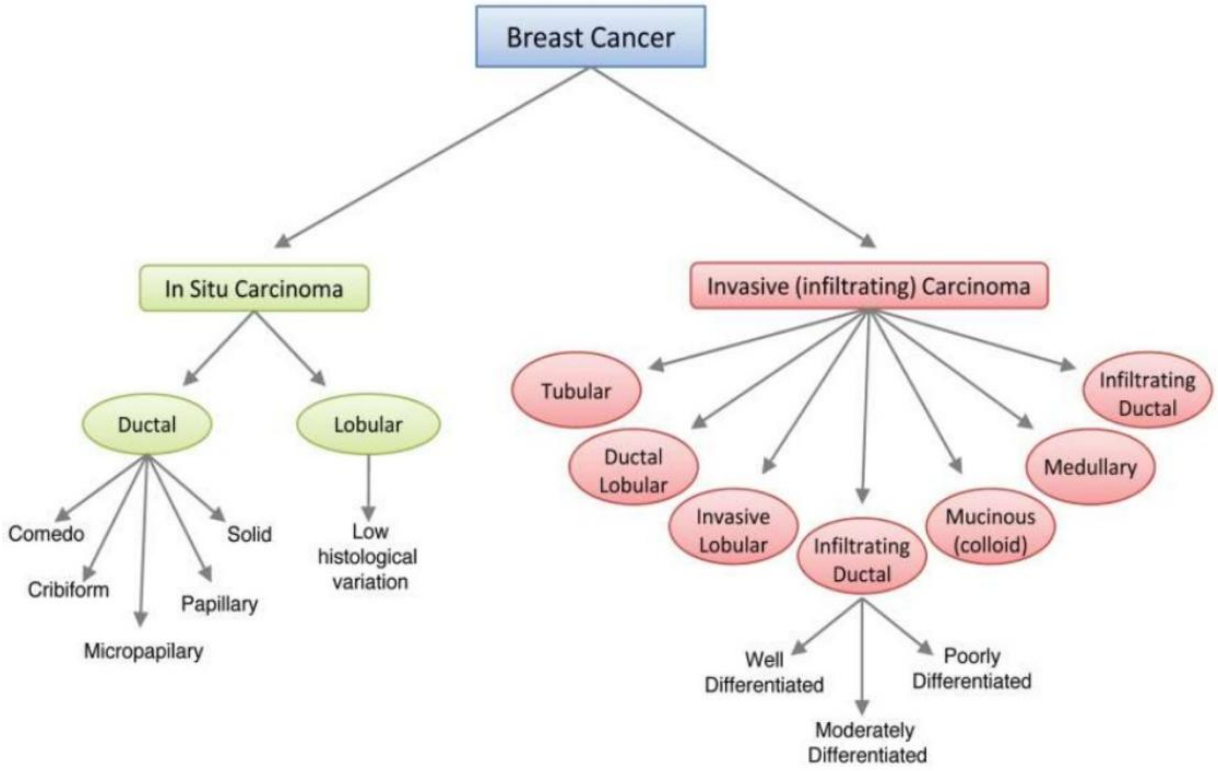

Figure 1. Histological classification of breast cancer subtypes. This scheme, currently used by clinicians, categorizes the heterogeneity found in breast cancer based on architectural features and growth patterns (Adapted from Malhotra G.K. et al., 2010).

1.1.4 MOLECULAR CLASSIFICATION

Breast cancer patients with the same histological subtype may display discrete prognosis and respond differently to the same treatment. Although the clinical observations indicate similarity within the same subgroup, genetic variations may reflect the overall outcome of the therapy (Perou C.M. et al., 2000). This situation entails the molecular classification of breast cancer.

Initially breast tumors are classified into two major groups as estrogen receptor positive (ER+) and estrogen receptor negative (ER-), and later more subtypes are added to this classification. ER+ tumors are divided into two subgroups as Luminal A and Luminal B (Figure 2). Luminal A tumors, which also express PR (progesterone receptor) but not

Her2 (Human epidermal growth factor receptor 2), are the most common type of breast cancer representing 50-60% of all cases (Perou C.M. et al., 2000; Sorlie T. et al., 2001). These cancers tend to be slow growing and less aggressive than other subtypes, and respond generally well to hormonal therapy, especially at the beginning of treatment (Anderson W.F. et al., 2014; Blows F.M. et al., 2010). Luminal B type tumors, which express PR and Her2, constitute 10-20 % of breast cancers. Compared to its counterpart Luminal A, Luminal B type cancers have a more aggressive phenotype, a higher histological grade (poorly differentiated) and a worse prognosis (Kennecke H. et al., 2010). Although ER is still expressed, the proliferation capacity of cells is quite high as indicated by Ki67 staining (indicator of a large proportion of actively dividing cells) and Her2 overexpression (Cheang M.C. et al., 2009; Parise C.A. et al., 2014).

ER- tumors are sub-classified into 4 groups including Her2 enriched, basal-like, Claudin Low and normal breast like (Figure 2). 15-20% of all breast cancer cases are Her2 enriched, which is characterized by high expression of Her2 and other genes associated with the Her2 pathway. These tumors are quite proliferative, have a higher histological grade and spread more aggressively than other breast tumors (Parker J.S. et al., 2009; Prat A. and Perou C.M., 2011). The basal-like breast cancer represents 10-20% of all breast carcinomas. Although they express genes usually present in normal breast cells, including cytokeratins, P-cadherin, caveolin 1 and 2, EGFR, they are devoid of three key receptors in breast cancer: ER, PR and Her2. Hence, they are often referred to as “triple negative (TN)” in clinical practice. Basal-like tumors tend to be invasive ductal carcinomas which are diagnosed at early ages with a large tumor size, and a high histological grade along with lymph node metastasis (Bosch A. et al., 2010; Livasy C.A. et al., 2006; Kreike B. et al., 2007). These tumors exhibit enormous aggressiveness and poor prognosis. They usually relapse within the first 3 years after chemotherapy (Dent R. et al., 2007). Genomic alterations such as high rates of p53 mutations (Sorlie T. et al., 2001) and decreased function of BRCA1 either by mutation or epigenetic mechanisms could be one of the explanations of the aggressive cancer phenotype (Bosch A. et al., 2010; Sorlie T. et al., 2003). Claudin Low type breast tumors are generally referred to as triple negative even though 20% of them are positive for hormone receptors. These tumors are named after their low expression profile of genes

involved in tight junctions and intercellular adhesion, including claudin-3,4 and 7, ocludin and E-cadherin (Parker J.S. et al., 2009; Prat A. et al., 2010; Prat A. and Perou C.M., 2011). Claudin Low tumors are quite metastatic and have a poor prognosis with acquired resistance to therapy (Prat A. et al., 2010). They carry cancer stem cell (CSC) properties due to overexpression of a subset of genes linked to mesenchymal differentiation and epithelial-mesenchymal transition (Hennessy B.T. et al., 2009). Despite other subtypes, normal breast like tumors are poorly characterized, and usually classified together with fibroadenomas and normal breast samples. They usually express characteristic genes of adipose tissue and lack the expression of ER, PR and Her2. Normal breast tumors represent about 5-10% of breast carcinomas (Perou C.M. et al., 2000).

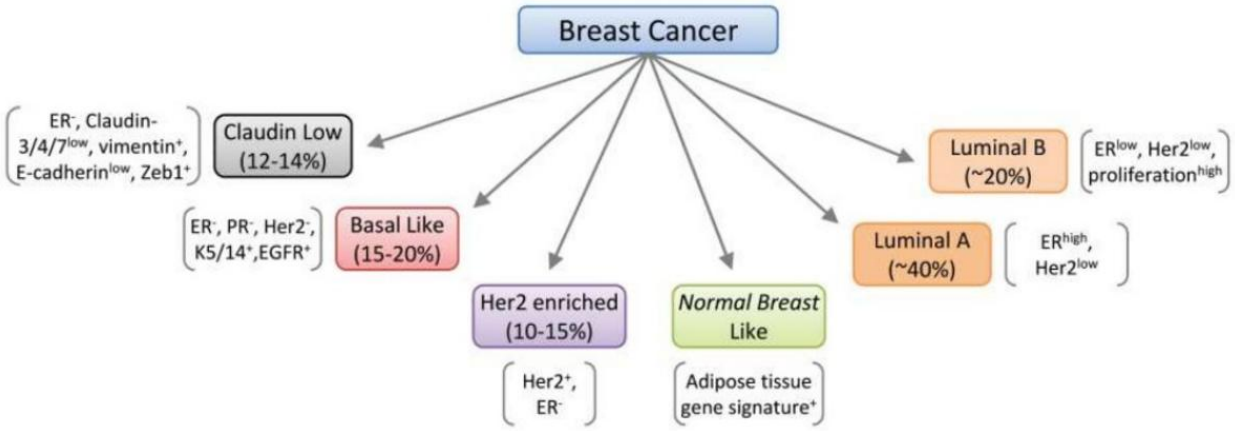

Figure 2. Molecular classification of breast cancer. This classification is based on the intrinsic molecular subtypes of breast cancer identified by microarray analysis of patient tumor specimens (Adapted from Malhotra G.K. et al., 2010).

1.1.5 TREATMENT

The treatment plan of breast cancer is decided after careful consideration of various parameters including the stage and biological characteristics of the cancer, the patient's age and preferences, and the risks and benefits associated with each option. Most women with early stage breast cancer will have some type of surgery along with other treatments such as radiation therapy, chemotherapy, endocrine (hormonal) therapy, to reduce the risk of recurrence. Patients with metastatic disease are mostly treated with systemic therapies including chemotherapy, targeted therapy, and hormonal therapy (Society, AC, 2015-2016).

1.1.5.1 Endocrine Therapy

Breast cancer is a hormone-dependent cancer, and estrogen is the major driver for the initiation and progression of the disease. Biological actions of estrogen are mediated with the estrogen receptor (ER) and 70% of breast tumors express the ER (Masood S. 1992; Mohibi S. et al., 2011). Hence targeting the ER using either ER antagonists or antiestrogens has been the standard therapy of choice for ER+ breast cancers. Endocrine therapy can be given prior or after surgery/radiotherapy; or it can be used in combination with chemotherapy. Introduction of adjuvant systemic therapy has led to a significant improvement in post-surgical survival and a reduction in disease relapse in women especially those diagnosed with early stage ER+ breast cancers (Aebi S. et al., 2011; Perez E.A. 2007). Endocrine therapy for breast cancer consists of:

-Ovarian suppression (OS)

-Selective estrogen receptor modulators (SERMs)

-Selective estrogen down-regulators (SERDs)

-Aromatase inhibitors (AIs) (Lumachi F. et al., 2013).

1.1.5.2 Estrogen Receptors

1.1.5.2.1 Structure of Estrogen Receptors

The three major forms of estrogen are estrone (E1), estradiol (E2), and estriol (E3). 17β-estradiol (E2), the most potent estrogen in the body, functions via diffusion through the plasma membrane of target cells and signaling through intra-cellular hormone-specific estrogen receptors (ERs) (Marino M. et al., 2006). Two isoforms of estrogen receptor in human, ERα and ERβ, are encoded by different genes located on different chromosomes, chromosome 6 and 14, respectively (Gosden J.R. et al., 1986; Enmark E. et al., 1997; Zhou W. et al., 2006). They belong to the nuclear receptor family and contain evolutionarily conserved structural and functional domains of the nuclear receptor family (Mangelsdorf D.J. et al., 1995). The DNA binding domain (DBD) (Figure 3, C region) and the multifunctional ligand-binding domain (LBD) in the COOH- terminus (Figure 3, E/F region) are the conserved domains. DBD facilitates receptor dimerization and receptor binding to specific DNA sequences called “estrogen response elements

(ERE) through its zinc finger structures. The hinge domain (Figure 3, D-region) has also a role in receptor dimerization and binding to chaperone heat-shock proteins (Hsp). The N-terminal domain of ER is not conserved and varies in sequence and length. This domain is involved in inter/intra-molecular interactions and activation of gene transcription. Transcriptional activation is facilitated by two regions called activation function (AF). Constitutively active AF-1 is located at the N-terminus (Figure 3, A/B region) whereas receptor and ligand-dependent AF-2 is located in the C- terminus in LBD (Figure 3, E-region,) (Nilsson S. et al., 2001; Mosselman S. et al., 1996; Claessens F. et al., 2004; Kumar R. et al., 2004). Both AF regions interact with a series of co-regulatory protein complexes upon receptor binding to the DNA (McEwan IJ 2004).

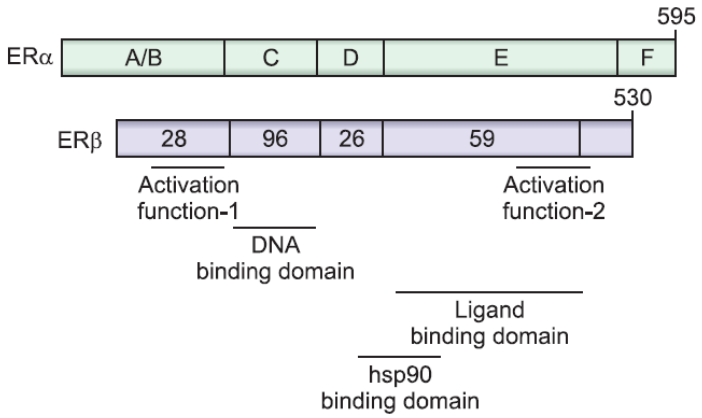

Figure 3: Schematic representation of the common structural and functional domains of ERα and ERβ. The functional domains of the receptors are indicated (A-F), as are the regions responsible for transcriptional activation, DNA binding, ligand binding, and heat shock protein (hsp) 90 binding. The percentage of amino acid homology between regions A through F in ERα and ERβ is indicated by the numbers written on the structure of ERβ. Two transcriptional activation domains, activation function (AF) domains are present in the A/B and E region of the ERs (Modified from Chang M., 2012).

1.1.5.2.2 Mechanism of Action

The ER signaling is a complex biological pathway, which is involved a variety of cellular events such as cell proliferation, inhibition of apoptosis, invasion, angiogenesis, tumor growth and survival. There are several distinct molecular pathways that are responsible for the regulatory actions of ER (Björnström L. and Sjöberg M., 2005).

In the classical genomic model, binding of estrogen to ER results in receptor dimerization. Further, ER dimers bind to estrogen response elements (ERE) at the promoters of the target genes and recruit protein complexes, coactivators and

corepressors, which can alter chromatin structure and facilitate the recruitment of RNA polymerase II transcriptional machinery to the specific DNA sites (Figure 4) (Schiff R. et al., 2010; Klinge C.M. et al., 2001).

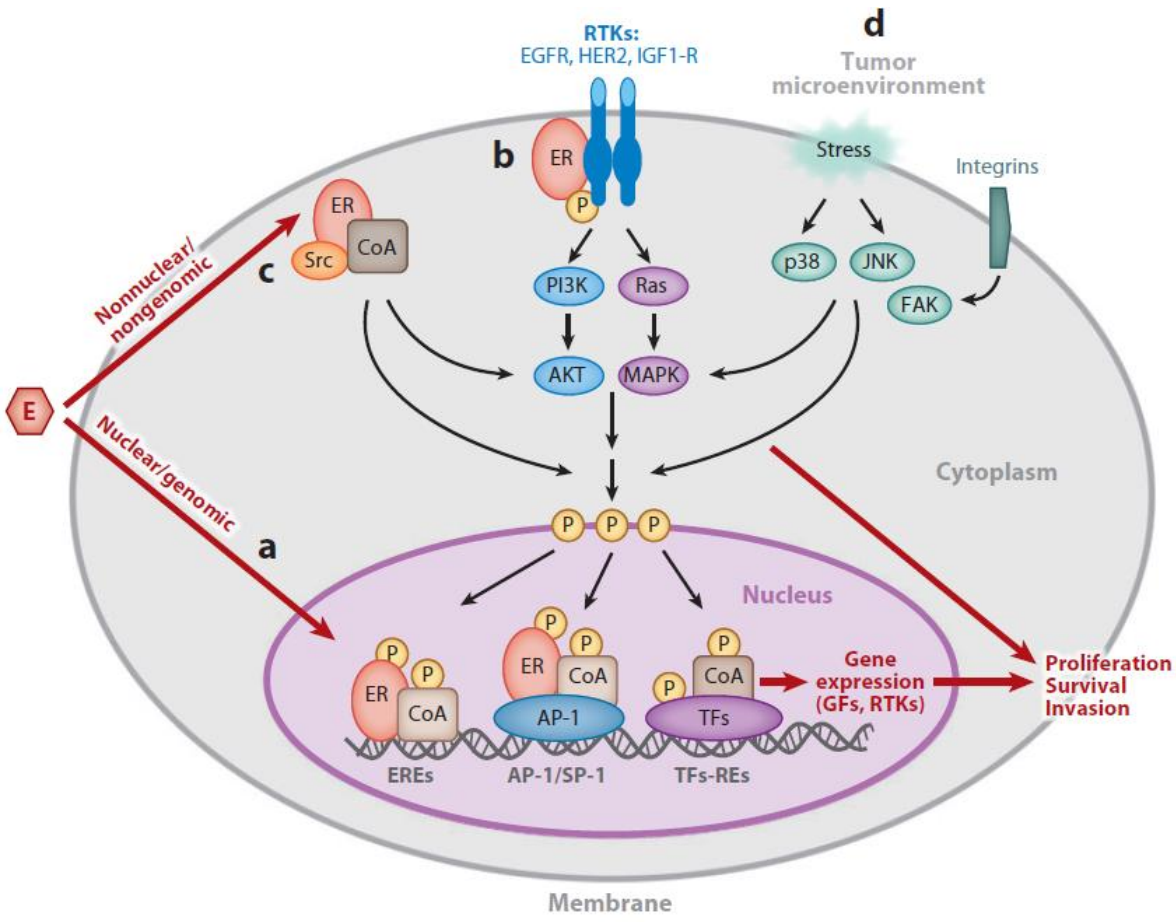

Figure 4. Mechanisms of estrogen receptor (ER) action in breast cancer. (a) Estrogen (E)-bound ER, in the nucleus (nuclear/genomic activity), binds to DNA sequences in promoter regions of target genes either directly (at ERE) or indirectly via protein-protein interaction with other transcription factors such as AP-1 or the SP-1. Upon estrogen binding, ER recruits coactivator complexes (CoA) to induce or modulate gene transcription, including genes encoding growth factors (GFs) and receptor tyrosine kinases (RTKs). A small subset of the cellular pool of ER localized outside the nucleus and/or at the cell membrane associates in response to estrogen with GF RTKs (EGFR, HER2, and IGF1-R) (b) and with additional signaling and coactivator molecules (Src kinase). (c) This interaction activates multiple downstream kinase pathways (SRC, PI3K/AKT, and Ras/p42/44 MAPK), which in turn phosphorylate various transcription factors (TFs) and coregulators. The non-nuclear/non-genomic activity is enhanced in the presence of overexpression and hyperactivation of RTKs. Overall, the nuclear/genomic and non-nuclear/ non-genomic ER activities work in concert to provide breast tumor cells with proliferation, survival, and invasion stimuli. (d) Signaling from the tumor microenvironment activates stress-related pathways and members of the integrin family. These pathways then trigger downstream kinase pathways such as FAK (focal adhesion kinase), JNK (c-Jun N-terminal kinase), and p38 MAPK. Alterations in each of these transcriptional and signaling elements can mediate resistance to endocrine therapy either by modulating ER activity or by acting as escape pathways to provide alternative proliferation and survival stimuli (Adapted from Osborne C.K. and Schiff R., 2011).

In the tethered version of classical model, estrogen bound ER doesn't bind directly to its target genes, but binds to other transcription factors such as AP-1 (activator protein-1) and SP-1 (specificity protein-1) at their specific sites on DNA. Hence ER can modulate the expression of the target genes which do not have EREs at their promoter regions (Figure 4) (Schiff R. et al., 2009; Kushner P.J. et al., 2000). In the non-genomic model, the ER signaling pathway is regulated by membrane receptor tyrosine kinases such as epidermal growth factor receptor (EGFR), Her2 and insulin-like growth factor receptor (IGF1-R). These membrane-associated kinases activate the pathway via phosphorylation of ER and receptor coregulators. This type of activation is called ligand-independent receptor activation (Figure 4) (Schiff R. et al., 2003; Shou J. et al., 2004; Wu R.C. et al., 2005; Schif R. et al., 2004). ER may also work through non-transcriptional mechanisms which are too rapid for a transcriptional effect to activate growth factor receptor signaling including the PI3K/AKT (Phosphatidylinositol 3-kinase/Akt) and the Ras/p42,44 MAPK (Ras/p22,44 Mitogen activated protein kinase) (Schiff R. et al 2004). Finally, the stress kinase pathway via p38 and JNK(c-Jun N-terminal kinase) (Wu R.C. et al., 2004; Lee H. and Bai W., 2004) and the tumor microenvironment along with the associated integrin signaling can also modulate ER function by phosphorylation of ER and its coregulators (Figure 4) (Pontiggia O. et al., 2009).

1.1.5.2.3 Selective Estrogen Receptor Modulators (SERMs)

Selective estrogen receptor modulators (SERMs) display mixed effects on estrogen sensitive tissues. Tamoxifen (TAM), the classic member of SERMs, acts as an antagonist on breast and mammary tissue, whereas it has partial agonist activity in bone and uterus. Administration of TAM has been the standard therapy choice in first line treatment in both pre- and postmenopusal patients with ER-positive metastatic breast cancer (Ward R.L. et al., 1993; Klotz D.M. et al., 2000; O'Regan R.M. and Jordan V.C., 2002).

Tamoxifen (Faslodex^{TM}) itself is a pro-drug with a low affinity for the estrogen receptor. It needs to be metabolized in the liver into active metabolites such as 4-hydroxytamoxifen (4-OHT) (afimoxifene) and N-desmethyl-4-hydroxytamoxifen

(endoxifen) (Desta Z. et al., 2004). These metabolites exert higher affinities for estrogen receptors. For example, 4-OHT has 78% and 338% of the affinity of estradiol for the ERα and ERβ, respectively, whereas Tamoxifen has only 7% and 6% of the affinity of estradiol (Kuhl H., 2005).

Tamoxifen functions through competitive binding to ERs and inhibiting E2 dependent gene transcription, cell proliferation and tumor growth (Maximov P.Y. et al., 2014; Massarweh S. et al., 2008). Upon binding to ER with a low affinity, TAM dissociates the heat shock protein 90 (HSP90) and dimerizes with ER. Later TAM-ER complex homo- or hetero-dimerizes and translocates to the cell nucleus, causing the activation of AF-1 and inhibition of AF-2. Although the TAM-ER complex dimer binds to EREs, transcription of E2 target genes is attenuated because of the inactive AF-2 domain and reduced binding of ER co-activators to the DNA (Figure 5) (Howell A. et al., 2000).

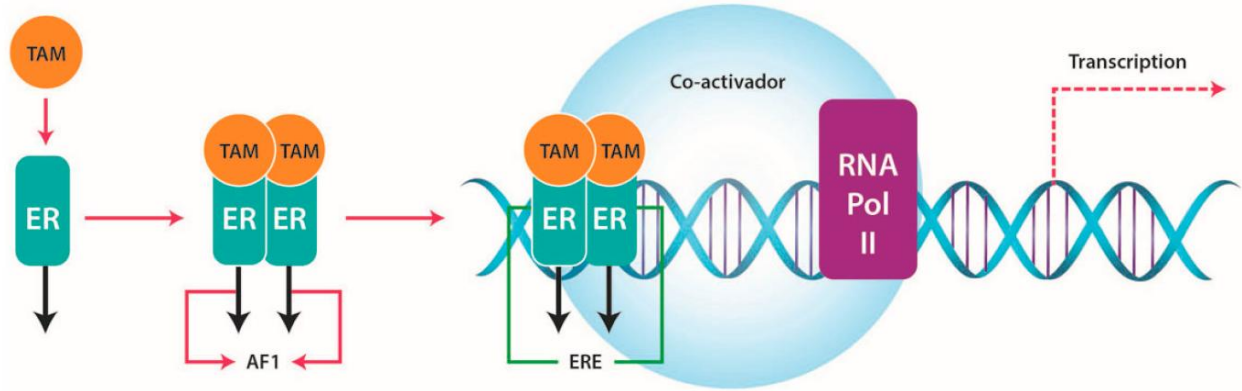

Figure 5. Mechanism of Tamoxifen. The tamoxifen-estrogen receptor (TAM-ER) complex activates the activation factor 1 (AF1) domain and inhibits the activation factor 2 (AF2) domain. The TAM-ER dimer binds to DNA at estrogen response element (ERE) sequences in the promotor region of E2 responsive genes. Transcription of these genes is attenuated because the AF2 domain is inactive (Adapted from Rondón-Lagos M. et al., 2016).

Tamoxifen inhibits cell proliferation *in vitro* and *in vivo* by inducing cell cycle arrest in the G0-G1 phase connected with increased apoptosis. The cell cycle arrest is associated with up-regulation of p53 and p21 concomitant with down-regulation of cyclin D1 and c-Myc. Down-regulation of Bcl-2, up-regulation of Bax, and the activation of caspase-9, -6- and 7 are indicative of an increased apoptotic response (Thiantanawat A. et al., 2003).

1.1.5.2.4 Selective Estrogen Receptor Down-regulators (SERDs)

Although Tamoxifen is an effective treatment for the early stages of ER+ breast cancers, during the treatment disease progression occurs evidently and the majority of the patients acquire resistance against the treatment. Moreover agonistic effects of Tamoxifen may result in stimulation of endometrium and tumor growth in these patients (Johnston S.R. 2001; Deshmane V. et al., 2007). These observed adverse effects brought forward the discovery of new drugs which display complete antagonistic effects on ER. So-called selective estrogen receptor down-regulators (SERDs) are pure anti-estrogens which down-regulate ER and promote proteasomal degradation of the ER at the same time (Wakeling A.E., 2000).

ICI 182,780 (Fulvestrant-Faslodex™) is the only SERD in clinical use at present. Fulvestrant has an ER binding affinity approximately 100 times greater than Tamoxifen and lacks agonist effects on the ER+ tissues such as endometrium and uterus (Kauffman R.F. et al., 1995; Wakeling A.E. et al., 1991; Dukes M. et al., 1991). It is used for the treatment of Tamoxifen resistant hormone receptor positive metastatic breast cancer or locally advanced inoperable breast tumors in postmenopausal women (Bundred M., 2005; Lee C.L. et al., 2017). Several studies have clarified that the partial agonistic activities of Tamoxifen is one of the mechanisms responsible for the acquired drug resistance. Moreover it was reported that Tamoxifen-resistant cells (Dukes M. et al., 1992; Coopman P. et al., 1994) and tumors (Hu X.F. et al., 1993; Osborne C.K. et al., 1994) remain sensitive to growth inhibiton by ICI 182,780*, in vitro* and *in vivo*, respectively. Fulvestrant functions through different mechanisms consisting of (Figure 6):

1) Increased proteosomal degradation of the ER (Dauvois S. et al., 1992; Nicholson R.I. et al., 1995; Borras M. et al., 1996; Pink J.J. and Jordan V.C., 1996; Alarid E.T. et al., 1999; Lonard D.M. et al., 2000; Nawaz Z. et al., 1999)

2) Impaired receptor dimerization (Chen D. et al., 1999)

3) Disrupted nuclear localization (Dauvois S. et al., 1993; Htun H. et al., 1999)

4) Rapid down-regulation of the ER following ICI 182,780 treatment (Dauvois S. et al., 1992; Nicholson R.I. et al. 1995; Borras M. et al., 1996; Pink J.J. and Jordan V.C., 1996)

5) Down-regulation of the ER mediated transcription of estrogen dependent genes (Blin C. et al., 1995; Huynh H.T. and Pollack M., 1993; Hyder S.M. et al., 1997; May F.E.B. et al., 1989; Nicholson R.I. et al., 1995; Osborne C.K. et al. 1995; DeFriend D.J. et al., 1995).

In conclusion, ICI 182,780 is more effective than Tamoxifen in inhibiting the growth of ER-positive breast cancer cells and potentially inhibits progesterone-positive tumors (Nawaz Z. et al., 1999). In addition, ICI 182,780 has the advantage of inhibiting basement membrane invasiveness by tumor cells which is an important mechanism in tumor progression (Thompson E.W. et al., 1989).

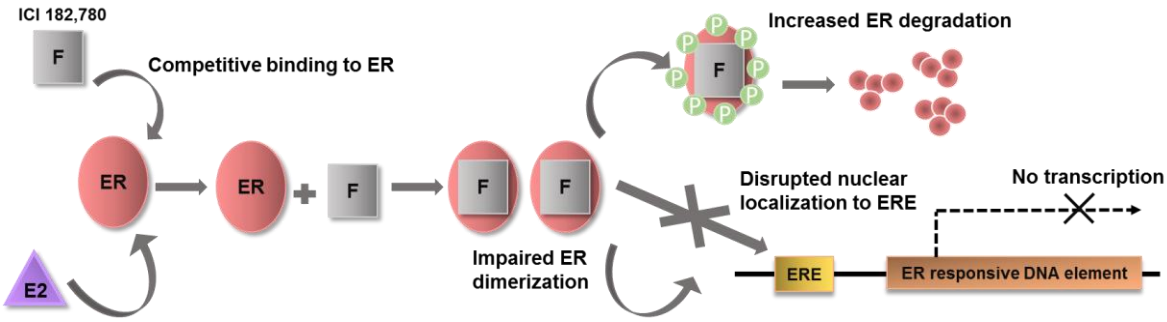

Figure 6. The molecular mechanism for the pure anti-estrogen fulvestrant (ICI 185,780). Fulvestrant binds competitively to ERα with a high affinity. It acts as an anti-estrogen chemical by reducing the half-life of ERα, resulting in a decrease in expression of ERα. Formation of the drug-receptor complex leads to stabilization of the receptor, which is degraded by an ubiquitin-proteasome complex. In addition, drug-receptor complex disrupts the nuclear localization of ER to ERE, and thereby down-regulates the transcription of estrogen responsive genes.

1.2 APOPTOSIS

Apoptosis is a programmed cell death which leads to characteristic morphological changes in the cells. These changes include blebbing, cell shrinkage, nuclear fragmentation, chromatin condensation, chromosomal DNA fragmentation, and global mRNA decay. Apoptosis occurs normally during development and aging as well as a response mechanism to stress conditions. In addition to corticosteroids, heat, hypoxia,

nutrient deprivation and viral infection; irradiation and chemotherapeutic drugs may trigger apoptosis as a result of DNA damage they caused. The mechanisms of apoptosis are highly complex involving energy dependent cascade of molecular events. Up to now, two major apoptotic pathways are described: the intrinsic and extrinsic pathways (Green D., 2011). The extrinsic pathway, also known as “death receptor pathway” is activated by the engagement of death receptors on the cell surface. The intrinsic pathway, also known as “mitochondrial pathway” comprises the release of cytochrome c (other proteins) from the mitochondria. At the end, both pathways leads to the activation of various caspases (enzyme-responsible for cell death). In vertebrates the majority of apoptosis proceeds through the mitochondrial pathway (Pelengaris S. and Khan M., 2006).

1.2.1 THE INTRINSIC (MITOCHONDRIAL) PATHWAY FOR APOPTOSIS

Upon activation by receptor-independent stimulus, the inner mitochondrial membrane permeability changes due to opening of the mitochondrial permeability transition (MPT) pore. These changes cause mitochondrial outer membrane permeabilization (MOMP) which is characterized by the loss of the mitochondrial transmembrane potential ($\Delta\Psi_m$), the release of pro-apoptotic proteins and the arrest of the bioenergetic function of the organelle.

The proteins released from the mitochondria are broadly classified into two groups. The first group involves proteins that activate the caspase dependent pathways such as cytochrome *c* (cyt *c*) and SMAC/Diablo (second mitochondria-derived activator of caspases). The second group involves other pro-apoptotic proteins such as apoptosis inducing factor (AIF) and endonuclease G (EndoG). After MOMP, holocytochrome *c* induces the oligomerization of its downstream binding partner, apoptotic protease-activating factor 1 (Apaf-1), thereby leading to the activation of caspase 9. The cyt *c*/ Apaf-1/ Caspase 9 complex forms the apoptosome and activates the executioner caspases 3 and 7. Activation of the caspase cascade results in cell dismantling through nuclear fragmentation. In parallel, SMAC/Diablo deactivates the inhibitor of apoptosis proteins (IAPs) to prevent the apoptosis arrest (Figure 7) (Hengartner M.O., 2000; Gross A. et al., 1999; Slee E.A. et al., 1999).

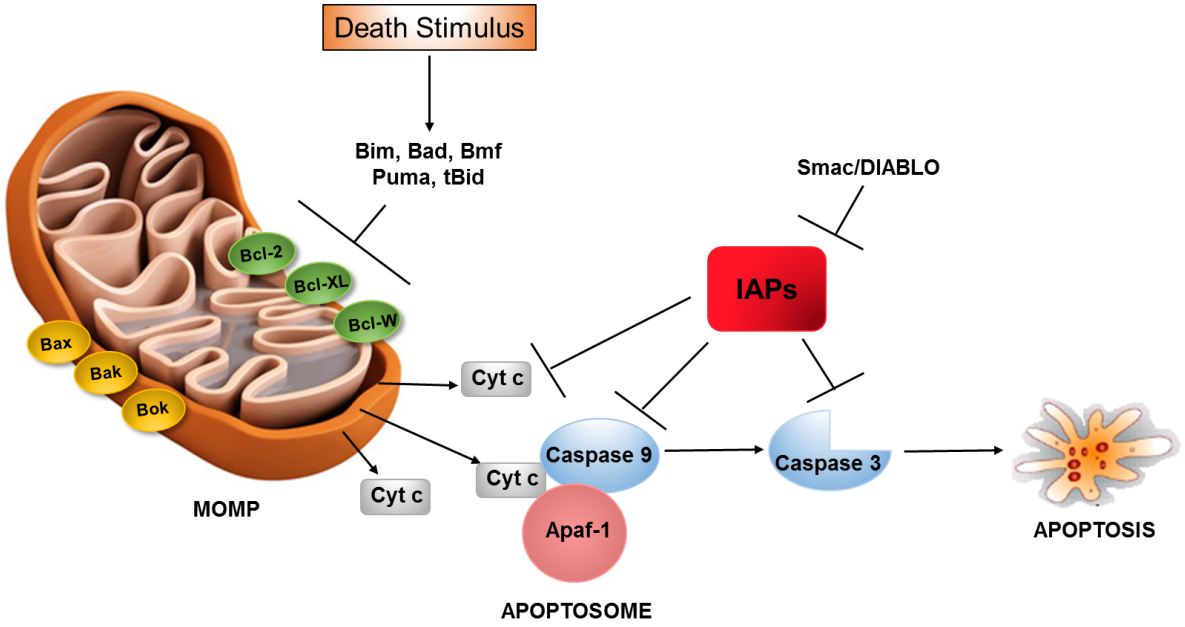

Figure 7. The molecular mechanism of the mitochondrial (intrinsic) pathway. The mitochondrial pathway is triggered by a variety of cellular stresses (e.g. DNA damage, hypoxia, depleted survival factors, or deregulated oncogenes). Once released into the cytosol, cytochrome *c* associates with APAF-1 creates the apoptosome along with caspase 9. Later caspase 9 activate downstream executioner caspases, such as caspase-3. Other proteins that are released from the mitochondria include Smac/DIABLO bind and inhibit, IAPs to prevent caspase-9 and caspase-3 inhibition.

1.2.2 REGULATION OF APOPTOSIS

1.2.2.1 The Bcl-2 Family of Proteins

The Bcl-2 family of proteins are essential regulators of apoptosis as they are necessary for the cytochrome *c* release from the mitochondria during MOMP. In addition, up-regulation of Bcl-2 family proteins is quite common in human tumors and dysregulation of these proteins favors cell survival preventing cell death in response to a variety of apoptotic stimuli. The blockade of apoptosis by Bcl-2 family proteins reduces sensitivity to antineoplastic drugs thus limiting the clinical efficacy of the antineoplastic drugs. The Bcl-2 family of proteins consists of both pro-apoptotic and anti-apoptotic members (Pelengaris S. and Khan M., 2006). Bcl-2, the founding member of the family (Tsujimoto Y. et al., 1984), shares common Bcl-2 homolog (BH) domains with the other members. All proteins of the Bcl-2 family are distinguished according to the BH domains they harbor (Figure 8) (Pelengaris S. and Khan M., 2006).

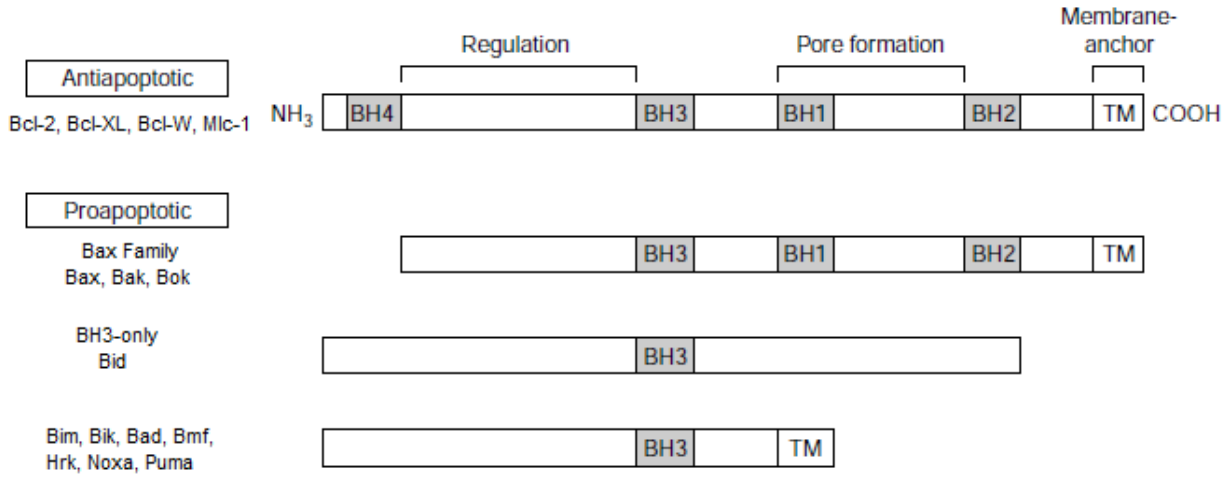

Figure 8. The Bcl-2 family of proteins. The Bcl-2 family of proteins can be divided into three categories according to their structure and function: the anti-apoptotic members promote cell survival, whereas members of the Bax family and 'BH3-only' family are pro-apoptotic and thus promote apoptosis. The Bcl-2 family members possess at least one of four conserved BH domains. Pore formation is enabled by residues of BH1, BH2, and BH3. During apoptosis, the pro-apoptotic members are activated, and presumably undergo a conformational change leading to exposure of the BH3 domain – an interaction domain that is necessary for their killing action. In this way, BH3-only proteins promote apoptosis by directly binding to their anti-apoptotic relatives (Pelengaris S. and Khan M., 2006).

The anti-apoptotic proteins, Bcl-2, Bcl-XL, Bcl-W and Mcl-1 have four BH domains (BH1-BH4). They also contain a hydrophobic carboxy terminal domain which enables the association with the cytoplasmic face of the outer mitochondria membrane (OMM), the nucleus, the endoplasmic reticulum and the nuclear envelope (Cory S. and Adams J.M., 2002). Although Bcl-2 is an integral membrane protein in all cells, Bcl-XL and Bcl-W only associates with the membrane after a cytotoxic signal (Figure 7). These proteins inhibit the release of cyt *c* by preventing the formation of mitochondrial pores and thereby the formation of the apoptosome (Brenner C. et al., 2000).

The pro-apoptotic proteins are sub-divided into two more groups consisting of the Bax family and the BH3-only family. Bax family of proteins, Bax, Bak and Bok share three BH domains (BH1-BH3). After an apoptotic trigger, Bax translocates into the mitochondria from the cytosol and inserts into the OMM (Figure 7). At the mitochondria, Bax homo- or heterodimerizes with other pro-apoptotic members such as Bak. Hence, Bax promotes the release of apoptogenic factors (cyt *c*) by disrupting the OMM integrity and by forming mitochondrial pores (Vyssokikh M.Y. et al., 2002). As the name implies, proteins of the BH3-only family (Bid, Bim, Bik, Bad, Bmf, Hrk, Noxa, Puma) have only

the short BH3 domain. They are direct antagonists of the anti-apoptotic members. After binding to specific Bcl-2 family proteins, they block their anti-apoptotic action via sequestration at the mitochondria (Whereas Bim, Puma, and truncated Bid bind to all anti-apoptotic Bcl-2 family proteins; Noxa binds only to Mcl-1 and A1; Bad and Bmf bind only to Bcl-2, Bcl-XL and Bcl-W (Figure 7) (Reed J.C., 1998).

1.2.2.2 The Inhibitors of Apoptotic Proteins

Once activated, caspases kill cells irreversibly. To circumvent unwanted death, cells have evolved a system in which inhibitors of apoptosis proteins (IAPs) play a central role. IAPs are a family of structurally related proteins that were initially identified in the genome of baculovirus owing to their ability to suppress apoptosis in infected host cells (Birnbaum M.J. et al., 1994). Up to now, eight mammalian IAPs have been described: c-IAP1 (cellular IAP1), c-IAP2 (cellular IAP2), NAIP (neuronal apoptosis inhibitory protein), Survivin, Livin, XIAP (X-linked inhibitor of apoptosis), BRUCE (BIR-containing ubiquitin conjugating enzyme), and Ts-IAP (Testis-specific IAP). These proteins can inhibit both intrinsic and extrinsic pathway mediated apoptosis by direct binding and inhibition of specific caspases (Ducket C.S. et al., 1996).

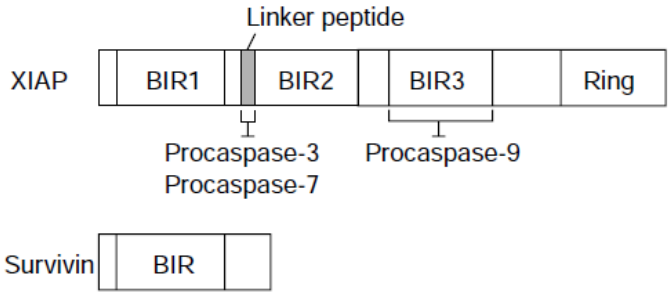

Figure 9. Proteins of the IAP family. XIAP, an IAP family member, contains three baculoviral IAP repeat (BIR) domains. The third BIR domain (BIR3) potently inhibits the activity of processed caspase-9, whereas the linker region between BIR1 and BIR2 specifically targets caspase-3 and caspase-7. On the other hand, Survivin contains a single BIR domain (Pelengaris S. and Khan M., 2006).

IAPs are characterized by the presence of their bacoloviral IAP repeat domain (BIR), an 80-amino acid zinc binding domain. For example, XIAP, c-IAP2 and c-IAP contain thee BIR domains, whereas Survivin contains a single BIR domain (Figure 9). IAPs are regulated by IAP binding proteins such as SMAC/Diablo. Upon an apoptotic stimulus, these proteins are proteolytically cleaved and released from the mitochondria into the

cytosol. Afterwards they associate with IAPs and prevent caspase inhibition (Ducket C.S., 2005).

One of the mechanisms by which tumor cells are believed to acquire resistance to apoptosis is by overexpression of IAPs. Of all IAPs, Survivin has been found to be overexpressed in a variety of tumors including breast cancer. Aberrant expression of surviving is associated with poor prognosis and drug resistance (Sohn D.M. et al., 2006; Pennati M. et al., 2007; Pennati M. et al., 2008).

1.3 RELATIONSHIP OF ZRF1 AND CANCER

The first link between Zrf1 and cancer was proposed due to the genomic locus of Zrf1. Chromosome 7, where Zrf1 is also located, is commonly altered in several types of human cancers, including breast, prostate, pancreatic, ovarian, gastric, colon, germ cell, glioblastoma, and head and neck malignancies (Resto V.A. et al., 2000). In accordance with this observation, Zrf1 was shown to be overexpressed in a variety of cancers such as head and neck squamous cell carcinoma (Resto V.A. et al., 2000), chronic myeloid leukemia (Schmitt M.et al., 2006), chronic lymphocytic leukemia (Giannopoulos K., et al., 2006) and acute myeloid leukemia (AML) (Greiner J. et al., 2003; Greiner J. et al., 2004 Siegel S. et al., 2012). A recent study demonstrated that Zrf1 controls *INK4-ARF* locus in oncogenic Ras overexpressing-fibroblasts and knockdown of Zrf1 induces neoplastic growth in these cells bypassing the oncogene-induced senescence (Riberio J.D. et al., 2013). On the contrary, Zrf1 depletion in human AML cells reduces cell proliferation, induces apoptosis and enhances cell differentiation. Further findings clarified this conflict and suggested a dual role for Zrf1 in transcriptional regulation. Zrf1 can either work as tumor suppressor or induce carcinogenesis depending on the cellular context (Demajo S. et al., 2013; Aloia L. et al., 2015).

2 AIM OF THE STUDY

Although Zrf1 plays an important role in many cancers, its role in breast cancer is poorly understood. A recent study analyzing the antibody response in sera of breast cancer patients suggests Zrf1 antigen and auto-antibodies as potential tumor markers particularly for detecting early breast cancers (Dyachenko D. et al., 2016). Thus, we hypothesized that Zrf1 might have a key role during breast cancer progression into a more metastatic and invasive stage.

3 MATERIAL AND METHODS

3.1 CBIOPORTAL SOFTWARE ANALYSIS

For genomic alteration and mRNA expression analysis, publicly available cBioPortal software was used: http://www.cbioportal.org/, citation: Gao et al. Sci. Signal. 2013 & Cerami et al. Cancer Discov. 2012. “June 30th, 2016” updated TCGA breast cancer dataset was chosen for the analysis. In the software, putative copy number calls on 1080 cases were determined using GISTIC 2.0. Values:-2=homozygous deletion; -1=hemizygous deletion; 0=neutral/no change; 1=gain; 2=high level amplification. Mutations were determined by whole exome sequencing. mRNA expression data were determined as mRNA z-scores (RNA Seq V2 RSEM) by comparison of the expression distribution of each gene tumors that are diploid for this gene.

3.2 CELL CULTURE

MCF7 cells were cultured in phenol red Dulbecco’s Modified Eagle Medium (Gibco) supplemented with 10% Fetal Bovine Serum (Gibco), L-Glutamine (Gibco) and Penicillin/Streptomycin (Gibco). Cells were passaged in every 4 days and their medium was exchanged in every 2 days. Prior to 17β-estradiol or ICI 182,780 treatments, cells were washed 2 times with 1XPBS and cultured in phenol red free DMEM supplemented with 5% charcoal-stripped FBS (Sigma-F6765), L-Glutamine (Gibco) and Penicillin/Streptomycin (Gibco) for 48 hours. During the starvation, the medium was changed every day.

3.3 GENERATION OF STABLE ZRF1 KNOCKDOWN CELL LINES

For the production of lentiviruses containing shRNA, HEK293T cells were grown overnight in 10 cm dishes and the next day the medium was replaced with OPTIMEM low serum medium (Gibco), two hours prior to transfection. For the transfection, 4 µg shRNA#55 or shRNA#58, 2 µg pMDLg/pRRe, 2 µg pRSV-Rev and 2 µg pMD2.G plasmids were mixed with 300 µl OPTIMEM and 30 µl PEI with OPTIMEM. 5 min later plasmids were mixed with PEI and 30 min later the mixture was added to the HEK293T cells. 18 hours post-transfection, the OPTIMEM was replaced with 6 ml complete cell

medium and the day after, the medium containing the viral particles was collected through centrifuge at 1500 rpm for 5 min. 1000 µl medium containing 500 µl shRNA#55 and shRNA#58 viral particles was added for transduction to $2x10^5$ MCF7 cells in a 6 well plate. 4 µg/ml polybrene was added to link the viral particle to the cells and 6 ml of fresh medium was added to HEK293T cells. After repeating the same procedure, cells were left to recover for 48 hrs. Knockdown cells were selected with 2 µg/mL puromycin (Sigma) for 3 days and then frozen or analyzed for RNA or protein expression.

Name	Company	DNA Barcode
shNMC: Mission pLKO.1-puro	Sigma	
shZrf1: TRCN0000254058	Sigma	5'CCGGCTGGAAGAACCAAGATCATTACTCGAG TAATGATCTTGGTTCTTCCAGTTTTTG3'
shZrf1: TRCN0000254055	Sigma	5'CCGGACAGATCAAAGCAGCTCATAACTCGAG TTATGAGCTGCTTTGATCTGTTTTT3'

Table 1. shRNA plasmids used for the cell line generation.

3.4 CELL GROWTH EXPERIMENT

For cell growth experiments, $1x10^5$ cells were seeded to 24 well plates in 9 replicates: pool of every 3 wells was accepted as 1 technical replicate. Cells were counted in every 2 days with hemocytometer and the medium was changed in 2 days.

3.5 PREPARATION AND USAGE OF CHEMICAL STOCKS

17β-estradiol (E8875) and 4-OH Tamoxifen (H7904) were purchased from Sigma. ICI 182,780 (1047) was purchased from TOCRIS. All the chemicals were prepared in 100% ethanol as 1000X and stored at -20^0C. Stock concentrations: 17β-estradiol 10 µM, 4-OH Tamoxifen 10 mM, ICI 182,780 either 1 mM or 100 µM.

3.6 MTT CELL PROLIFERATION ASSAY

Prior to MTT assay, cells were starved for 48 hours and seeded at a density of $6x10^3$ to the 48 well plates in 8 replicates (Day 0). Next day either 10 nM 17β-estradiol or 100 nM ICI 182,780 was added to the plates and the experiment was continued until day 7. At the end of day 7, cells were washed twice with 1XPBS and added 200 µl fresh medium with no treatment. MTT (Sigma) powder was dissolved in 1XPBS at a concentration of

5mg/ml. Then 20 µl of MTT solution was added to each well and incubated at 37^0C in the dark for 4 hours. After incubation, medium was collected carefully and 200 µl 0.04N HCl was added to each well to dissolve the formazan crystals. Absorbance was measured at 570 nm in TECAN plate reader.

3.7 KI67 STAINING

MCF7 cells grown on coverslips were washed with 1xPBS and fixed for 20 min with freshly thawed 4 % PFA. They were washed twice with 1xPBS and incubated for 10 min in 0.5% Triton in 1xPBS for permeabilization. After permeabilization, cells were washed twice with 1xPBS and blocked for 1 hour at room temperature in 5% FBS/0.1%Triton/1xPBS (blocking solution). The blocked cells were incubated over night at 4°C with Ki67 antibody (Abcam-ab15580) diluted in blocking solution. After overnight incubation, stained cells were washed with 0.1 % Triton/1xPBS (wash buffer) three times and incubated with secondary antibodies prepared in wash buffer for 1.5 hour at room temperature in dark. Cells were washed with wash buffer three times for 10 min each in dark, mounted with VECTASHIELD Antifade Mounting Medium with DAPI (Vector) and sealed. Fluorescence images were acquired on a Leica SP5 microscope.

3.8 WOUND HEALING ASSAY

Cells were grown to 100% confluence in 6 well plates and the cell monolayer was scraped in a straight line to create a "wound" with a p200 pipet tip. Cell debris were removed, the edge of the wounds were smoothened by washing the cells and 1 ml of fresh medium was added to each well. To obtain the same field during the image acquisition, markings were created on the lid of 6 well plate to be used as reference points close to the wound. Starting from 0h, images were taken every 24 hours until 96 hours at Leica DM-IL microscope. The healing in each time point was calculated in ImageJ and represented in % wound area graph as quantification of cell motility.

3.9 TRANSWELL CELL MIGRATION ASSAY

96 well transwell migration plate (Corning) was separated as reservoir plate and insert plate, and 150 µl attractant medium (DMEM supplemented 20%FBS) was added to the each well of reservoir plates. Insert plate was placed in a regular 96 well and 50 µl

DMEM without FBS was added to each well before cell seeding. $2x10^4$ cells in 50 µl DMEM without FBS was added to the insert well and they were placed back into the reservoir plate. Cells were left for migration for 24h. Next day, supernatant was aspirated carefully and cells were fixed in 3.7%formaldehyde in 1xPBS (100 µl per well) for 2 min at RT. After 2 times wash with 1xPBS, cells were permeabilized in 100 µl 100% methanol for 20 min at RT. Cells were washed 2 times with 1xPBS. Insert plate was turned upside down, and each transwell was incubated with 50 µl 1% crystal violet (prepared in methanol and filtered) for 15 min at RT. After incubation, the insert plate was placed back into the reservoir plate, washed 3 times with 1xPBS and the remaining stains in the upper part of the transwell were wiped off with Kimtech paper. Images of migrated cells on the lower part of the transwell was acquired at Leica DM-IL microscope and migrated cells number from 12 wells was calculated.

3.10 CELL ADHESION EXPERIMENT

1 hour in advance, collagen coated 24 well plates (ZenBio) were blocked with 1% BSA dissolved in only DMEM. After incubation, wells are washed 2 times with 1xPBS and $2x10^5$ cells suspended in 1ml DMEM (no supplements) were added to each well in 4 replicates. Cells were allowed to attach to the plate surface for 1 hour at 37^0C. Then cells were washed 3 times with 1xPBS and fixed with 4% PFA (paraformaldehyde) for 10 min at RT. After washing with 2 times with 1xPBS, cells were stained with crystal violet (5mg/ml prepared in 20% ethanol and filtered) for 10 min. Cells were washed 2 times with 1xPBS and left for air dry. After taking the microscopy images at Leica DM-IL microscope, the crystal violet was dissolved in 33% acetic acid and the absorbance was measured at 550 nm in TECAN plate reader. Cell adhesion capacity was calculated as fold change after background normalization of absorbance values.

3.11 ORGANOID LIKE STRUCTURE GENERATION IN SUSPENSION CULTURE

Regular tissue culture 96 well plates were covered with 100 µL 1% agarose dissolved in sterile 1xPBS and left for air dry for 30 min at the cell culture hood. Meantime, MCF7 cells were prepared at $5x10^6$ concentration in regular DMEM and 100 µL of cell suspension was added to each well of 96 well plates. Cells were left in suspension to

generate organoid like structures for 4 days. At the end of 4 day, images per well were acquired at Leica DM-IL microscope. Organoid generation efficiency was calculated: Total organoid number/ 96 (for each replicate). The ferret dimaters of organoids were calculated with ImageJ.

3.12 DETECTION OF APOPTOSIS

After 7 days of either ICI 182,780 or vehicle treatment, cells were collected in 15 ml falcons and washed 2 times with 1xPBS. Prior to use, 10X Annexin V binding buffer (0.1M HEPES ph.7.4, 1.4M NaCl, 25 mM CaCl2) was diluted to 1X with distilled water freshly. Cells were resuspended at a concentration of $1x10^6$ cells in 100 µl 1X Annexin V binding buffer. 5 µl Annexin V-FITC (Biolegend-640906) and 5 µl PI (stock: 0.5 mg/ml; Sigma) was added directly to the cells. Control samples including only Annexin V, only PI and no staining were also prepared. After gently wortexing, cells were incubated with dyes for 15 min at RT in the dark. At the end of incubation, 400 µl of 1X Annexin V binding buffer was added and samples were analyzed in the flow cytometry (BD LSFORTESSA) immediately. Gating was determined by single staining controls and necessary compensation was done. Apoptotic cell distributions were calculated by FlowJo.

3.13 CELL CYCLE ANALYSIS

After cell synchronization and 17β-estradiol treatment, the cell medium was aspirated. 1 ml fresh medium plus 10 µl BrdU from a 1 mM stock was added to cells and incubated 30 min at 37^0C for 30 min. End of incubation, cells were collected in 15 ml falcons and washed 2 times with 1xPBS. Cells were resuspended in 100 µl 1xPBS and fixed by adding dropwise of 400 µl ice-cold 100% ethanol (last concentration: 70%). Cells were either kept in fixation buffer at least 1 hour or stored in -20^0C. After fixation, cells were pelleted by centrifuge at 1200 rpm for 5 min and washed 2 times with 1xPBS. To hydrolize DNA, 300 µl permeabilization and denaturation buffer (0.5% Triton X-100, 2M HCl in water) was added to cell pellets and incubated for 20 min at RT. After spinning down, samples were resuspended in 500 µl 0.1M Na2B4O7 (pH 9.0) for neutralization and centrifuged again. Samples were washed one more time with 1xPBS and

resuspended in 300 µl 1xPBS + 0.1% BSA. RNase was added to samples at a concentration of 100µg/ml and incubated for 30 min at 37^0C to complete RNA digestion. After spinning down, samples were washed and blocked with blocking buffer (1% BSA and 0.25% Tween in 1xPBS) for 10 min at RT. After one more spinning down, samples were resuspended in 80µl blocking buffer with 1:10 dilution of Anti-BrdU-488 AlexaFluor (Biolegend) and incubated 1 hour at RT in the dark. Samples were washed 2 times with blocking buffer, resuspended in 1xPBS and stained with DAPI at 1:1000 concentration (stock 5 mg/ml) for additional 30 min in the dark. After spinning down, samples were resuspended in 500 µl 0.1% BSA in 1xPBS and analyzed in the flow cytometry (BD LSFORTESSA). Gating was determined by non BrdU treated cells and necessary compensation was done. Cell cycle distributions were calculated by FlowJo.

3.14 WESTERN BLOT

MCF7 cell pellets were collected and washed with 1xPBS. Samples were resuspended in 2xLaemmli buffer according to their pellet size and sonicated for 15 cycles (30 sec on/ 30 sec off) at high setting using a Diagenode Bioruptor plus. Samples were boiled for 20 min at 95°C and centrifuged for 15 at room temperature at maximum speed. Boiled proteins were separated on 10 % SDS-PAGE for Western Blot analysis.

Antibody Name	Company	Code	Dilution
Zrf1	Homemade		1:500
Cleaved PARP	Abcam	ab4830	1:1000
β-actin	Sigma	a5441	1:10000
α-Tubulin	Sigma	AB15708	1:10000

Table 2. Antibodies used in western blot experiments.

3.15 RNA EXTRACTION, CDNA SYNTHESIS AND RT-QPCR

RNA was extracted by lysis with 1 mL Trizol Reagent (Ambion) MCF7 derived cell pellets. Lysis was carried out by proper mixing and homogenization by passing the lysate through a syringe with a 0.9 x 40 mm 20G needle. Homogenized lysate was transferred in phase lock Heavy 2 mL tubes and incubated for 5 min at RT. 0.2 mL Chloroform (Sigma) was added and samples were shacked vigorously for 15 sec and incubated at RT for 3 min. Samples were centrifuged for 15 min at 4 °C, at 12.000 g and

aqueous phase was transferred to a new tube. 0.5 mL analytical grade Isopropanol was added and RNA was precipitated by incubation at RT for 10 min followed by centrifugation at 4 °C, 12.000 g for 10 min. The RNA pellet was washed once with 75% Ethanol and centrifuged for 5 min at 4 °C at 7500 g. After Ethanol removal the pellet was resuspended in 60 µL Nuclease Free Water (NFW) and incubated for 5 min at 57 °C. RNA was re-precipitated to remove any Trizol traces by adding 6 µL NaOAc 3M and 1 mL Ethanol. Precipitation was carried out at -80 °C from 1 hr to overnight. Samples were centrifuged for 20 min at max speed at 4 °C and washed twice with 1 mL ice-cold 75% Ethanol. Pellets were air-dried and resuspended in 20 µL NFW.

500 ng or 1 µg of RNA was used for cDNA synthesis by using the First Strand cDNA Synthesis Kit (Fermentas) with random hexamer primers. cDNA was diluted with NFW and 2 µL were used for qPCR. For each qPCR reaction, 2 µL cDNA and 2 µL NFW were combined with the following master mix at a final volume of 10 µL per reaction: Cyber Green Mix 2x (Life Technologies) 5 µL + Forward Primer (10 µM) 0.5 µL + Reverse Primer (10 µM) 0.5 µL.

qPCRs, were carried out using a Viia7 cycler (Life Technologies) at normal settings and expression was analyzed by using the ddCt method. The oligos were designed to span exon-exon junctions of transcripts and the results were normalized by using GAPDH oligos as reference (Table 3).

PRIMER LIST FOR RT-QPCR			
Name	**Forward**	**Reverse**	**Ref.**
GAPDH	AATCCCATCACCATCTTCCA	TGGACTCCACGACGTACTCA	
Cdk1	CTGGGGTCAGCTCGTTACTC	TCTGAATCCCCATGGAAAAG	
CCND1	TGGTGAACAAGCTCAAGTGG	TGTTTGCGGATGATCTGTTT	
P16	GGTTTTCGTGGTTCACATCC	CTAGACGCTGGCTCCTCAGT	
P15	TCTTATCTGGCCCTCGACAC	TCCCTCAGAAAACCCTGAAA	
Bcl-2	CTGCACCTGACGCCCTTCACC	CACATGACCCCACCGAACTCAAAGA	
Bcl-XL	CATTTAGGGGCCACTTTTGA	GCTTCTGGAGGACATTTGGA	
Bcl-W	GCGGAGTTCACAGCTCTATAC	AAAAGGCCCCTACAGTTACCA	
Bax	GGGACGAACTGGACAGTAACA	TTGAAGTTGCCGTCAGAAAA	
Bid	GCTCCGTGATGTCTTTCACA	TCGAGCTTTAGCCAGTCACA	
Bad	CCTCAGGCCTATGCAAAAAG	AACTTCCGATGGGACCAAG	
Survivin	ATGTGGATCTCGGCTTCTGT	TAGCCATGAGGGTCTGGTTT	
XIAP	TATCAGACACCATATACCCGAGG	TGGGGTTAGGTGAGCATAGTC	
BIRC3	AAGCTACCTCTCAGCCTACTTT	CCACTGTTTTCTGTACCCGGA	HPB

Table 3. Primers used in RT-qPCR experiments. HPB: Harvard primer bank.

4 RESULTS

4.1 ZRF1 IS OVEREXPRESSED IN BREAST INVASIVE DUCTAL CARCINOMA

To elucidate Zrf1's potential involvement in breast cancer, we analyzed the TCGA breast cancer dataset (June 30th, 2016 dated) for any genomic alteration or mRNA expression change of Zrf1 that might be associated using the publicly available cBioPortal software (Figure 1).

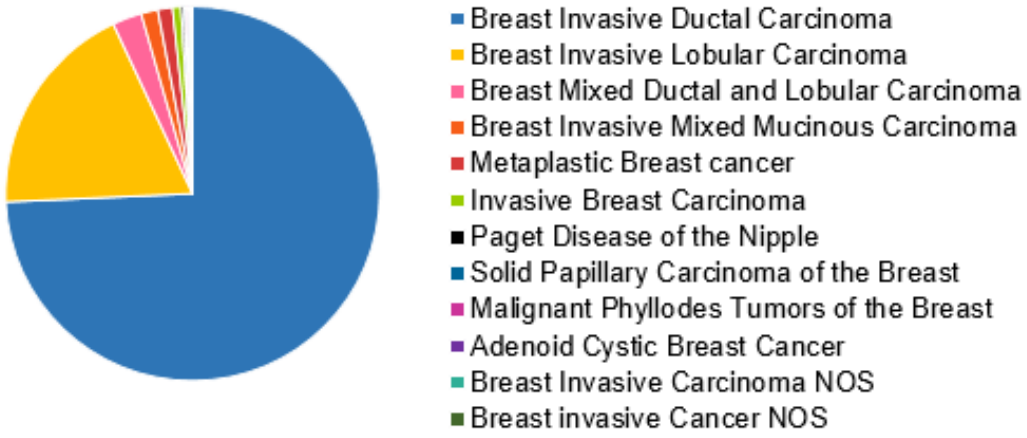

Figure 1. Representative pie chart of the breast cancer type distribution in the TCGA dataset. The TCGA dataset includes a total of 1105 biopsy samples from patients with different types of breast cancer.

Firstly we examined the copy number alterations (CNA) of Zrf1, which could be either amplification (copy number increase) or deep deletion (copy number decrease). To gain a better understanding, we analyzed Zrf1 together with the high CNA profile genes (e.g. amplification **MYC, RAD21, EXT1, NDRG1, CCND1**; e.g. deletion **DUSP4, PTEN, PCM1, ESCO2, WRN**) and the top 5 mostly mutated (**PIK3CA, TP53, CDH1, GATA3, MAP3K1**) genes within the same dataset. Based on the CNA analysis, MYC exhibited the highest frequency of alteration with 21% of the sequenced cases and compared to this gene Zrf1 exhibited a lower frequency of alteration with 0.9% of the sequenced cases (Figure 2A). According to the heatmap, most of these alterations occurred in the breast invasive ductal carcinoma. Further analysis of CNA alterations clarified that Zrf1 is mostly amplified rather than deleted (Figure 2B).

A)

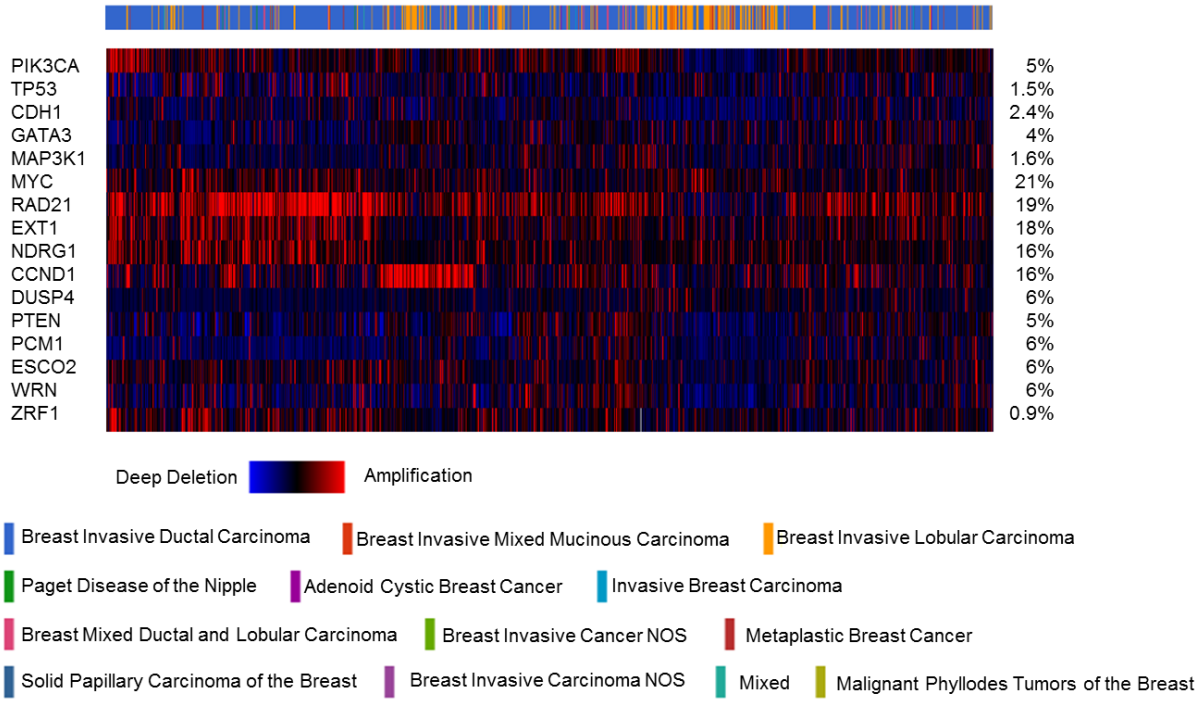

B)

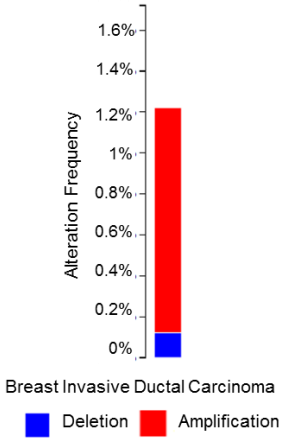

Figure 2. CNA analysis of Zrf1. (A) Heatmap of CNA analysis indicates a 0.9% frequency of alterations in Zrf1, mostly in breast invasive ductal carcinoma. (B) Zrf1 exhibits an increased copy number in breast invasive ductal carcinoma. Whereas amplification is observed in 9 cases, deletion is observed in only 1 case in a total of 10 cases.

Next we investigated the somatic mutation rates and the mutation types of Zrf1 along with the top 2 highly mutates genes, PIK3CA and TP53, in the dataset (Figure 3). Whereas PIK3CA and TP53 have higher somatic mutation rates (28.9% and 27%, respectively), Zr1 has only 0.4% somatic mutation rate. The type of the mutations are missense and truncating mutations without a documented effect in clinics. One of the missense mutations is in front of the DnaJ domain causing a deletion of the region. The second missense mutation lies in front of the one of the DNA binding domains leading

to a gain of function. The last missense mutation is also in front of the other DNA binding domain and results in diploidy. The only truncating mutation is in the ribosome-associated complex head domain and this mutation also results in diploidy. Lastly, we analyzed the mRNA expression profile of Zrf1. In this dataset, RAD21 and CCND1 have the highest frequency of mRNA alteration, 30% and 16%, respectively. Compared to these genes, expression of Zrf1 was altered in 8% of total cases (Figure 4A) and its expression was upregulated (Figure 4B), mostly in breast invasive ductal carcinoma (Figure 4C). Collectively these findings suggest an overrepresentation of Zrf1 either through gene amplification or mRNA upregulation in invasive ductal breast carcinoma.

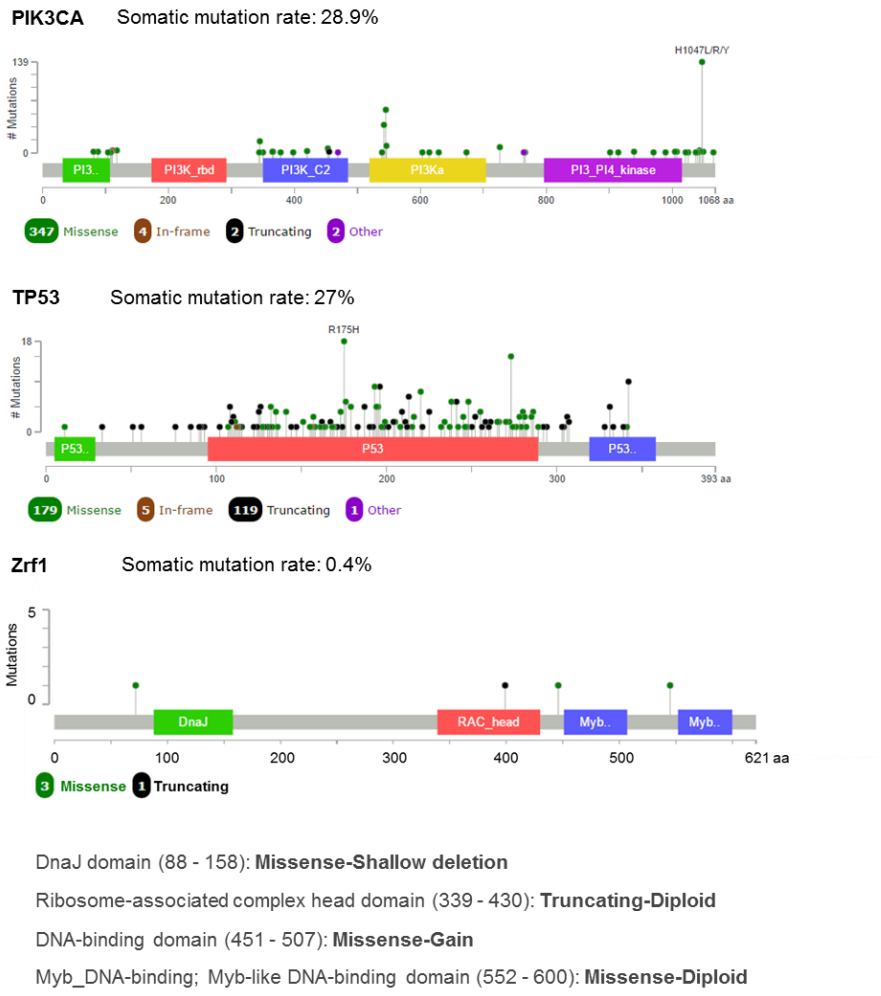

Figure 3. Somatic mutation rate and types of Zrf1. Whereas PIK3CA and TP53 have higher somatic mutation rates, 28.9 and 27, respectively; Zr1 has only 0.4% somatic mutation rates. Zrf1 has 3 missense and 1 truncating mutations without a documented effect in clinic.

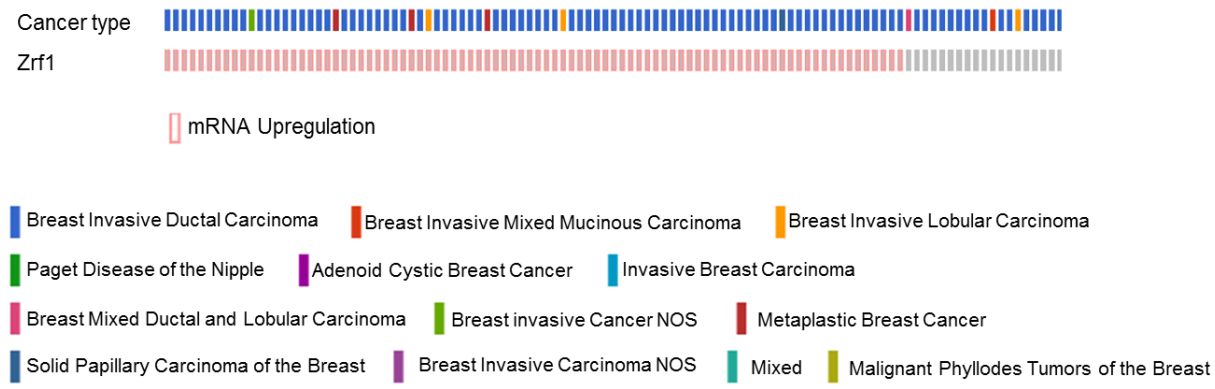

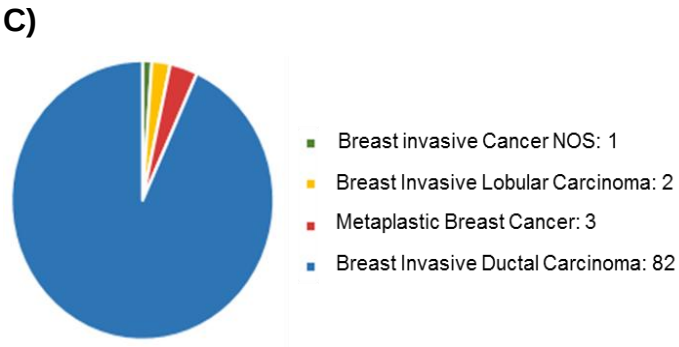

Figure 4. mRNA expression profile of Zrf1. (A) Heatmap of mRNA expression indicates a 8% mRNA alteration frequency for Zrf1 in all sequenced cases. (B) Zrf1 is mostly upregulated in breast cancers. (C) Pie chart represents the mRNA expression change of Zrf1 in different cancers. Zrf1 is particularly upregulated in breast invasive ductal carcinoma.

4.2 ZRF1 DISPLAYS A DUAL ROLE ON CELL PROLIFERATION IN MICROENVIRONMENT CONTEXT

Having shown that Zrf1 is amplified or overexpressed mostly in invasive ductal breast carcinoma, we decided to focus on Zrf1's role in this breast cancer type. For this purpose, we used the MCF7 cell line which represents the invasive ductal breast carcinoma *in vitro*. We generated control and Zrf1 knockdown cells either expressing a non-specific shRNA (shNMC) or shRNA targeting Zrf1 (shZrf1) by viral infection (Figure 5A and 5B) and characterized both cell lines to explore Zrf1's potential role. First we assessed the growth rates of control and Zrf1 knockdown cells. After seeding the same number of cells, we counted the cell numbers during 10 days and plotted them in a growth curve (Figure 5C). Zrf1 knockdown cells grew significantly less (20% less) compared to the control cells at most of the time points.

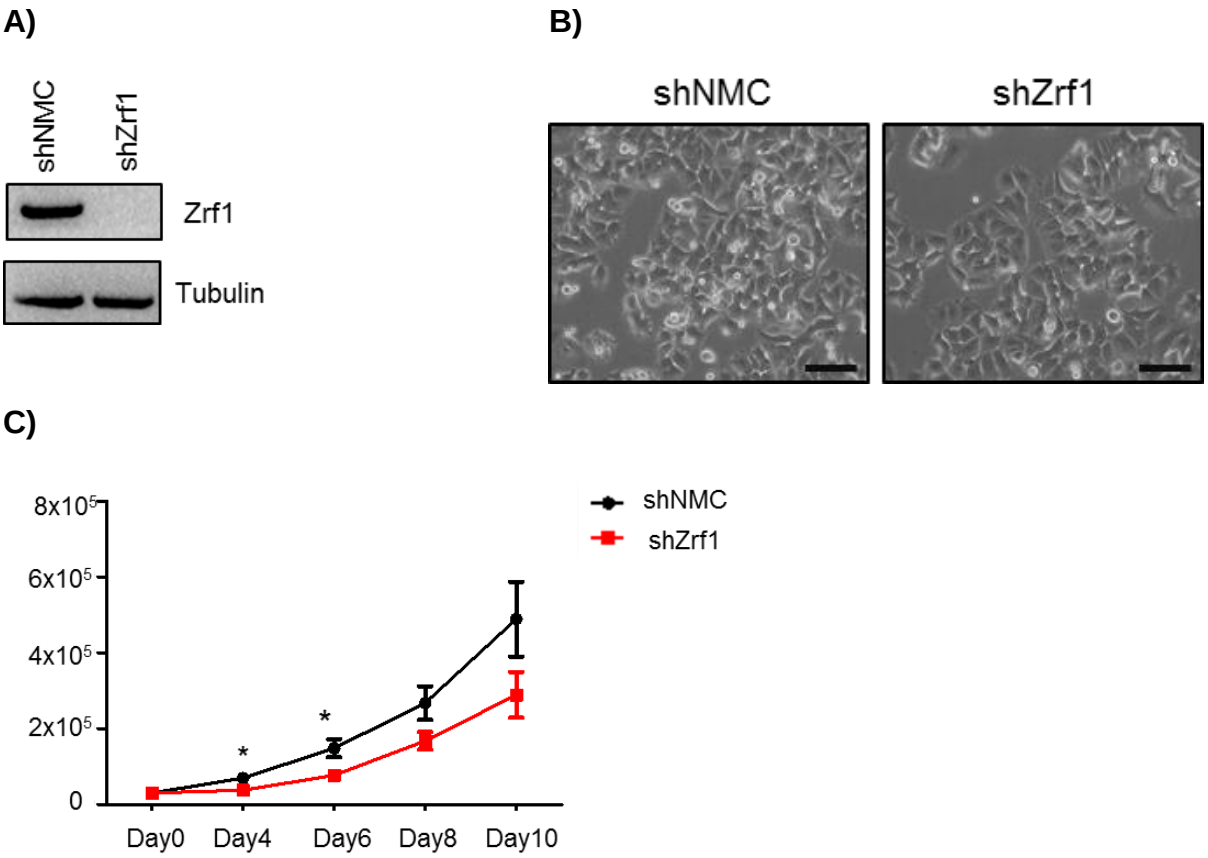

Figure 5. Zrf1 knockdown cells grow significantly less compared to control cells in normal conditions. (A) Western blot for Zrf1 after viral induction. Alpha tubulin was used as a loading control. (B) Representative microscopy images of control and Zrf1 knockdown cells. Scale bar, 200 µm. (C) Growth curve for MCF7 control and Zrf1 knockdown cells during 10 days. Data represent the average of three experiments, +/- S.E.M. *p<0.5, calculated by two-tailed unpaired t test.

Zrf1 regulates the expression of *p15* and *p16* tumor suppressor genes, which prevent cell cycle progression from G1 to S phase (Riberio JD et al., 2013). Thus, we investigated if the observed decrease in cell growth was caused by disruption of the cell cycle. For this purpose, we starved and synchronized cells in growth factor deprived medium for 48 hours and then treated them with 10nM 17β-estradiol (E2) to promote cell division. Next we analyzed the cell cycle distribution of both cell lines by flow cytometry after double staining with BrdU and DAPI (Figure 6A). Strikingly, however, upon serum starvation, we observed more cells in S phase (1.8 fold more) and G2-M (1.7 fold more) in Zrf1 knockdown cells. After 24h of E2 treatment, we observed increased numbers (11.8 fold more) of control cells in S phase almost, whereas shZrf1 cells only showed a 7.2 fold increase in S phase. After 48h of E2 treatment, the cell cycle distribution of both cell lines reached almost similar levels. To further confirm our findings, we carried out immunostainings with Ki67 antibody which is a nuclear marker expressed during all phases of the cell cycle except for G0 (Figure 6B). After serum starvation, most of the control cells were in the G0 phase with no significant Ki67 staining. In line with the cell cycle analysis, Zrf1 knockdown cells have a significant number of cells in S phase as indicated by homogenous Ki67 staining in the nucleus (white arrows in Figure 6B). In summary, Zrf1 depleted cells compared to control cells show a higher S phase ratio when the growth factors are withdrawn from the medium.

We examined the cell proliferation of both cell lines in serum starved and E2 induced conditions to explore whether the increased cell numbers in S phase observed in Zrf1 knockdown cells could lead to increased cell proliferation (Figure 7). 48 hours after serum starvation, we maintained control and shZrf1 cells in either vehicle or 10 nM E2 induced starvation medium for 7 days to circumvent unwanted growth effects by other factors. After 7 days, we assessed the cell proliferation of both cell lines with the MTT assay which is a colorimetric assay used for the detection of proliferating cells based on their enzymatic activity to convert the tetrazolium dye MTT into insoluble formazan crystals. Zrf1 knockdown cells proliferated strikingly more (3 fold) compared to control cells in serum starved conditions. Control cells were more responsive to E2 treatment and proliferated 2.5 fold more compared to their vehicle treated counterparts, whereas

shZrf1 cells were less responsive to E treatment and proliferated only 1.3 fold more compared to their vehicle treated counterparts.

A)

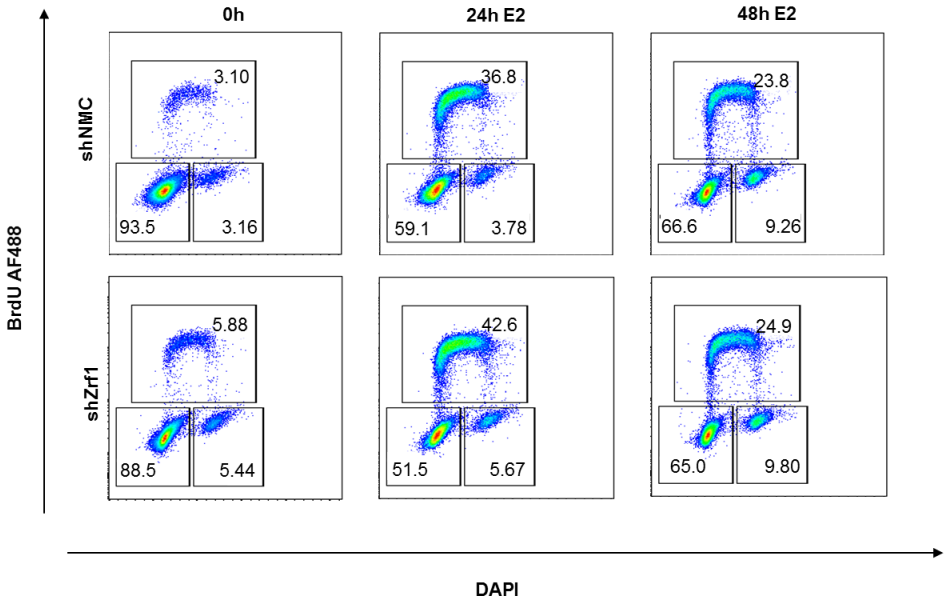

B)

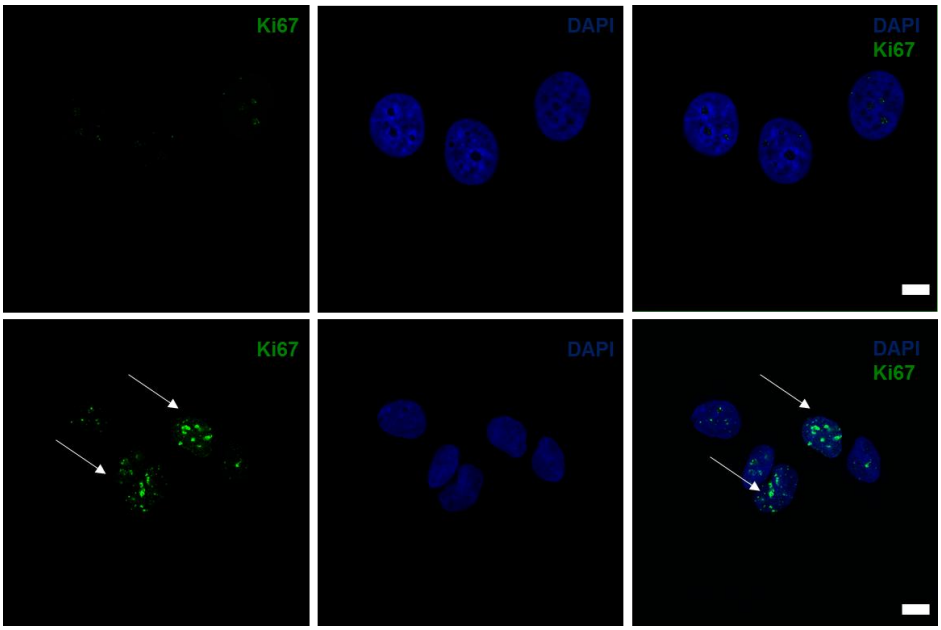

Figure 6. Zrf1 depletion stimulates S phase transition of cells. (A) Flow cytometry analysis of cell cycle distribution of control and shZrf1 cells in synchronized and E2 induced conditions for 24h and 48h. In each graph, the upper box represents the S phase, the left lower box represents the G0-G1 and the right lower box represents the G2-M phase. (B) Microscopy images of Ki67 staining for control and Zrf1 knockdown cells in serum starved conditions. White arrows show homogenous distribution of Ki67 staining which indicates cells in S phase. Scale bar, 7.5 μm.

Collectively these data suggest that Zrf1 knockdown cells proliferate less compared to control cells in normal medium conditions. However upon serum starvation, Zrf1 depletion stimulates cell proliferation in accordance with increased S phase transition of cells. Interestingly, the same cells have less proliferation capacity after estrogen treatment. In summary, Zrf1 has a dual role during cellular proliferation in a microenvironment context and Zrf1 knockdown has a significant impact on cell growth in a hormone-independent microenvironment.

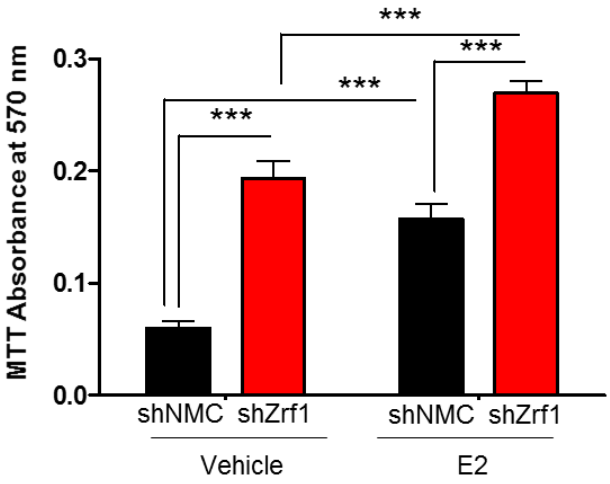

Figure 7. Zrf1 depleted cells proliferated significantly more upon growth factor withdrawal. MTT absorbance at 570 nm represents the cellular proliferation of control and shZrf1 cells in vehicle and E2 treated conditions. Data represent the average of three experiments, +/- S.E.M. ***p<0.001, calculated by One-way ANOVA.

4.3 ZRF1 KNOCKDOWN CELLS EXHIBIT MORE AGGRESSIVE CANCER PHENOTYPE

To further characterize Zrf1's effect on breast cancer progression, we performed experiments to analyze the cell migration and cell-cell adhesion capacity of Zrf1 knockdown cells. Because increased cell motility together with decreased cell adhesion are key steps in the cancer progression. The loss of cellular adhesion allows malignant cells to dissociate from the primary tumor mass. With the help of increased motility, these cells invade to the surrounding tissues and may enter the bloodstream where they eventually produce a secondary tumor. We carried out both wound healing and transwell migration assays to analyze the motility of Zrf1 knockdown cells. For wound healing experiments, we generated a scar tissue in the monolayer of control and shZrf1 cells. Then we monitored them for their wound healing capacity during 72 hours and captured images every 24 hours (Figure 8A). At each time point, Zrf1 knockdown cells closed their wound significantly faster than control cells (Figure 8B). To support the wound healing data, we performed a transwell cell migration assay. In this assay, cells are able to crawl and pass through the 8 μm pores in the membrane from a serum free medium to a serum containing medium. After resuspending in serum free medium, control and shZrf1 cells were placed into a transwell system and allowed to migrate through the transwells into the 20% serum containing medium. In line with our previous findings, Zrf1 knockdown cells migrated almost 2 fold more compared to control cells (Figure 8C and 8D). These data indicate that Zrf1 limits the cell migration of cancerous cells into other tissues.

Later we assessed the cell adhesion capacity of Zrf1 knockdown cells using collagen coated plates. Collagen here helps to mimic the cell-cell adhesion events functioning as an extracellular matrix protein. After blocking the plates with 1% BSA, we left cells to attach the surface for 1 hour and then stained only the attached cells with crystal violet (Figure 9A). To quantify the adhesion capacity of the cells, we measured the absorbance of the dye. Compared to the control cells, Zrf1 knockdown cells had significantly less crystal violet fluorescence indicating less cellular adhesion (Figure 9B).

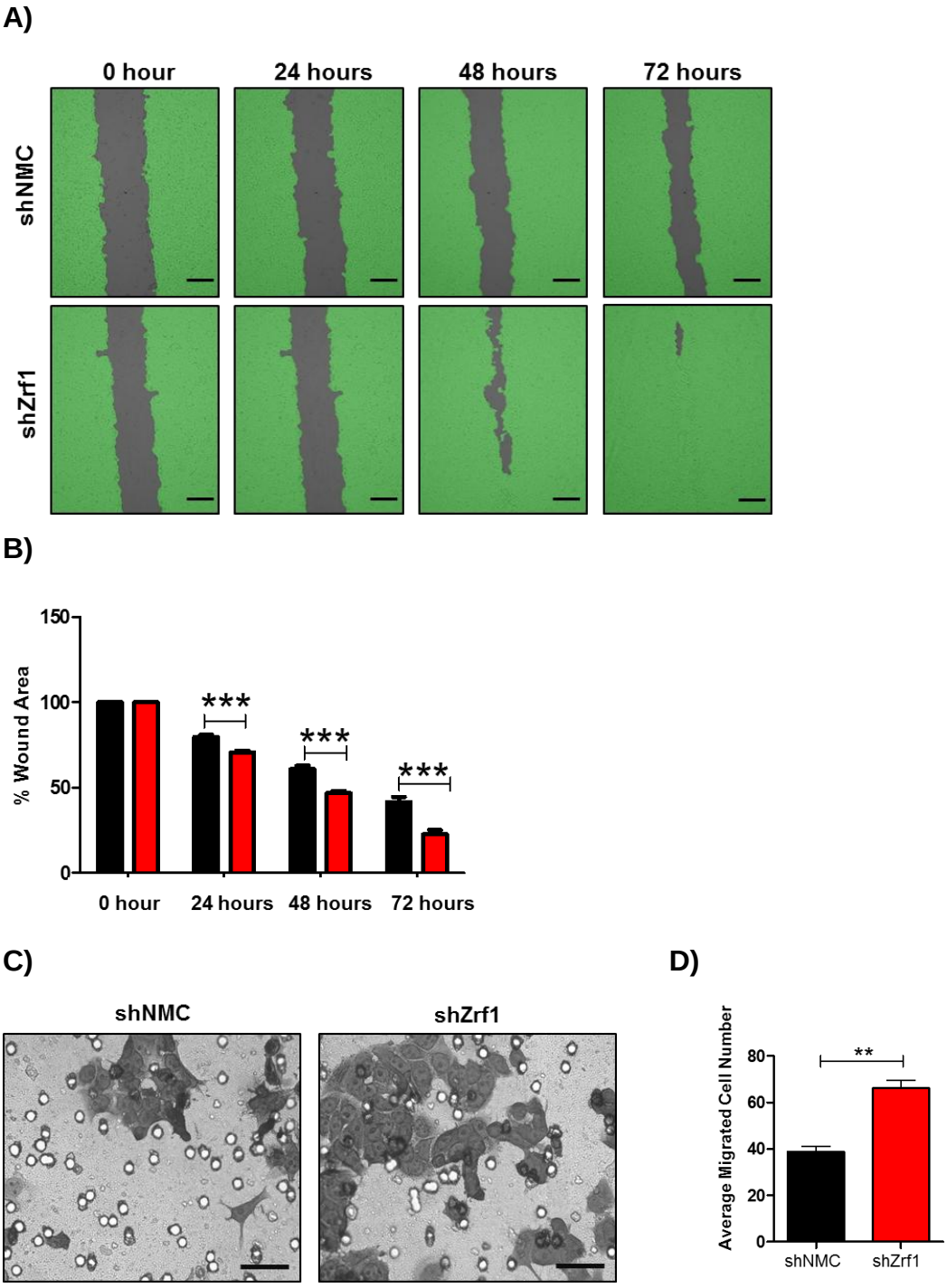

Figure 8. Zrf1 knockdown cells migrate significantly more compared to control cells. (A) Wound healing assay of control and shZrf1 cells for 72 hours. Images were taken at every 24 hours. Scale bar, 500 μm. (B) Quantification of cell migration was calculated as percentage wound area healed after the scratch. Data represent the average of three experiments, +/- S.E.M. *** $p<0.001$ as calculated by two-tailed unpaired t test. (C). Representative microscopy images of transwell migration assay of control and shZrf1 cells after 24 hours. Scale bar, 100 μm. (D) Quantification of the transwell cell migration assay. Migrated cells from 12 different fields randomly chosen were counted and calculated as average cell number. Data represent the average of three experiments, +/- S.E.M. ** $p<0.01$, calculated by two-tailed unpaired t test.

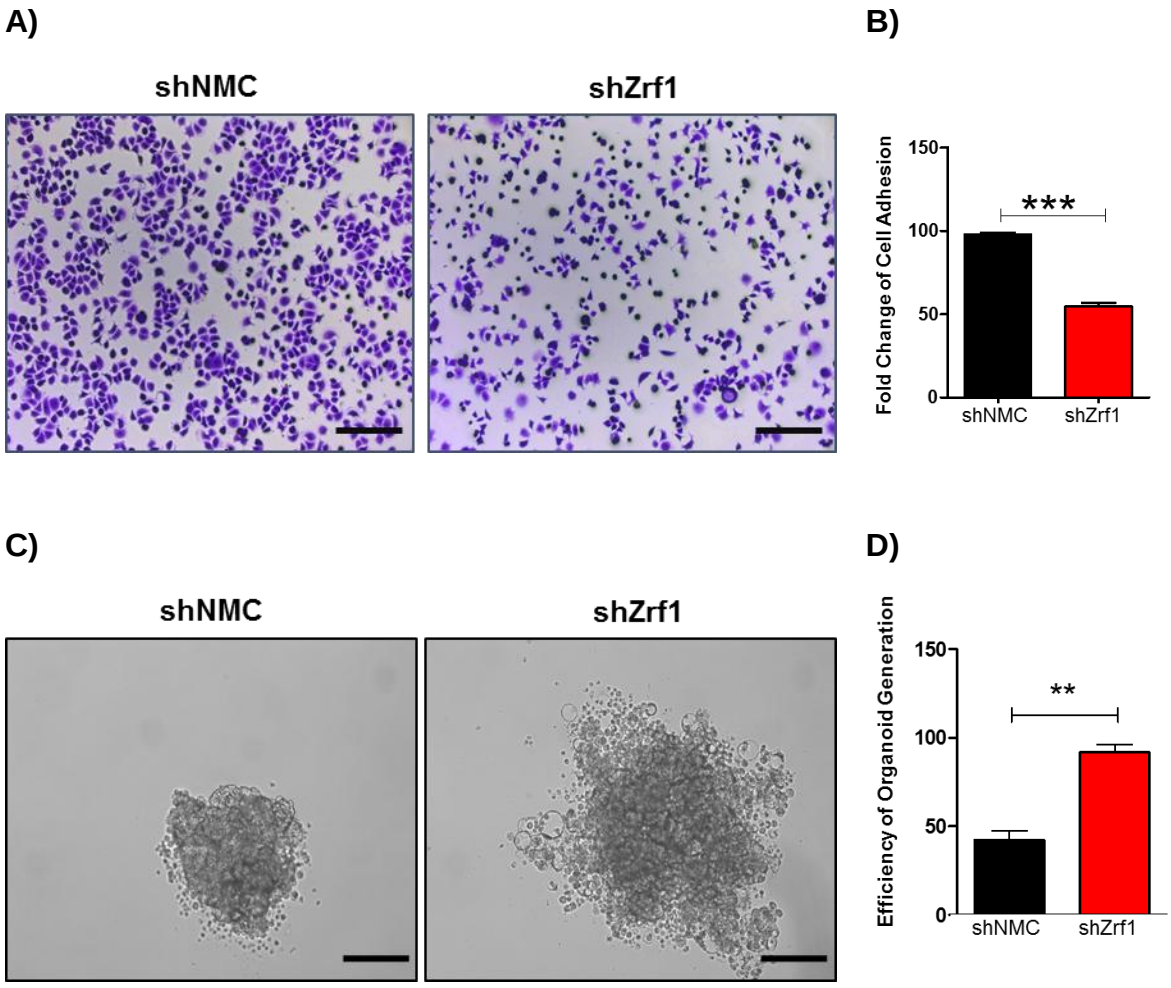

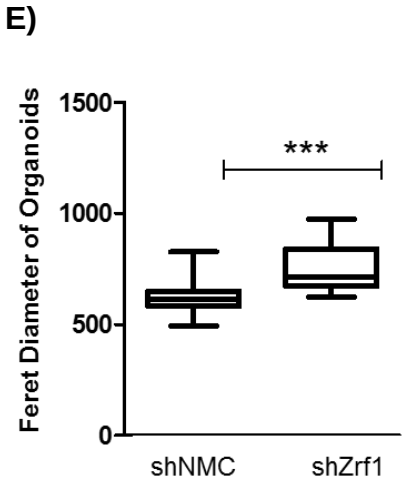

Figure 9. Zrf1 depletion results in the decrease of cellular adhesion properties. (A) Representative microscopy images of control and Zrf1 knockdown cells attached to the collagen coated plates after 1 hour. Scale bar, 200 μm. (B) Quantification of cell adhesion was calculated as fold change of crystal violet fluorescence in each cell line. Data represent the average of three experiments, +/- S.E.M. *** $p<0.001$ as calculated by two-tailed unpaired t test.(C) Representative microscopy images of organoid like structures generated by control and shZrf1 cell line after 4 days in suspension culture. Scale bar, 200 μm. (D) Efficiency of organoid generation was calculated as total organoid/ total well number and represented as fold change. Data represent the average of three experiments, +/- S.E.M. ** $p<0.01$ as calculated by two-tailed unpaired t test. (E) Box plot representing the feret diameters of organoids generated by both cell line at the end of day 4. Feret diameter unit is μm. Data represent the average of three experiments, +/- S.E.M. *** $p<0.001$ as calculated by two-tailed unpaired t test.

These results prompted us to further check whether these less adhesive cells are capable of also generating 3D organoid like structures in suspension culture (Figure 9C, D and E). For this purpose, we coated regular 96 well cell culture plates with agarose to prevent the cell attachment to the surface and maintained both cell lines in suspension during 4 days. After 4 days, Zrf1 knockdown cells generated almost two fold more organoid like structures compared to control cells (Figure 9C). According to feret diameter analysis of the organoids generated by both cell lines, we observed that shZrf1 cells were able to form larger organoids compared to control cells (Figure 9D). Decreased cell-cell adhesion was most probably the reason of larger cell clusters observed in Zrf1 knockdown cells. Taken together, Zrf1 depletion increases the cell motility significantly and affects the cellular adhesion, thereby promoting a more aggressive cancer phenotype in MCF7 cells.

4.4 ZRF1 KNOCKDOWN CELLS ARE RESISTANT TO ENDOCRINE THERAPY

Estrogen is the major driver of ERα+ breast cancers, hence the drugs targeting ERα are a first line choice for the treatment of invasive ductal breast carcinoma. Having shown that knockdown of Zrf1 causes an aggressive cancer phenotype in MCF7 cells, we asked whether Zrf1 knockdown cells are also resistant to anti-estrogen therapy. To answer this question, we treated control and shZrf1 cells with 10 µl partial anti-estrogen 4-OH Tamoxifen (active form of Tamoxifen) for 2 days. Prior to drug treatment, we synchronized cells for 48 hours and used the same volume of vehicle as control for each experiment. We analyzed the apoptotic response of both cell lines in flow cytometry based on their Annexin V and PI double staining (Figure 10A). Upon 4-OH Tamoxifen (TAM) treatment, control cells became dramatically apoptotic and the ratio of late apoptotic cells increased 6 fold more compared to their control condition. On the contrary, shZrf1 cells did not respond well to the treatment and the ratio of late apoptotic cells increased only 1.5 compared to the control condition.

Since Zrf1 knockdown cells exhibited such a robust phenotype after TAM treatment, we investigated their response against pure anti-estrogen ICI 182,780 (ICI) which is used against Tamoxifen resistant breast cancer cells in the clinic. After 48 hours of synchronization, we treated cells with 100 nM ICI 182,780 for 7 days and analyzed their

apoptotic response in flow cytometry (Figure 10B). In accordance with the TAM results, shZrf1 cells were resistant to ICI treatment and their total apoptotic cell number was almost 3 fold less compared to control cells. The total apoptotic cell number after ICI 182,780 treatment was less compared to 4-OH Tamoxifen due to the drug dosage used in the experiment. To further confirm the apoptosis phenotype, we assessed the level of cleaved-PARP protein which is used as a marker for the detection of apoptosis (Figure 10C). After a time course of ICI 182,780 treatment, Zrf1 knockdown cells had less cleaved PARP protein compared to control cells. Although we monitored a slight increase of protein levels at 2 hours and 8 hours, shZrf1 cells did not show an increase in cleaved PARP levels when compared with control cells, supporting the previous findings. Collectively these data reveal that Zrf1 depletion causes a significant resistance to endocrine therapy.

In addition, we observed a less apoptotic population in shZrf1 cells, almost half of the control (control: 17.28%; shZrf1: 8.5%), after 9 days of starvation (2 day synchronization + 7 days vehicle treatment) (Figure 10B). Since 0.1% vehicle volume does not have any effect on cells, we interpreted this observation as decreased apoptotic response in shZrf1 cells. Normally growth factor removal from cell culture medium leads to apoptosis in cells due to the stress conditions. In order to study the molecular mechanism underlying the role of Zrf1 in apoptosis, we investigated the mRNA expression of Bcl-2 and IAP family genes, which have essential roles in the regulation of the intrinsic apoptotic pathway, in control and shZrf1 cells after 1 μM ICI 182,780 treatment for 48h (Figure 11). To have a better understanding of early transcriptional changes, we chose a 48h drug treatment. Therefore we used 10 fold concentration of ICI 182,780 in this particular experiment. We compared the results of each cell line and each conditions (indicated as vehicle and ICI) separately because we observed less apoptotic response both in serum starved and drug induced condition. Zrf1 depletion increased the expression of anti-apoptotic genes significantly in both conditions. However the expression of pro-apoptotic genes were similar to control cells in both conditions. Bcl-2, Bcl-W, Survivin and BIRC3 genes were dramatically upregulated upon ICI 182,780 treatment indicating a drug specific response which can cause resistance in shZrf1 cells.

A)

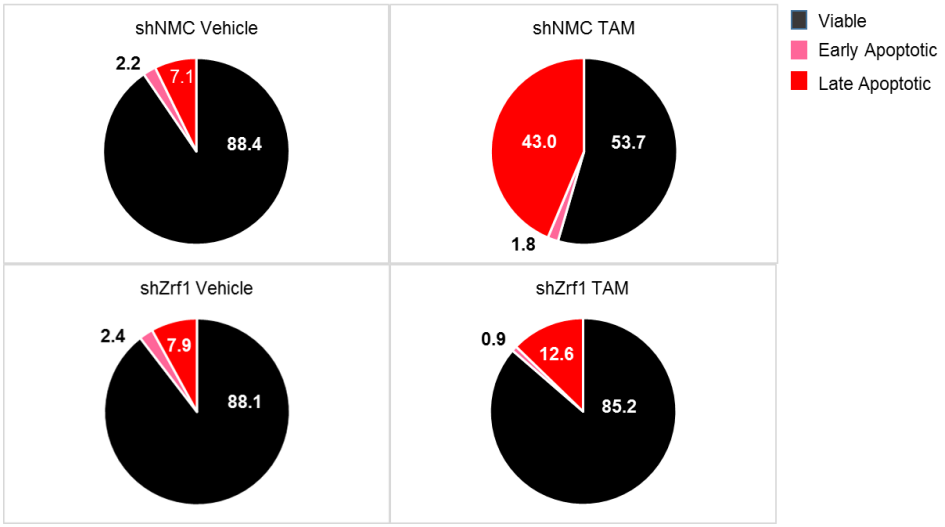

B)

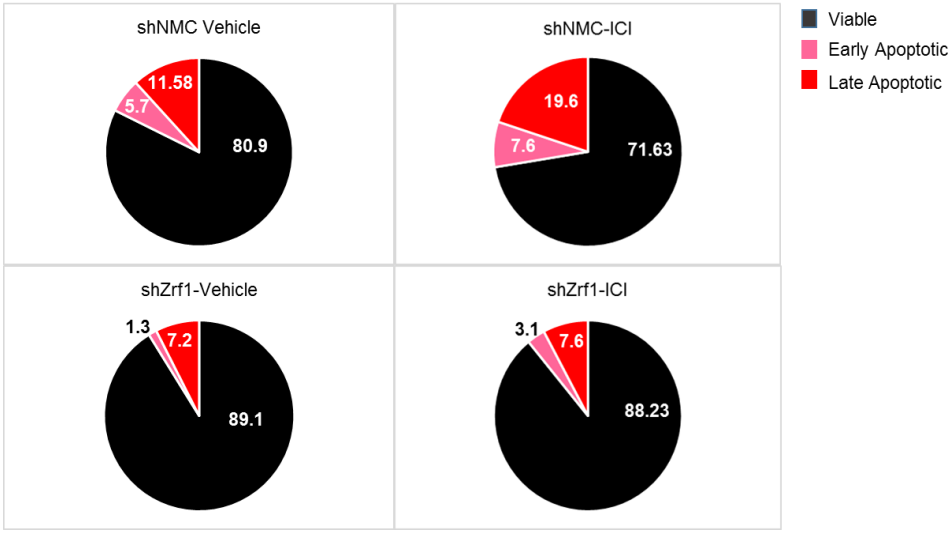

C)

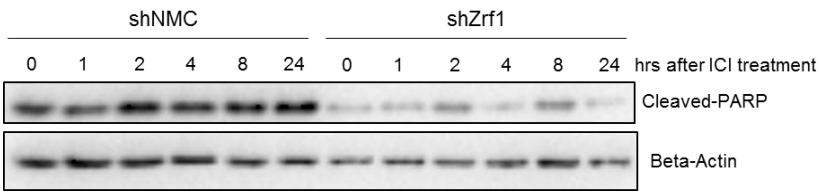

Figure 10. Zrf1 knockdown cells are resistant to endocrine therapy. (A) Representative pie charts of apoptotic cell distribution after 48h Tamoxifen treatment in control and shZrf1 cells. Data represent the average of three independent experiments. (B) Representative pie charts of apoptotic cell distribution after 7 days of ICI 182,780 treatment in control and shZrf1 cells. Data represent the average of three independent experiments. (C) Western blot of Cleaved-PARP protein in control and shZrf1 cells after a time course of ICI 182,780 treatment. Beta-Actin was used as a loading control.

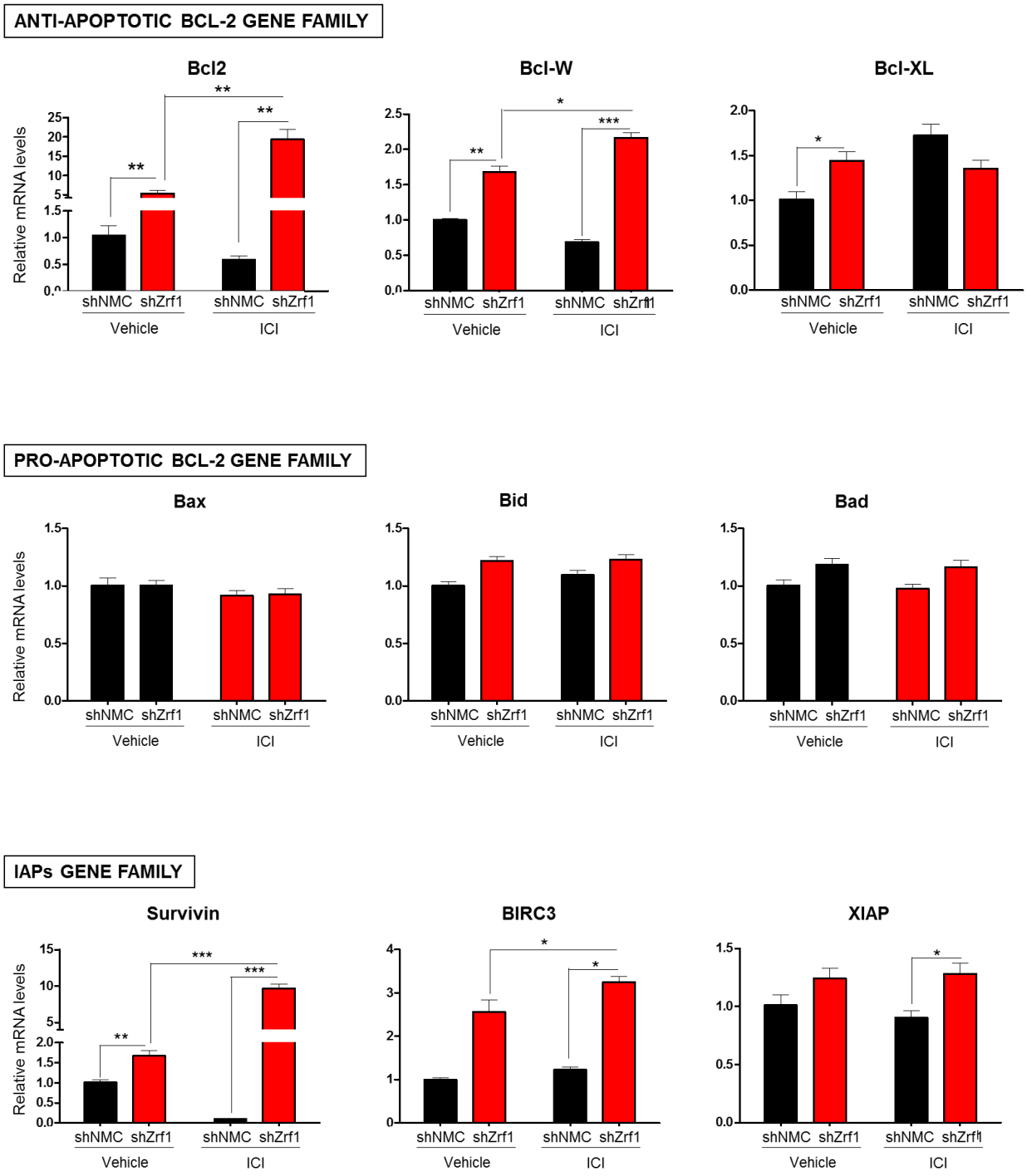

Figure 11. Zrf1 regulates the expression of anti-apoptotic genes. Real-time qPCR of Bcl-2 and IAPS family genes in control and shZrf1 cells after 1uM ICI 182,780 treatment for 48 hours. Expression was normalized to the housekeeping gene GAPDH. Data represent the average of three experiments, +/- S.E.M. *p<0.5, **p<0.01, ***p<0.001 as calculated by two-tailed unpaired t test between the samples indicated.

In summary, Zrf1 depletion impairs the balance between anti-apoptotic and pro-apoptotic genes and favors cell survival upon endocrine treatment.

5 DISCUSSION

Breast cancer is the most frequent carcinoma in females, and the second most common cause of cancer related mortality in women. The mortality rates of BC reduced over the past 15 years due to advances in early detection and therapeutic regimens. Despite these improvements, nearly 30% of all patients with early stage breast cancer have recurring, mostly metastatic forms of the disease. Hence BC remains the leading cause of death in women over the age 50 (Lumachi F. and Basso S.M.M., 2004; Zheng B. 2008). In this respect, understanding the molecular basis of events which govern the progression of an early stage breast cancer towards a metastatic form is quite essential to prevent the relapse and ultimately decrease mortality.

In this report, we have studied the function of Zrf1, a recently characterized epigenetic factor that is amplified in breast invasive ductal carcinoma. We demonstrate that Zrf1 is an important factor of breast cancer progression. Zrf1 depletion mimics events during cancer metastasis *in vitro.* It increases cell motility, decreases cellular adhesion and leads to the formation of organoid like structures in cell suspension. Furthermore Zrf1 knockdown contributes to hormone independent growth of MCF7 cells which represents a phenotype that is observed in more aggressive forms of breast cancer. Lastly, Zrf1 depletion may disrupt the balance between anti-apoptotic and pro-apoptotic genes, thereby favoring cell survival and contributing to drug resistance *in vitro* (Figure 12).

Our data provide evidence that Zrf1 depletion decreases the cell proliferation in normal conditions acting as a repressor factor but stimulates the cell proliferation when cells are deprived from the growth factors acting as a positive regulator. Understanding why Zrf1 switches from a growth repressor to a growth activator in hormone deprived conditions will certainly be a focus of future research. Because hormone independent breast cancer grows faster and is usually less differentiated compared to hormone-dependent breast cancers. Moreover hormone independent breast cancer is more aggressive than other types of breast cancers and requires radical therapies such as chemotherapy and radiotherapy for treatment.

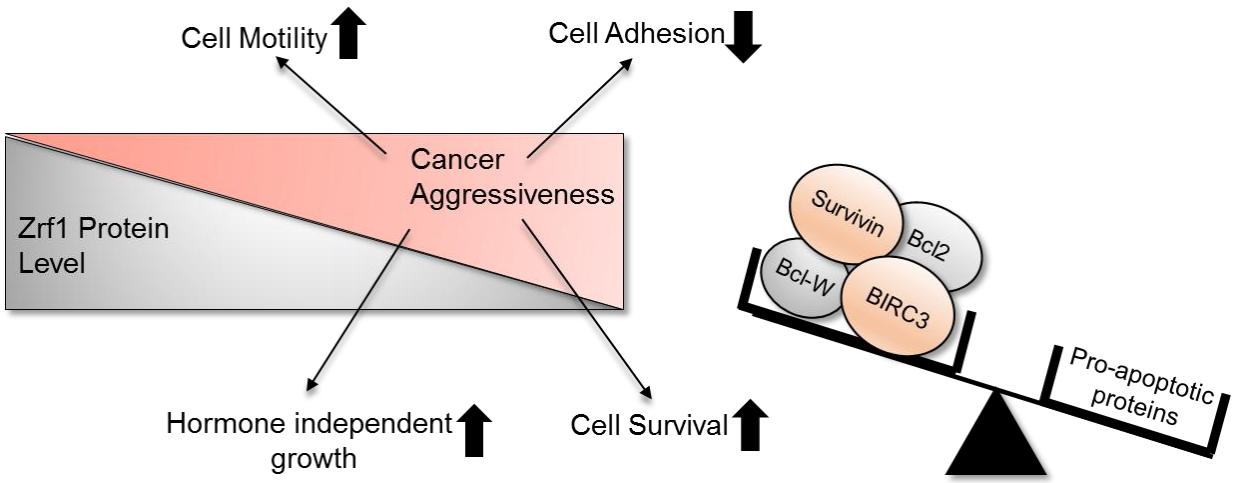

Figure 12. Summary of Zrf1's role in breast invasive ductal carcinoma. Depletion of Zrf1 in breast invasive ductal carcinoma cells results in increased cell motility and hormone independent growth. In addition, decreased cell-cell adhesion facilitates the formation of 3D organoid like structures in cell suspension. Furthermore, Zrf1 contributes to anti-hormonal drug resistance in same cells by promoting cell survival with its positive effects on anti-apoptotic genes such as Bcl-2, Bcl-W, Survivin and BIRC3.

Zrf1 depletion strongly induces the expression of anti-apoptotic genes (Bcl-2, Bcl-W, Survivin and BIRC3) but does not affect the expression of pro-apoptotic genes after pure ICI 182,780 treatment. It is generally accepted that the balance between proliferation and apoptosis influences the response of tumors to treatments such as hormonal therapy (Dowsett M. et al., 1999), radiation (Rupnow B.A. and Knox S.J., 1999) and chemotherapy (McKnight J.J. et al., 2005). Dysregulation of apoptosis is usually the reason of treatment failures in the clinic. Hence, overexpression of Bcl-2 upon ICI 182,780 treatment might be an important cause of intrinsic resistance observed in shZrf1cells.

In the context of chemotherapy, clinical breast cancer samples were analyzed before and after neoadjuvant chemotherapy and suggested a strong link between increased Bcl-2 and chemoresistance (Ellis P.A. et al., 1998). In accordance with this finding, metastatic human breast cancer cell lines with high Bcl-2 levels were found to be less sensitive to taxanes (Real P.J. et al., 2002) and Adriamycin (Teixeira C. et al., 1995). Furthermore, Tamoxifen treated ER+ breast cancers often increase Bcl-2 and Bcl-xL levels which leads to a decreased acute tumor response and ultimately to a long-term resistance to Tamoxifen (Musgrove E.A. and Sutherland R.L., 2009).

Interestingly, long term survival of ER+ breast cancers in hormone deprived conditions is shown to be supported by increased activity of Bcl-2 at the mitochondria. Upon long term hormone deprivation, endoplasmic reticulum chaperone proteins facilitate Bcl-2 and Bak/Bax interaction by sequestering the pro-apoptotic protein Bik thereby preventing the intrinsic mediated apoptosis (Zhou W. et al., 2011). Increased Bcl-2 levels observed in shZrf1 cells upon serum starvation may stimulate the cell survival and proliferation in similar manners. Notably, Zrf1 acts as a molecular chaperone in the cytoplasm and belongs to the DnaJ family proteins which are key regulators of apoptosome formation (Takayama S. et al., 2003). It would be an intriguing hypothesis to test whether Zrf1 has a specific function on apoptosome formation during intrinsic mediated apoptosis.

Zrf1 also controls the expression of IAPs in addition to anti-apoptotic Bcl-2 family members. Survivin, an important member of IAPs, is upregulated almost 20 fold more in shZrf1 cells upon ICI 182,780 treatment. This gene is expressed minimal in normal tissues, whereas it is overexpressed in a large number of malignancies (Ambrosini G. et al., 1997; Fukuda S. et al., 2006). The expression level of Survivin is correlated with a more aggressive disease and poor clinical outcome (Salz W. et al., 2005; Khan Z. et al., 2010; Khan Z. et al., 2013). Survivin plays also important roles in multidrug resistance in MCF7 cells (Liu F. et al., 2010) and may induce resistance in triple negative breast cancer cells by preventing apoptosis (Gritsko T. et al., 2006). Therefore Survivin has been proposed as a promising target for new anticancer interventions. *In vitro* and *in vivo* studies targeting Survivin have promising results such as reduced tumor-growth or increased sensitivity to chemotherapeutic drugs (Zaffaroni N. and Daidone M.G., 2002). Therefore, further understanding the role of Zrf1 in the regulation of Survivin could assist the new anticancer therapy studies.

BIRC3 is another IAPs family gene which is upregulated in shZrf1 cells after drug treatment. Studies have demonstrated that BIRC3 promotes resistance of cancer cells towards apoptosis (Peterson S.L. et al., 2007, Karasawa H. et al., 2009; Peterson S.L. et al., 2010). It has been shown that nuclear factor-κB (NF-κB) induces BIRC3 to promote survival of breast cancer cells (Frasor J. et al., 2009).

Collectively, Zrf1 depletion contributes to cell survival and drug resistance in breast invasive ductal carcinoma via regulation of anti-apoptotic genes. Our data suggest that Zrf1 is a potential novel target to be explored for new treatment strategies for breast cancer, moreover it plays a critical regulatory role in the breast cancer progression. Our findings support the clinical data indicating a decreased Zrf1 antigen and auto-antibody response in the sera of patients with more aggressive breast cancer (Dyachenko D. et al., 2016).

6 REFERENCES

Aebi S, Davidson T, Gruber G, Cardoso F; ESMO Guidelines Working Group. Primary breast cancer: ESMO Clinical Practice Guidelines for diagnosis, treatment and follow-up. Ann. Oncol., 2011, 22 (Suppl 6), vi12-vi24.

Ahmad A, Shahabuddin S, Sheikh S, Kale P, Krishnappa M, Rane RC, Ahmad I. Endoxifen, a new cornerstone of breast cancer therapy: demonstration of safety, tolerability, and systemic bioavailability in healthy human subjects. Clin Pharmacol Ther. 2010 Dec;88(6):814-7.

Alarid ET, Bakopoulos N, Solodin N. Proteasome-mediated proteolysis of estrogen receptor: A novel component in autologous down-regulation. Mol. Endocrinol 1999, 13, 1522–1534.

Albrektsen G, Heuch I, Hansen S, Kvale G. Breast cancer risk by age at birth, time since birth and time intervals between births: exploring interaction effects. British J Cancer. 2005;92: 167-175.

Aloia L, Demajo S, Di Croce L. ZRF1: a novel epigenetic regulator of stem cell identity and cancer. Cell Cycle. 2015;14(4):510-5.

Ambrosini G, Adida C, Altieri DC. A novel anti-apoptosis gene, survivin, expressed in cancer and lymphoma. Nat Mad. 1997;3:917–21.

Anderson KN, Schwab RB, Martinez ME. Reproductive risk factors and breast cancer subtypes: a review of the literature. Breast Cancer Res Treat. 2014;144: 1-10.

Anderson WF, Rosenberg PS, Prat A, Perou CM, Sherman ME. How many etiological subtypes of breast cancer: two, three, four, or more? J Natl Cancer Inst. 2014;106(8).

Antoniou A, Pharoah PD, Narod S, Risch HA, Eyfjord JE, Hopper JL, Loman N, Olsson H, Johannsson O, Borg A, Pasini B, Radice P, Manoukian S, Eccles DM, Tang N, Olah E, Anton-Culver H, Warner E, Lubinski J, Gronwald J, Gorski B, Tulinius H, Thorlacius S, Eerola H, Nevanlinna H, Syrjäkoski K, Kallioniemi OP,

Thompson D, Evans C, Peto J, Lalloo F, Evans DG, Easton DF. Average risks of breast and ovarian cancer associated with BRCA1 or BRCA2 mutations detected in case series unselected for family history: a combined analysis of 22 studies. Am J Hum Genet. 2003;72: 1117-1130.

Birnbaum MJ, Clem RJ, Miller LK. An apoptosis-inhibiting gene from a nuclear polyhedrosis virus encoding a polypeptide with Cys/His sequence motifs. J Virol. 1994 Apr;68(4):2521-8.

Björnström L, Sjöberg M. Mechanisms of estrogen receptor signaling: convergence of genomic and nongenomic actions on target genes. Mol Endocrinol. 2005 Apr;19(4):833-42.

Blin C, L'Horset F, Leclerc T, Lambert M, Colnot S, Thomasset M, Perret C. Contrasting effects of tamoxifen and ICI 182780 on estrogen-induced calbindin-D 9k gene expression in the uterus and in primary culture of myometrial cells. J Steroid Biochem Mol Biol. 1995 Oct;55(1):1-7.

Blows FM, Driver KE, Schmidt MK, Broeks A, van Leeuwen FE, Wesseling J, Cheang MC, Gelmon K, Nielsen TO, Blomqvist C, Heikkilä P, Heikkinen T, Nevanlinna H, Akslen LA, Bégin LR, Foulkes WD, Couch FJ, Wang X, Cafourek V, Olson JE, Baglietto L, Giles GG, Severi G, McLean CA, Southey MC, Rakha E, Green AR, Ellis IO, Sherman ME, Lissowska J, Anderson WF, Cox A, Cross SS, Reed MW, Provenzano E, Dawson SJ, Dunning AM, Humphreys M, Easton DF, García-Closas M, Caldas C, Pharoah PD, Huntsman D. Subtyping of breast cancer by immunohistochemistry to investigate a relationship between subtype and short and long term survival: a collaborative analysis of data for 10,159 cases from 12 studies. PLoS Med. 2010;7(5): e1000279.

Borras M, Laios I, El Khissiin A, Seo H-S, Lempereur F, Legros N, Leclercq G Estrogenic and antiestrogenic regulation of the half-life of covalently labeled estrogen receptor in MCF-7 breast cancer cells. J Steroid Biochem Mol Biol. 1996 Feb;57(3-4):203-13.

Bosch A, Eroles P, Zaragoza R, Vina JR, Lluch A. Triple-negative breast cancer: molecular features, pathogenesis, treatment and current lines of research. Cancer Treat Rev 2010;36(3):206–15.

Brenner C, Cadiou H, Vieira HL, Zamzami N, Marzo I, Xie Z, Leber B, Andrews D, Duclohier H, Reed JC, Kroemer G. Bcl-2 and Bax regulate the channel activity of the mitochondrial adenine nucleotide translocator. Oncogene. 2000 Jan 20;19(3):329-36.

Britt K, Ashworth A, Smalley M. Pregnancy and the risk of breast cancer. Endocrine-Related Cancer. 2007;14: 907-933.

Bundred N. Preclinical and clinical experience with fulvestrant (Faslodex) in postmenopausal women with hormone receptor-positive advanced breast cancer. Cancer Investigation 2005;23(2):173–81.

Chang M. Tamoxifen resistance in breast cancer. Biomol Ther (Seoul). 2012 May;20(3):256-67.

Cheang MC, Chia SK, Voduc D, Gao D, Leung S, Snider J, Watson M, Davies S, Bernard PS, Parker JS, Perou CM, Ellis MJ, Nielsen TO. Ki67 index, HER2 status, and prognosis of patients with luminal B breast cancer. J Natl Cancer Inst. 2009 May 20;101(10):736-50.

Chen D, Pace PE, Coombes RC, Ali S. Phosphorylation of human estrogen receptor α by protein kinase A regulates dimerization. Mol Cell Biol. 1999 Feb;19(2):1002-15.

Chen S, Parmigiani G. Meta-analysis of BRCA1 and BRCA2 penetrance. J Clin Oncol. 2007;25: 1329-1333.

Claessens, F., Gewirth, D.T. DNA recognition by nuclear receptors. In: McEwan, I.J. (Ed.), Essay in Biochemistry: The Nuclear Receptor Superfamily Portland Press, London, 2004, 59-72.

Collaborative Group on Hormonal Factors in Breast Cancer. Familial breast cancer: collaborative reanalysis of individual data from 52 epidemiological studies including

58,209 women with breast cancer and 101,986 women without the disease. *Lancet*. 2001;358: 1389-1399

Connolly J, Kempson R, LiVolsi V, Page D, Patchefsky A, Silverberg S. Recommendations for the reporting of breast carcinoma. Association of Directors of Anatomic and Surgical Pathology 2004.

Coopman P, Garcia M, Brünner N, Derocq D, Clarke R, Rochefort H. Anti-proliferative and antiestrogenic effects of ICI 164, 384 and ICI 182, 780 in 4-OH-tamoxifen-resistant human breast cancer cells. Int J Cancer. 1994 Jan 15;56(2):295-300.

Cory S, Adams JM. The Bcl2 family: regulators of the cellular life-or-death switch. Nat Rev Cancer. 2002 Sep;2(9):647-56.

Dauvois S, Danielian PS, White R, Parker MG. Antiestrogen ICI 164,384 reduces cellular estrogen receptor content by increasing its turnover. Proc Natl Acad Sci U S A. 1992 May 1;89(9):4037-41

Dauvois S, White R, Parker MG. The antiestrogen ICI 182,780 disrupts estrogen receptor nucleocytoplasmic shuttling. J Cell Sci. 1993 Dec;106 (Pt 4):1377-88.

DeFriend DJ, Howell A, Nicholson RI, Anderson E, Dowsett M, Mansel RE, BlameyRW, Bundred N, Robertson JF, Saunders C, Baum M, Walton P, Sutcliffe F, Wakeling AE. Investigation of a new pure antiestrogen (ICI 182780) in women with primary breast cancer. Cancer Res. 1994 Jan 15;54(2):408-14.

Demajo S, Uribesalgo I, Gutierrez A, Ballare C, Capdevila S, Roth M, Zuber J, Martin-Caballero J, Di Croce L. ZRF1 controls the retinoic acid pathway and regulates leukemogenic potential in acute myeloid leukemia. Oncogene 2013; 33(48):5501-10.

Dent R, Trudeau M, Pritchard KI, Hanna WM, Kahn HK, Sawka CA, Lickley LA, Rawlinson E, Sun P, Narod SA. Triple-negative breast cancer:clinical features and patterns of recurrence. Clin Cancer Res 2007;13(15):4429–34.

Deshmane V, Krishnamurthy S, Melemed AS, Peterson P, Buzdar AU. Phase III double-blind trial of arzoxifene compared with tamoxifen for locally advanced or metastatic breast cancer. J Clin Oncol. 2007; 25:4967–73

Desta Z, Ward BA, Soukhova NV, Flockhart DA. Comprehensive evaluation of tamoxifen sequential biotransformation by the human cytochrome P450 system in vitro: prominent roles for CYP3A and CYP2D6. J Pharmacol Exp Ther. 2004 Sep;310(3):1062-75.

Dowsett M, Archer C, Assersohn L, Gregory RK, Ellis PA, Salter J, Chang J, Mainwaring P, Boeddinghaus I, Johnston SR, Powles TJ, Smith IE. Clinical studies of apoptosis and proliferation in breast cancer. Endocr Relat Cancer. 1999 Mar;6(1):25-8.

Duckett CS, Nava VE, Gedrich RW, Clem RJ, Van Dongen JL, Gilfillan MC, Shiels H, Hardwick JM, Thompson CB. A conserved family of cellular genes related to the baculovirus iap gene and encoding apoptosis inhibitors. EMBO J. 1996 Jun 3;15(11):2685-94.

Duckett CS. IAP proteins: sticking it to Smac. Biochem J. 2005 Jan 1;385(Pt 1):e1-2.

Dukes M., Miller D., Wakeling AE, Waterton JC. Antiuterotrophic effects of a pure antiestrogen, ICI 182, 780: magnetic resonance imaging of the uterus in ovariectomized monkeys. J. Endocrinol.135 (2) (1992) 239–247.

Dyachenko L, Havrysh K, Lytovchenko A, Dosenko I, Antoniuk S, Filonenko V, Kiyamova R. Autoantibody Response to ZRF1 and KRR1 SEREX Antigens in Patients with Breast Tumors of Different Histological Types and Grades. Dis Markers. 2016;2016:5128720.

Ellis PA, Smith IE, Detre S, Burton SA, Salter J, A'Hern R, Walsh G, Johnston SR, Dowsett M. Reduced apoptosis and proliferation and increased Bcl-2 in residual breast cancer following preoperative chemotherapy. Breast Cancer Res Treat. 1998;48:107–116.

Enmark, E., Pelto-Huikko, M., Grandien, K., Lagercrantz, S., Lagercrantz, J., Fried, G., Nordenskjold, M., Gustafsson, J.-Å. Human estrogen receptor β-gene structure, chromosomal localization, and expression pattern. J. Clin. Endocrinol. Metab. 1997, 82: 4258- 4265.

Faupel-Badger JM, Arcaro KF, Balkam JJ, Eliassen AH, Hassiotou F, Lebrilla CB, Michels KB, Palmer JR, Schedin P, Stuebe AM, Watson CJ, Sherman ME. Postpartum remodeling, lactation, and breast cancer risk: summary of a National Cancer Institute-sponsored workshop. J Natl Cancer sInst. 2013;105: 166-174.

Frasor J, Weaver A, Pradhan M, Dai Y, Miller LD, Lin CY, Stanculescu A. Positive Crosstalk between Estrogen Receptor and NFκB in Breast Cancer. Cancer Res. 2009 Dec 1; 69(23): 8918–8925.

Fukuda S, Pelus LM. Survivin, a cancer target with an emerging role in normal adults tissues. Mol Cancer Ther. 2006;5:1087–98.

Giannopoulos K, Li L, Bojarska-Junak A, Rolinski J, Dmoszynska A, Hus I, Greiner J, Renner C, Döhner H, Schmitt M. Expression of RHAMM/CD168 and other tumor-associated antigens in patients with B-cell chronic lymphocytic leukemia. Int J Oncol 2006; 29: 95–103.

Gosden, J.R., Middleton, P.G., Rout, D. Localization of the human oestrogen receptor gene to chromosome 6q24-q27 by in situ hybridization. Cytogenet. Cell Genet. 1986, 43: 218-220.

Green, Douglas Means to an End: Apoptosis and other Cell Death Mechanisms. Cold Spring Harbor, NY: Cold Spring Harbor Laboratory Press. 2011 ISBN 978-0-87969-888-1.

Greiner J, Ringhoffer M, Taniguchi M, Hauser T, Schmitt A, Döhner H, Schmitt M. Characterization of several leukemia-associated antigens inducing humoral immune responses in acute and chronic myeloid leukemia. Int J Cancer 2003; 106:224–231.

Greiner J, Ringhoffer M, Taniguchi M, Li L, Schmitt A, Shiku H, Döhner H, Schmitt M. mRNA expression of leukemia-associated antigens in patients with acute myeloid

leukemia for the development of specific immunotherapies. Int J Cancer 2004;108: 704–711.

Gritsko T, Williams A, Turkson J, Kaneko S, Bowman T, Huang M, Nam S, Eweis I, Diaz N, Sullivan D, Yoder S, Enkemann S, Eschrich S, Lee JH, Beam CA, Cheng J, Minton S, Muro-Cacho CA, Jove R. Persistent activation of stat3 signaling induces survivin gene expression and confers resistance to apoptosis in human breast cancer cells. Clin Cancer Res. 2006 Jan 1;12(1):11-9.

Gross A, McDonnell JM, Korsmeyer SJ. BCL-2 family members and the mitochondria in apoptosis, Genes Dev. 13 (1999) 1899–1911

Hengartner MO. The biochemistry of apoptosis, Nature 407 (2000) 770–776.

Hennessy BT, Gonzalez-Angulo AM, Stemke-Hale K, Gilcrease MZ, Krishnamurthy S, Lee JS, Fridlyand J, Sahin A, Agarwal R, Joy C, Liu W, Stivers D, Baggerly K, Carey M, Lluch A, Monteagudo C, He X, Weigman V, Fan C, Palazzo J, Hortobagyi GN, Nolden LK, Wang NJ, Valero V, Gray JW, Perou CM, Mills GB. Characterization of a naturally occurring breast cancer subset enriched in epithelial-to-mesenchymal transition and stem cell characteristics. Cancer Res 2009;69(10):4116–24.

Howell, A.; Osborne, C.K.; Morris, C.; Wakeling, A.E. ICI 182,780 (Faslodex): Development of a novel, “pure” antiestrogen. Cancer 2000, 89, 817–825.

Howlader N, Noone AM, Krapcho M, et al. SEER Cancer Statistics Review, 1975-2012. http://seer.cancer.gov/csr/1975_2012/, based on November 2014 SEER data submission, posted to the SEER web site, April 2015. Bethesda, MD: National Cancer Institute, 2015.

Htun H, Holth LT, Walker D, Davie JR, Hager GL. Direct visualization of the human estrogen receptor α reveals a role for ligand in the nuclear distribution of the receptor. Mol Biol Cell. 1999 Feb;10(2):471-86.

Hu XF, Veroni M, De Luise M, Wakeling A, Sutherland R, Watts CK, Zalcberg JR. Circumvention of tamoxifen resistance by the pure anti-estrogen ICI 182,780. Int J Cancer. 1993 Nov 11;55(5):873-6.

Huynh HT, Pollack M. Insulin-like growth factor-I gene expression in the uterus is stimulated by tamoxifen and inhibited by the pure antiestrogen ICI 182780. Cancer Res. 1993 Dec 1;53(23):5585-8.

Hyder SM, Chieppetta C, Murthy L, Stancel GM. Selective inhibition of estrogen-regulated gene expression in vivo by the pure antiestrogen ICI 182,780. Cancer Res. 1997 Jul 1;57(13):2547-9.

Johnston SR. Endocrine manipulation in advanced breast cancer: recent advances with SERM therapies. Clin Cancer Res. 2001; 7:4376s–4387s.

Karasawa H, Miura K, Fujibuchi W, Ishida K, Kaneko N, Kinouchi M, Okabe M, Ando T, Murata Y, Sasaki H, Takami K, Yamamura A, Shibata C, Sasaki I. Down-regulation of cIAP2 enhances 5-FU sensitivity through the apoptotic pathway in human colon cancer cells. Cancer Sci. 2009;100(5):903–913.

Kauffman R.F., Bryant H.U. Selective estrogen receptor modulators. Drug News Perspect. 8 (9) (1995) 531–539.

Kennecke H, Yerushalmi R, Woods R, Cheang MC, Voduc D, Speers CH, Nielsen TO, Gelmon K. Metastatic behavior of breast cancer subtypes. J Clin Oncol 2010;28(20):3271–7

Khan Z, Bisen PS. Oncoapoptotic signaling and deregulated target genes in cancers: special reference to oral cancer. Biochim Biophys Acta. 2013;1836:123–45.

Khan Z, Khan N, Tiwari RP, Patro IK, Prasad GB, Bisen PS. Down-regulation of survivin by oxaliplatin diminishes radioresistance of head and neck squamous carcinoma cells. Radiother Oncol. 2010;96:267–73.

Klinge CM. Estrogen receptor interaction with estrogen response elements. Nucleic Acids Res. 2001 Jul 15;29(14):2905-19.

Klotz DM, Hewitt SC, Korach KS, Diaugustine RP. Activation of a uterine insulin-like growth factor I signaling pathway by clinical and environmental estrogens: requirement of estrogen receptor-alpha. Endocrinology. 2000 Sep 1;141(9):3430-3439.

Kreike B, van Kouwenhove M, Horlings H, Weigelt B, Peterse H, Bartelink H, van de Vijver MJ.Gene expression profiling and histopathological characterization of triple-negative/basal-like breast carcinomas. Breast Cancer Res 2007;9(5):R65.

Kuhl H. Pharmacology of estrogens and progestogens: influence of different routes of administration. Climacteric 2005 Aug;8 Suppl 1: 3–63.

Kumar R, Johnson BH, Thompson, EB. Overview of the structural basis for transcription regulation by nuclear hormone receptors. In: McEwan, I.J. (Ed.), Essay in Biochemistry: The Nuclear Receptor Superfamily Portland Press, London, 2004, pp. 27-39.

Kushner PJ, Agard DA, Greene GL, Scanlan TS, Shiau AK, Uht RM, Webb P. Estrogen receptor pathways to AP-1. J Steroid Biochem Mol Biol. 2000 Nov 30;74(5):311-7.

Lakhani S, Ellis I, Schnitt S, et al.: WHO Classification of Tumours of the Breast, 4th ed. Lyon, IARC Press, 2012

Lee CI, Goodwin A, Wilcken N. Fulvestrant for hormone-sensitive metastatic breast cancer. Cochrane Database Syst Rev. 2017 Jan 3;1:CD011093

Lee H, Bai W. Regulation of estrogen receptor nuclear export by ligand-induced and p38-mediated receptor phosphorylation. Mol Cell Biol. 2002 Aug;22(16):5835-45.

Li CI, Uribe DJ, Daling JR. Clinical characteristics of different histologic types of breast cancer. Br J Cancer 2005; 93:1046-52.

Liu F, Liu S, He S, Xie Z, Zu X, Jiang Y. Survivin transcription is associated with P-glycoprotein/MDR1 overexpression in the multidrug resistance of MCF-7 breast cancer cells. Oncol Rep. 2010 May;23(5):1469-75.

Livasy CA, Karaca G, Nanda R, Tretiakova MS, Olopade OI, Moore DT, Perou CM. Phenotypic evaluation of the basal-like subtype of invasive breast carcinoma. Mod Pathol 2006;19(2):264–71.

Lonard DM, Nawaz Z, Smith CL, O'Malley BW. The 26S proteasome is required for estrogen receptor-alpha and coactivator turnover and for efficient estrogen-alpha transcription. Mol. Cell 2000, 5, 939–948.

Lumachi F, Basso SMM. Serum tumor markers in patients with breast cancer. Expert Rev. Anticancer Ther., 2004, 4, 921-31.

Lumachi F, Brunello A, Maruzzo M, Basso U, Basso SM. Treatment of estrogen receptor-positive breast cancer. Curr Med Chem. 2013;20ss(5):596-604.

Malhotra GK, Zhao X, Band H, Band V. Histological, molecular and functional subtypes of breast cancers. Cancer Biol Ther. 2010 Nov 15;10(10):955-60.

Mangelsdorf DJ, Thummel C, Beato M, Herrlich P, Schütz G, Umesono K, Blumberg B, Kastner P, Mark M, Chambon P, Evans RM.(1995) The nuclear receptor superfamily: the second decade. Cell 1995 83, 835-839.

Masood, S. Estrogen and progesterone receptors in cytology: a comprehensive review. Diagn. Cytopathol., 1992, 8, 475-491.

Massarweh S, Osborne CK, Creighton CJ, Qin L, Tsimelzon A, Huang S, Weiss H, Rimawi M, Schiff R. Tamoxifen resistance in breast tumors is driven by growth factor receptor signaling with repression of classic estrogen receptor genomic function. Cancer Res. 2008, 68, 826–833.

Mavaddat N, Peock S, Frost D, Ellis S, Platte R, Fineberg E, Evans DG, Izatt L, Eeles RA, Adlard J, Davidson R, Eccles D, Cole T, Cook J, Brewer C, Tischkowitz M, Douglas F, Hodgson S, Walker L, Porteous ME, Morrison PJ, Side LE, Kennedy MJ, Houghton C, Donaldson A, Rogers MT, Dorkins H, Miedzybrodzka Z, Gregory H, Eason J, Barwell J, McCann E, Murray A, Antoniou AC, Easton DF; EMBRACE. Cancer risks for BRCA1 and BRCA2 mutation carriers: results from prospective analysis of EMBRACE. J Natl Cancer Inst. 2013;105: 812-822.

Maximov PY, McDaniel RE, Fernandes DJ, Bhatta P, Korostyshevskiy VR, Curpan RF, Jordan VC. Pharmacological relevance of endoxifen in a laboratory simulation of breast cancer in postmenopausal patients. J. Natl. Cancer Inst. 2014, 106.

May FEB, Johnson MD, Wiseman LR, Wakeling AE, Kastner P, Westley BR. Regulation of progesterone receptor mRNA byoestradiol and antioestrogens in breast cancer cell lines. J Steroid Biochem. 1989 Dec;33(6):1035-41.

McEwan, IJ. Sex, drugs and gene expression: signalling by members sof the nuclear receptor superfamily. In: McEwan, I.J. (Ed.), Essays in Biochemistry: the Nuclear Receptor Superfamily. Portland Press, London, 2004, pp. 1-10.

McKnight JJ, Gray SB, O'Kane HF, Johnston SR, Williamson KE. Apoptosis and chemotherapy for bladder cancer. J Urol. 2005 Mar;173(3):683-90.

Mohibi S, Mizra S, Band H, Band V. Mouse models of estrogen receptor-positive breast cancer. J. Carcinog., 2011, 10, 35.

Mosselman S, Polman J, Dijkema R. ERα: identification and characterization of a novel human estrogen receptor. FEBS Lett. 1996, 392: 49-53.

Musgrove EA, Sutherland RL. Biological determinants of endocrine resistance in breast cancer. Nat Rev Cancer. 2009;9:631–643.

Nawaz Z, Lonard DM, Dennis AP, Smith, CL, O'Malley BW. Proteasome-dependent degradation of the human estrogen receptor. Proc. Natl. Acad. Sci. USA 1999, 96, 1858–1862.

Nawaz Z, Stancel GM, Hyder SM. The pure antiestrogen ICI 182,780 inhibits progestin-induced transcription. Cancer Res 1999;59:372-6

Neilson HK, Friedenreich CM, Brockton NT, Millikan RC. Physical activity and postmenopausal breast cancer: proposed biologic mechanisms and areas for future research. Cancer Epidemiol Biomarkers Prev. 2009;18: 11-27.

Nicholson RI, Gee JMW, Manning DL, Wakeling AE, Montano MM, Katzenellenbogen BS. Responses to pure antioestrogens (ICI 164384, ICI 182780) in estrogen-sensitive and -resistant experimental and clinical breast cancer. Ann N Y Acad Sci. 1995 Jun 12;761:148-63.

Nilsson S, Mäkelä S, Treuter E, Tujague M, Thomsen J, Andersson G, Enmark E, Pettersson K, Warner M, Gustafsson JA.Mechanisms of estrogen action. Physiol Rev. 2001 Oct;81(4):1535-65.

O'Regan RM, Jordan VC. The evolution of tamoxifen therapy in breast cancer: selective oestrogen-receptor modulators and downregulators. Lancet Oncol. 2002 Apr;3(4):207-14.

Osborne CK, Jarman M, McCague R, Coronado EB, Hilsenbeck SG, Wakeling AE. The importance of tamoxifen metabolism in tamoxifen-stimulated breast tumor growth. Cancer Chemother Pharmacol. 1994;34(2):89-95

Osborne CK, Schiff R. Mechanisms of endocrine resistance in breast cancer. Annu Rev Med. 2011;62:233-47.

Parise CA, Caggiano V. Breast Cancer Survival Defined by the ER/PR/HER2 Subtypes and a Surrogate Classification according to Tumor Grade and Immunohistochemical Biomarkers. J Cancer Epidemiol. 2014;2014: 469251

Parker JS, Mullins M, Cheang MC, Leung S, Voduc D, Vickery T, Davies S, Fauron C, He X, Hu Z, Quackenbush JF, Stijleman IJ, Palazzo J, Marron JS, Nobel AB, Mardis E, Nielsen TO, Ellis MJ, Perou CM, Bernard PS. Supervised risk predictor of breast cancer based on intrisic subtypes. J Clin Oncol. 2009 Mar 10;27(8):1160-7.

Pelengaris S, Kean M. The Molecular Biology of Cancer. 6th edition, Blackwell Publishing 2006 pp.251-357.

Pennati M, Folini M, Zaffaroni N. Targeting survivin in cancer therapy. Expert Opin Ther Targets. 2008;12:463–76.

Pennati M, Folini M, Zaffaroni N. Targeting survivin in cancer therapy: fulfilled promises and open questions. Carcinogenesis. 2007;28:1133–9.

Perez, EA. Safety profiles of tamoxifen and aromatase inhibitors in adjuvant therapy of hormone-responsive early breast cancer. Ann. Oncol., 2007, 18 Suppl 8, viii26-viii35.

Perou CM, Sørlie T, Eisen MB, van de Rijn M, Jeffrey SS, Rees CA, Pollack JR, Ross DT, Johnsen H, Akslen LA, Fluge O, Pergamenschikov A, Williams C, Zhu SX, Lønning PE, Børresen-Dale AL, Brown PO, Botstein D. Molecular portraits of human breast tumours. Nature. 2000 Aug 17;406(6797):747-52.

Petersen SL, Peyton M, Minna JD, Wang X. Overcoming cancer cell resistance to Smac mimetic induced apoptosis by modulating cIAP-2 expression. Proc Natl Acad Sci USA. 2010;107 (26):11936–11941.

Petersen SL, Wang L, Yalcin-Chin A, Li L, Peyton M, Minna J, Harran P, Wang X. Autocrine TNFalpha signaling renders human cancer cells susceptible to Smac-mimetic-induced apoptosis. Cancer Cell. 2007;12(5):445–456.

Pink JJ, Jordan VC. Models of estrogen receptor regulation by estrogens and antiestrogens in breast cancer cell lines. Cancer Res. 1996 May 15;56(10):2321-30.

Pontiggia O, Rodriguez V, Fabris V, Raffo D, Bumaschny V, Fiszman G, de Kier Joffé EB, Simian M. Establishment of an in vitro estrogen-dependent mouse mammary tumor model: a new tool to understand estrogen responsiveness and development of tamoxifen resistance in the context of stromal-epithelial interactions. Breast Cancer Res Treat. 2009 Jul;116(2):247-55.

Prat A, Parker JS, Karginova O, Fan C, Livasy C, Herschkowitz JI, He X, Perou CM. Phenotypic and molecular characterization of the claudin-low intrinsic subtype of breast cancer. Breast Cancer Res. 2010;12(5):R68.

Prat A, Perou CM. Deconstructing the molecular portraits of breast cancer. Mol Oncol. 2011 Feb;5(1):5-23.

Real PJ, Sierra A, De Juan A, Segovia JC, Lopez-Vega JM, Fernandez-Luna JL. Resistance to chemotherapy via Stat3-dependent overexpression of Bcl-2 in metastatic breast cancer cells. Oncogene. 2002;21:7611–7618.

Reed JC. Bcl-2 family proteins. Oncogene. 1998 Dec 24;17(25):3225-36.

Resto VA, Caballero OL, Buta MR, Westra WH, Wu L, Westendorf JM, Jen J, Hieter P, Sidransky DA. Putative oncogenic role for MPP11 in head and neck squamous cell cancer. Cancer Res 2000; 60:5529-35.

Ribeiro JD, Morey L, Mas A, Gutierrez A, Luis NM, Mejetta S, Richly H, Benitah SA, Keyes WM, Di Croce L. ZRF1 controls oncogene-induced senescence through the INK4-ARF locus. Oncogene 2013; 32:2161-8.

Rondón-Lagos M, Villegas VE, Rangel N, Sánchez MC, Zaphiropoulos PG. Tamoxifen Resistance: Emerging Molecular Targets. Int J Mol Sci. 2016 Aug 19;17(8). pii: E1357.

Rupnow BA, Knox SJ. The role of radiation-induced apoptosis as a determinant of tumor responses to radiation therapy. Apoptosis. 1999 Apr;4(2):115-43.

Salz W, Eisenberg D, Plescia J, Garlick DS, Weiss RM, Wu XR, et al. A survivin gene signature predicts aggressive tumor behavior. Cancer Res. 2005;65:3531–4.

Schiff R, Massarweh S, Shou J, Osborne CK. Breast cancer endocrine resistance: how growth factor signaling and estrogen receptor coregulators modulate response. Clin Cancer Res. 2003 Jan;9(1 Pt 2):447S-54S.

Schiff R, Massarweh SA, Shou J, Bharwani L, Mohsin SK, Osborne CK. Cross-talk between estrogen receptor and growth factor pathways as a molecular target for overcoming endocrine resistance. Clin Cancer Res. 2004 Jan 1;10(1 Pt 2):331S-6S.

Schiff R, Osborne CK, Fuqua SA. Clinical aspects of estrogen and progesterone receptors. In Diseases of the Breast, ed. JR Harris, ME Lippman, M Morrow, CK Osborne pp. 408–30. Philadelphia: Wolters Kluwer/Lippincott Williams & Wilkins. 2009 4th ed.

Schmitt M, Li L, Giannopoulos K, Chen J, Brunner C, Barth T, Schmitt A, Wiesneth M, Döhner K, Döhner H, Greiner J.Chronic myeloid leukemia cells express tumor-associated antigens eliciting specific CD8þ T-cell responses and are lacking costimulatory molecules. Exp Hematol 2006; 34:1709–1719.

Shou J, Massarweh S, Osborne CK, Wakeling AE, Ali S, Weiss H, Schiff R. Mechanisms of tamoxifen resistance: increased estrogen receptor-HER2/neu cross-talk in ER/HER2-positive breast cancer. J Natl Cancer Inst. 2004 Jun 16;96(12):926-35.

Siegel S, Wirth S, Schweizer M, Schmitz N, Zeis M. M-phase phosphoprotein 11 is a highly immunogenic tumor antigen in patients with acute myeloid leukemia. Acta Haematol 2012; 127: 193–197.

Slee EA, Harte MT, Kluck RM, Wolf BB, Casiano CA, Newmeyer DD, Wang HG, Reed JC, Nicholson DW, Alnemri ES, Green DR, Martin SJ. Ordering the cytochromec-initiated caspase cascade: hierarchical activation of caspases-2, -3, -6,-7, -8, and -10 in a caspase-9-dependent manner. J Cell Biol. 1999 Jan 25;144(2):281-92.

Society, AC, Breast Cancer Facts and Figures, 2015-2016. p.1-2

Society, AC, Cancer Facts and Figures, 2016. p. 9-10

Sohn DM, Kim SY, Baek MJ, Lim CW, Lee MH, Cho MS, Kim TY. Expression of survivin and clinical correlation in patients with breast cancer. Biomed Pharmacother. 2006;60:289–92.

Sørlie T, Perou CM, Tibshirani R, Aas T, Geisler S, Johnsen H, Hastie T, Eisen MB, van de Rijn M, Jeffrey SS, Thorsen T, Quist H, Matese JC, Brown PO, Botstein D, Lønning PE, Børresen-Dale AL. Gene expression patterns of breast carcinomas distinguish tumor subclasses with clinical implications. Proc Natl Acad Sci USA 2001;98(19):10869–74.

Sorlie T, Tibshirani R, Parker J, Hastie T, Marron JS, Nobel A, Deng S, Johnsen H, Pesich R, Geisler S, Demeter J, Perou CM, Lønning PE, Brown PO, Børresen-Dale AL, Botstein D. Repeated observation of breast tumor subtypes in independent gene expression data sets. Proc Natl Acad Sci USA 2003;100(14):8418–23.

Stingl J, Caldas C. Molecular heterogeneity of breast carcinomas and the cancer stem cell hypothesis. Nat Rev Cancer 2007; 7:791-9.

Takayama S, Reed JC, Homma S. Heat-shock proteins as regulators of apoptosis. Oncogene. 2003 Dec 8;22(56):9041-7.

Teixeira C, Reed JC, Pratt MA. Estrogen promotes chemotherapeutic drug resistance by a mechanism involving Bcl-2 proto-oncogene expression in human breast cancer cells. Cancer Research. 1995;55:3902–3907.

Thiantanawat A, Long BJ, Brodie AM. Signaling pathways of apoptosis activated by aromatase inhibitors and antiestrogens. Cancer Res 2003; 63(22):8037-8050

Thompson EW, Katz D, Shima TB, Wakeling AE, Lippman ME, Dickson RB. ICI 164 384, a pure antagonist of estrogen-stimulated MCF-7 cell proliferation and invasiveness. Cancer Res 1989;49:6929-34.

Tsujimoto Y, Finger LR, Yunis J, Nowell PC, Croce CM. Cloning of the chromosome breakpoint of neoplastic B cells with the t(14;18) chromosome translocation. Science. 1984 Nov 30;226(4678):1097-9.

Vyssokikh MY, Zorova L, Zorov D, Heimlich G, Jürgensmeier JJ, Brdiczka D. Bax releases cytochrome c preferentially from a complex between porin and adenine nucleotide translocator. Hexokinase activity suppresses this effect. Mol Biol Rep. 2002;29(1-2):93-6.

Wakeling AE, Dukes M, Bowler J. A potent specific pure antiestrogen with clinical potential, Cancer Res. 51 (15) (1991) 3867–3873

Wakeling AE. Similarities and distinctions in the mode of action of different classes of antioestrogens. Endocrine-Related Cancer 2000;7(1):17–28.

Ward RL, Morgan G, Dalley D, Kelly PJ. Tamoxifen reduces bone turnover and prevents lumbar spine and proximal femoral bone loss in early postmenopausal women. Bone Miner. 1993 Aug;22(2):87-94.

Wu RC, Qin J, Yi P, Wong J, Tsai SY, Tsai MJ, O'Malley BW. Selective phosphorylations of the SRC-3/AIB1 coactivator integrate genomic reponses to multiple cellular signaling pathways. Mol. Cell 15:937–49

Wu RC, Smith CL, O'Malley BW. Transcriptional regulation by steroid receptor coactivator phosphorylation. Endocr Rev. 2005 May;26(3):393-9.

Zaffaroni N, Daidone MG. Survivin expression and resistance to anticancer treatments: perspectives for new therapeutic interventions. Drug Resist Updat. 2002 Apr;5(2):65-72.

Zhang M, Rosen JM. Developmental Insights into Breast Cancer Intratumoral Heterogeneity. Trends Cancer. 2015 Dec 1;1(4):242-251.

Zheng, B. Breast cancer: computer-aided detection. In Methods of Cancer Diagnosis, Therapy, and Prognosis, Hayat, M.A., Ed.; Springer: Heidelberg, 2008; Vol. 1, pp. 5-27.

Zhou H, Zhang Y, Fu Y, Chan L, Lee AS. Novel mechanism of anti-apoptotic function of 78-kDa glucose-regulated protein (GRP78): endocrine resistance factor in breast cancer, through release of B-cell lymphoma 2 (BCL-2) from BCL-2-interacting killer (BIK) Journal of Biological Chemistry. 2011;286:25687–25696.

Zhou W, Liu Z, Wu J, Liu JH, Hyder SM, Antoniou E, Lubahn DB. Identification and characterization of two novel splicing isoforms of human estrogen-related receptor β. J. Clin. Endocrinol. Metab. 2006, 91: 569-579.